



## UvA-DARE (Digital Academic Repository)

### Modulators of ventricular arrhythmias in structurally normal and abnormal hearts

ten Sande, J.N.

**Publication date**

2017

**Document Version**

Final published version

**License**

Other

[Link to publication](#)

**Citation for published version (APA):**

ten Sande, J. N. (2017). *Modulators of ventricular arrhythmias in structurally normal and abnormal hearts*. [Thesis, fully internal, Universiteit van Amsterdam].

**General rights**

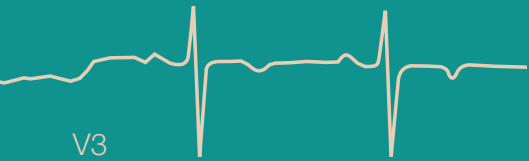
It is not permitted to download or to forward/distribute the text or part of it without the consent of the author(s) and/or copyright holder(s), other than for strictly personal, individual use, unless the work is under an open content license (like Creative Commons).

**Disclaimer/Complaints regulations**

If you believe that digital publication of certain material infringes any of your rights or (privacy) interests, please let the Library know, stating your reasons. In case of a legitimate complaint, the Library will make the material inaccessible and/or remove it from the website. Please Ask the Library: <https://uba.uva.nl/en/contact>, or a letter to: Library of the University of Amsterdam, Secretariat, Singel 425, 1012 WP Amsterdam, The Netherlands. You will be contacted as soon as possible.

# Modulators of ventricular arrhythmias in structurally normal and abnormal hearts

Judith N. ten Sande





# **Modulators of Ventricular Arrhythmias in Structurally Normal and Abnormal Hearts**

Judith N. ten Sande

Layout and printing: Optima Grafische Communicatie, Rotterdam, The Netherlands

© Judith N. ten Sande, 2016

All rights reserved. No part of this thesis may be reproduced, stored in a retrieval system, or transmitted in any form or by any means, electronic, mechanical, photocopying, recording or otherwise without permission of the author or the copyright owning journal.

ISBN 978-90-77595-17-6

Financial support by the Dutch Heart Foundation for publication of this thesis is gratefully acknowledged.

Additional financial support for printing this thesis was kindly provided by: Academic Medical Center – University of Amsterdam, Bayer B.V., BioSemi B.V., BIOTRONIK Nederland B.V., Boehringer Ingelheim, ChipSoft, Sanofi, St. Jude Medical Nederland B.V., Servier Nederland Farma B.V.

Modulators of Ventricular Arrhythmias in Structurally  
Normal and Abnormal Hearts

**ACADEMISCH PROEFSCHRIFT**

ter verkrijging van de graad van doctor  
aan de Universiteit van Amsterdam  
op gezag van de Rector Magnificus  
prof. dr. ir. K.I.J. Maex  
ten overstaan van een door het College voor Promoties ingestelde commissie,  
in het openbaar te verdedigen in de Agnietenkapel  
op 26 januari 2017, te 10:00 uur

door

**Judith Nicolien ten Sande**  
geboren te Amersfoort

## PROMOTIECOMMISSIE

### Promotores:

Prof. dr. ir. J.M.T. de Bakker      Universiteit van Amsterdam

Prof. dr. A.A.M. Wilde              Universiteit van Amsterdam

### Copromotores:

Dr. P.F.H.M. van Dessel            Universiteit van Amsterdam

Dr. R. Coronel                        Universiteit van Amsterdam

### Overige leden:

Prof. dr. R.J.G. Peters              Universiteit van Amsterdam

Prof. dr. Y.M. Pinto                 Universiteit van Amsterdam

Prof. dr. D.J. van Veldhuisen      Rijksuniversiteit Groningen

Prof. dr. M.A. Vos                  Universiteit Utrecht

Dr. C.E. Conrath                    Universiteit van Amsterdam

Dr. P.G. Postema                    Universiteit van Amsterdam

Dr. J.P. van Tintelen                Universiteit van Amsterdam

Faculteit der Geneeskunde

## CONTENTS

Chapter 1	Introduction and outline	7
-----------	--------------------------	---

### **Part I Markers of Vulnerability for Ventricular Arrhythmias**

Chapter 2	Value of Serial Heart Rate Variability Measurement for Prediction of Appropriate ICD Discharge in Patients with Heart Failure <i>Journal of Cardiovascular Electrophysiology</i> 2014 Jan;25(1):60-5	23
Chapter 3	Myocardial Fibrosis as an Early Feature in Phospholamban p.Arg14del Mutation Carriers: Phenotypical Insights using Cardiovascular Magnetic Resonance Imaging <i>Submitted</i>	39
Chapter 4	Detailed Characterization of Familial Idiopathic Ventricular Fibrillation Linked to the <i>DPP6</i> Locus <i>Heart Rhythm</i> 2016 Apr;13(4):905-12	57

### **Part II Characteristics of Arrhythmogenic Substrates of Ventricular Arrhythmias**

Chapter 5	Differences in Left Ventricular Remodeling between Patients with Ischemic and Dilated Cardiomyopathy <i>In preparation</i>	77
Chapter 6	ST-segment Elevation and Fractionated Electrograms in Brugada Syndrome Patients Arise from the Same Structurally Abnormal Subepicardial RVOT Area but Have a Different Mechanism <i>Circulation: Arrhythmia and Electrophysiology</i> 2015 Dec;8(6):1382-92	91
Chapter 7	Differential Mechanisms of Myocardial Conduction Slowing by Adipose Tissue-Derived Stromal Cells Derived From Different Species <i>STEM CELLS Translational Medicine</i> , 2016;5:1-9	113
Chapter 8	Summary and future directions	141
Chapter 9	Samenvatting en toekomstperspectieven	153
	Portfolio	165
	Contributing authors	167
	Curriculum Vitae	175
	Dankwoord (Dutch)	171

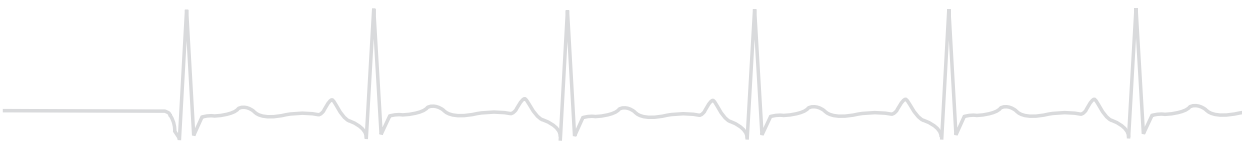




# CHAPTER 1

## Introduction and outline

Judith N. ten Sande





## INTRODUCTION AND OUTLINE

Sudden cardiac death (SCD) is a major cause of death in the Western world<sup>1</sup> and it accounts for approximately 25% of the cardiovascular deaths.<sup>2</sup> SCD is defined by unexpected death with a cardiac origin, generally within 1 hour from the onset of symptoms, and it is mainly caused by ventricular tachycardia (VT) or ventricular fibrillation (VF).<sup>4</sup> Most SCD victims have coronary artery disease including those with an acute coronary syndrome<sup>5</sup> and/or heart failure (HF). Less frequently, SCD is caused by mutation in ion channel genes (f.e. long QT syndromes<sup>6</sup>) and in rare cases such as Brugada syndrome (BrS) the pathophysiological substrate is more complex and incompletely understood.<sup>7</sup> In some cases (idiopathic SCD/VF) the causes remain unknown despite extensive investigation.<sup>8</sup>

Extensive knowledge of the underlying disease, inherited or acquired, gives opportunities to identify patients at risk and anticipate on the triggering factors before patients succumb to lethal ventricular arrhythmias (VA). Hence, one needs to understand the mechanisms, circumstances and conditions in which VA can occur and which factors are a prerequisite.

One of the founding fathers of modern arrhythmology was Philippe Coumel. His research resulted in Coumel's three components of arrhythmogenesis (figure).<sup>3</sup> In order to develop ventricular or atrial arrhythmias, the concurrence of a pre-existing arrhythmogenic condition (the substrate) and an initiating factor (the trigger) is required. Both trigger and substrate can be changed by modulating factors (in the original graph represented by the autonomic nervous system). This concept of Coumel has been modulated to a triangle and can be used for every arrhythmia. In addition, each determinant could be a target for anti-arrhythmic therapy. Antiarrhythmic therapy then can be considered a modulating factor as well.

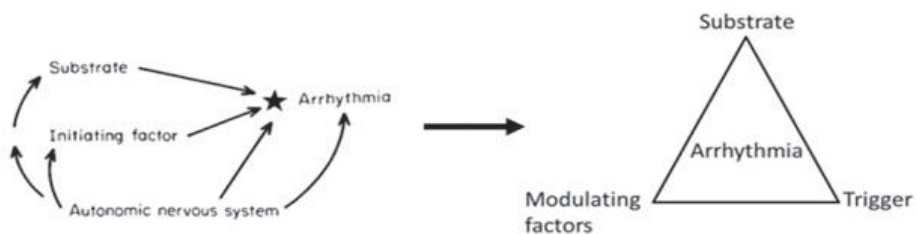


**Figure.** Left: Coumel's three components of arrhythmogenesis.<sup>3</sup> Right: adjusted triangle of arrhythmia.

This thesis will focus on the arrhythmogenic substrate and its modulators of VA with Coumel's triangle as a backbone. It aims to provide insight in the etiology and pathophysiology of VA in various cardiac diseases. The exact electrophysiological mechanism of VA occurring in association with diseases is often unknown. As a result, the substrate, trigger and modulating factors pertinent to the arrhythmia are difficult to identify. Characterization of markers for arrhythmogenesis in large patient populations may lead to the identification of

the vulnerable factors pertaining to the specific arrhythmia. PART I will deal with the various markers in SCD and assess the clinical value of these markers in clinical risk stratification. PART II will concentrate on the characteristics of the arrhythmogenic substrate in various specific diseases, and the potential creation of an arrhythmogenic substrate by therapy.

### **PART I Markers of Vulnerability for Ventricular Arrhythmias**

Remarkable effort has been put in basic as well as clinical research to identify patients at risk for SCD. Risk stratification for SCD is, however, still ill-defined and this is the main reason that implantable cardioverter defibrillator (ICD) therapy is often the first choice of treatment.<sup>1</sup> Essentially, this is caused by the fact that the arrhythmogenic substrate/trigger is unknown (and/or unpredictable) for the particular arrhythmia at hand. In case of structural heart disease, ICD has proven to be more efficient than anti-arrhythmic drug therapy to reduce SCD in primary as well as secondary prevention patients.<sup>9-14</sup> However, two third of the patients with an ICD for primary prevention will never experience an appropriate shock during 5 year follow-up<sup>15</sup>, even though they are exposed to the same complications and negative side effects occurring during and/or after the implantation as the other patients.<sup>16-18</sup>

Currently, most guidelines mention a reduced left ventricular ejection fraction (LVEF) of less than 35% as the best risk factor for primary prevention. Clearly, a better risk stratification is warranted because of the lack of accuracy and reproducibility of this parameter<sup>19-22</sup> to predict VA.<sup>1</sup> Numerous studies have evaluated new indicators of SCD risk based on clinical, electrophysiological, imaging and genetic parameters, but none of these potential predictors have led to application in clinical practice.<sup>1</sup> Parameters including autonomic cardiac activity, microvolt T-wave alternans and arrhythmia inducibility by programmed electrical stimulation have been investigated. Although these tests appear to have reasonable negative predictive value, their role in predicting appropriate ICD therapy is less well established.<sup>23-25</sup> Several studies suggest that decreased heart rate variability (HRV) plays an important role in the pathophysiology of SCD.<sup>26, 27</sup> In CHAPTER 2 the predictive value of HRV as an independent predictor for imminent appropriate ICD shocks is evaluated in patients with an ICD implanted for primary or secondary prevention, capable of automatic assessment and storage of HRV parameters.

Structural abnormalities as seen in HF patients can have a genetic origin. For example, in 20% of the patients with dilated cardiomyopathy (DCM) a genetic cause is identified.<sup>28, 29</sup> In the Netherlands, one of the main contributors is a common founder mutation in the phospholamban (PLN) gene.<sup>30</sup> The PLN p.Arg14del mutation is associated with arrhythmogenic cardiomyopathy (AC) in patients who have been initially diagnosed with DCM or arrhythmogenic right ventricular cardiomyopathy. PLN is a transmembrane sarcoplasmic reticulum phosphoprotein and is involved in the calcium homeostasis.<sup>31</sup> In the Netherlands, in 10-15% of patients diagnosed with AC, a mutation in the PLN R14del gene is found.

These patients show frequent malignant ventricular arrhythmias, suffer from end-stage heart failure and have low voltages on the electrocardiogram (ECG) as the most prominent manifestation.<sup>32</sup> Especially in this disease, low voltages on the ECG may indicate the presence of cardiac fibrosis.<sup>33</sup> The reduced QRS amplitudes could be the first indication of fibrosis resulting in cardiac electrical instability and heart failure. In CHAPTER 3 the possible correlation between low voltage signals on standard 12 lead ECG, segmental fibrosis on cardiac magnetic resonance imaging and severity of the cardiomyopathy is investigated to assess the diagnostic potential of these non-invasive parameters.

If VF occurs without ischemic or structural heart disease and no inheritable arrhythmic syndrome is uncovered, idiopathic ventricular fibrillation (IVF) is diagnosed.<sup>8</sup> This rather rare entity may also occur in a hereditary pattern. In previous research we discovered an association between familial IVF and a risk haplotype on chromosome 7q36 (which harbors the *DPP6* gene).<sup>34</sup> Up to now, no prognostic markers of risk for SCD in IVF have been found in those who have not died or have been resuscitated to guide treatment besides confirmation of the 7q36 risk haplotype.<sup>35</sup> Further insight in the clinical parameters and the mechanism will help us to identify patients at risk. In CHAPTER 4 familial idiopathic ventricular fibrillation is characterized and the possible substrate is discussed.

## PART II Characteristics of Arrhythmogenic Substrates of Ventricular Arrhythmias

The understanding of pathophysiological mechanisms of the arrhythmogenic substrate leading to ventricular arrhythmias may give direction toward better tailored therapy. In coronary artery disease extensive research of VA related substrate has been conducted, but there are also more rare diseases in which the arrhythmogenic substrate is less well understood.<sup>1,36</sup> In PART II of this thesis the arrhythmogenic substrate of various, sometimes less frequently occurring cardiac diseases is outlined.

It is known that patients with HF have an increased risk of SCD depending on severity and etiology of the underlying disease.<sup>37</sup> Several factors are associated with increased occurrence of VA in HF. In ischemic heart failure, for example, inhomogeneous scarring occurs due to areas consisting of scar intermingled with surviving myocardium.<sup>38</sup> This may result in areas of altered conduction, a lengthening of pathways, altered anisotropy of conduction and surviving conducting myocardial channels within scar, leading to the development of re-entrant VA.<sup>39-42</sup> Also, the expression and distribution of connexin43 (Cx43) is of importance, since heterogeneous distribution of Cx43, which may occur in heart disease, is associated with dispersion in conduction and enhanced susceptibility to VA.<sup>43-46</sup> Impaired conduction is a major component for reentry-based VA, but triggered activity and increased normal or abnormal automaticity may cause rhythm disturbances in the remodeled hearts as well. Some studies refer to a focal mechanism for VA in patients with dilated cardiomyopathy, but the arrhythmic substrate suggests that reentry can also

be a good candidate<sup>47, 48</sup>. These two aspects can be responsible in remodeled hearts at the same time.

Since the causes of HF are multiple, the onset, progression and arrhythmogenic causes and consequences of electrical and structural remodeling are also diverse and differ among the etiology of heart failure. In CHAPTER 5 we report on the differences in the arrhythmogenic substrate on cellular and molecular level, based on the etiology of heart failure by biopsies obtained during thoracic surgery of patients with a left ventricular assist device (LVAD).

Brugada syndrome (BrS) is characterized by a typical ECG pattern (coved-type ST-segment elevation and a negative T-wave in right precordial leads).<sup>49</sup> In Brugada syndrome controversy remains in defining the substrate, trigger and in some cases the modulating factors of this disease. The typical ST-segment elevation, as seen on the type I BrS-ECG, is incompletely understood and no consensus exists about its pathophysiological importance in relation to the substrate. Several hypotheses have been proposed but none with a conclusive answer.<sup>7, 50, 51</sup> One mechanism, the repolarization hypothesis, is based on transmural dispersion in repolarization of the right ventricle/right ventricular outflow tract (RV/RVOT). A second mechanism is based on activation delay and/or excitation failure in the subepicardium of the RV/RVOT (depolarization hypothesis). Whether activation delay in the RVOT by itself is sufficient to explain all phenotypic electrocardiographic Brugada syndrome changes is questioned. It has been suggested recently that ST-segment elevation may be caused by propagation failure due to current-to-load mismatch (caused by modulators) resulting excitation failure in the terminal epicardial part of the RVOT in the setting of the already present abnormal conduction in the structurally abnormal subepicardium of the RV/RVOT.<sup>52-54</sup> The latter has led to the proposal of a unifying hypothesis, explaining the electrocardiographic changes, the presence of structural abnormalities and the role of the sodium channel mutation. In CHAPTER 6 clinical observations supporting this newly postulated mechanism of the ST-segment elevation in the right precordial leads on the surface ECG in BrS are described.

The prognosis of myocardial infarction has improved over time, predominantly as a result of reperfusion therapy.<sup>37</sup> However, a significant number of patients develops heart failure and arrhythmias.<sup>55</sup> Besides the optimal medical treatment, e.g. life-style, drug therapy and devices, to change the course of nature in heart failure, regenerative medicine is a promising alternative.<sup>56-58</sup> Stem cell-based therapy has been investigated extensively *in vitro* as well as *in vivo* to improve cardiac function by directly influencing contractility or indirectly influencing remodeling and angiogenesis with contradicting results. Direct effects of the stem cells as well as indirect effects produced by paracrine factors may affect the cardiomyocytes.<sup>59</sup> The use of stromal –stem cell like- cells to repair the damaged myocardium and/or improve cardiac performance has proven to be promising. However, several studies suggest that stem cells can have a proarrhythmic effect by electrotonic coupling or by

paracrine effects.<sup>59, 60</sup> In CHAPTER 7 the direct and indirect effects of different types of stem cells on the host myocardium are investigated.

The final chapter of this thesis consists of a summary and discussion combining the different topics and future directions for investigation and treatment strategies are presented.



## REFERENCES

1. Wellens HJ, Schwartz PJ, Lindemans FW, Buxton AE, Goldberger JJ, Hohnloser SH, Huikuri HV, Kaab S, La Rovere MT, Malik M, Myerburg RJ, Simoons ML, Swedberg K, Tijssen J, Voors AA and Wilde AA. Risk stratification for sudden cardiac death: current status and challenges for the future. *Eur Heart J*. 2014;35:1642-51.
2. Priori SG, Blomstrom-Lundqvist C, Mazzanti A, Blom N, Borggrefe M, Camm J, Elliott PM, Fitzsimons D, Hatala R, Hindricks G, Kirchhof P, Kjeldsen K, Kuck KH, Hernandez-Madrid A, Nikolaou N, Norekval TM, Spaulding C, Van Veldhuisen DJ, Authors/Task Force M and Document R. 2015 ESC Guidelines for the management of patients with ventricular arrhythmias and the prevention of sudden cardiac death: The Task Force for the Management of Patients with Ventricular Arrhythmias and the Prevention of Sudden Cardiac Death of the European Society of Cardiology (ESC) Endorsed by: Association for European Paediatric and Congenital Cardiology (AEPC). *Eur Heart J*. 2015;36:2793-867.
3. Coumel P. The management of clinical arrhythmias. An overview on invasive versus non-invasive electrophysiology. *Eur Heart J*. 1987;8:92-9.
4. Zipes DP and Wellens HJ. Sudden cardiac death. *Circulation*. 1998;98:2334-51.
5. Myerburg RJ and Junttila MJ. Sudden cardiac death caused by coronary heart disease. *Circulation*. 2012;125:1043-52.
6. Schwartz PJ. The congenital long QT syndromes from genotype to phenotype: clinical implications. *Journal of internal medicine*. 2006;259:39-47.
7. Hoogendijk MG, Opthof T, Postema PG, Wilde AA, de Bakker JM and Coronel R. The Brugada ECG pattern: a marker of channelopathy, structural heart disease, or neither? Toward a unifying mechanism of the Brugada syndrome. *Circ Arrhythm Electrophysiol* 2010;3:283-290.
8. Priori SG, Wilde AA, Horie M, Cho Y, Behr ER, Berul C, Blom N, Brugada J, Chiang CE, Huikuri H, Kannankeril P, Krahn A, Leenhardt A, Moss A, Schwartz PJ, Shimizu W, Tomaselli G and Tracy C. Executive summary: HRS/EHRA/APHRS expert consensus statement on the diagnosis and management of patients with inherited primary arrhythmia syndromes. *Heart Rhythm*. 2013; 10:e85-108.
9. Moss AJ, Hall WJ, Cannom DS, Daubert JP, Higgins SL, Klein H, Levine JH, Saksena S, Waldo AL, Wilber D, Brown MW and Heo M. Improved survival with an implanted defibrillator in patients with coronary disease at high risk for ventricular arrhythmia. Multicenter Automatic Defibrillator Implantation Trial Investigators. *The New England journal of medicine*. 1996;335: 1933-40.
10. comparison of antiarrhythmic-drug therapy with implantable defibrillators in patients resuscitated from near-fatal ventricular arrhythmias. The Antiarrhythmics versus Implantable Defibrillators (AVID) Investigators. *The New England journal of medicine*. 1997;337:1576-1583.
11. Buxton AE, Lee KL, Fisher JD, Josephson ME, Prystowsky EN and Hafley G. A randomized study of the prevention of sudden death in patients with coronary artery disease. Multicenter Unsustained Tachycardia Trial Investigators. *The New England journal of medicine*. 1999;341: 1882-1890.
12. Connolly SJ, Gent M, Roberts RS, Dorian P, Roy D, Sheldon RS, Mitchell LB, Green MS, Klein GJ and O'Brien B. Canadian implantable defibrillator study (CIDS) : a randomized trial of the implantable cardioverter defibrillator against amiodarone. *Circulation*. 2000;101:1297-302.
13. Moss AJ, Zareba W, Hall WJ, Klein H, Wilber DJ, Cannom DS, Daubert JP, Higgins SL, Brown MW and Andrews ML. Prophylactic implantation of a defibrillator in patients with myocardial

- infarction and reduced ejection fraction. *The New England journal of medicine*. 2002;346:877-883.
14. Bardy GH, Lee KL, Mark DB, Poole JE, Packer DL, Boineau R, Domanski M, Troutman C, Anderson J, Johnson G, McNulty SE, Clapp-Channing N, Davidson-Ray LD, Fraulo ES, Fishbein DP, Luceri RM and Ip JH. Amiodarone or an implantable cardioverter-defibrillator for congestive heart failure. *The New England journal of medicine*. 2005;352:225-237.
  15. van Welsenes GH, van Rees JB, Borleffs CJ, Cannegieter SC, Bax JJ, van Erven L and Schalij MJ. Long-term follow-up of primary and secondary prevention implantable cardioverter defibrillator patients. *Europace : European pacing, arrhythmias, and cardiac electrophysiology : journal of the working groups on cardiac pacing, arrhythmias, and cardiac cellular electrophysiology of the European Society of Cardiology*. 2011;13:389-94.
  16. van Rees JB, de Bie MK, Thijssen J, Borleffs CJ, Schalij MJ and van EL. Implantation-related complications of implantable cardioverter-defibrillators and cardiac resynchronization therapy devices: a systematic review of randomized clinical trials. *J Am Coll Cardiol* 2011;58:995-1000.
  17. Daubert JP, Zareba W, Cannom DS, McNitt S, Rosero SZ, Wang P, Schuger C, Steinberg JS, Higgins SL, Wilber DJ, Klein H, Andrews ML, Hall WJ and Moss AJ. Inappropriate implantable cardioverter-defibrillator shocks in MADIT II: frequency, mechanisms, predictors, and survival impact. *J Am Coll Cardiol* 2008;51:1357-1365.
  18. Poole JE, Johnson GW, Hellkamp AS, Anderson J, Callans DJ, Raitt MH, Reddy RK, Marchlinski FE, Yee R, Guarnieri T, Talajic M, Wilber DJ, Fishbein DP, Packer DL, Mark DB, Lee KL and Bardy GH. Prognostic importance of defibrillator shocks in patients with heart failure. *The New England journal of medicine*. 2008;359:1009-1017.
  19. Bellenger NG, Burgess MI, Ray SG, Lahiri A, Coats AJ, Cleland JG and Pennell DJ. Comparison of left ventricular ejection fraction and volumes in heart failure by echocardiography, radionuclide ventriculography and cardiovascular magnetic resonance; are they interchangeable? *Eur Heart J*. 2000;21:1387-96.
  20. Cheitlin MD, Armstrong WF, Aurigemma GP, Beller GA, Bierman FZ, Davis JL, Douglas PS, Faxon DP, Gillam LD, Kimball TR, Kussmaul WG, Pearlman AS, Philbrick JT, Rakowski H and Thys DM. ACC/AHA/AASE 2003 guideline update for the clinical application of echocardiography--summary article: a report of the American College of Cardiology/American Heart Association Task Force on Practice Guidelines (ACC/AHA/AASE Committee to Update the 1997 Guidelines for the Clinical Application of Echocardiography). *J Am Coll Cardiol*. 2003;42:954-70.
  21. Hoffmann R, von Bardeleben S, ten Cate F, Borges AC, Kasprzak J, Firschke C, Lafitte S, Al-Saadi N, Kuntz-Hehner S, Engelhardt M, Becher H and Vanoverschelde JL. Assessment of systolic left ventricular function: a multi-centre comparison of cineventriculography, cardiac magnetic resonance imaging, unenhanced and contrast-enhanced echocardiography. *Eur Heart J*. 2005;26:607-16.
  22. Grothues F, Smith GC, Moon JC, Bellenger NG, Collins P, Klein HU and Pennell DJ. Comparison of interstudy reproducibility of cardiovascular magnetic resonance with two-dimensional echocardiography in normal subjects and in patients with heart failure or left ventricular hypertrophy. *Am J Cardiol*. 2002;90:29-34.
  23. Gold MR, Bloomfield DM, Anderson KP, El-Sherif NE, Wilber DJ, Groh WJ, Estes NA, 3rd, Kaufman ES, Greenberg ML and Rosenbaum DS. A comparison of T-wave alternans, signal averaged electrocardiography and programmed ventricular stimulation for arrhythmia risk stratification. *J Am Coll Cardiol*. 2000;36:2247-53.

24. Lahiri MK, Kannankeril PJ and Goldberger JJ. Assessment of autonomic function in cardiovascular disease: physiological basis and prognostic implications. *J Am Coll Cardiol* 2008;51: 1725-1733.
25. Chow T, Kereiakes DJ, Onufer J, Woelfel A, Gursoy S, Peterson BJ, Brown ML, Pu W, Benditt DG and Investigators MT. Does microvolt T-wave alternans testing predict ventricular tachyarrhythmias in patients with ischemic cardiomyopathy and prophylactic defibrillators? The MASTER (Microvolt T Wave Alternans Testing for Risk Stratification of Post-Myocardial Infarction Patients) trial. *J Am Coll Cardiol*. 2008;52:1607-15.
26. La Rovere MT, Pinna GD, Hohnloser SH, Marcus FI, Mortara A, Nohara R, Bigger JT, Jr., Camm AJ and Schwartz PJ. Baroreflex sensitivity and heart rate variability in the identification of patients at risk for life-threatening arrhythmias: implications for clinical trials. *Circulation*. 2001; 103:2072-2077.
27. Fauchier L, Babuty D, Cosnay P and Fauchier JP. Prognostic value of heart rate variability for sudden death and major arrhythmic events in patients with idiopathic dilated cardiomyopathy. *J Am Coll Cardiol* 1999;33:1203-1207.
28. Petretta M, Pirozzi F, Sasso L, Paglia A and Bonaduce D. Review and metaanalysis of the frequency of familial dilated cardiomyopathy. *Am J Cardiol*. 2011;108:1171-6.
29. Gersh BJ, Maron BJ, Bonow RO, Dearani JA, Fifer MA, Link MS, Naidu SS, Nishimura RA, Ommen SR, Rakowski H, Seidman CE, Towbin JA, Udelson JE, Yancy CW, American College of Cardiology Foundation/American Heart Association Task Force on Practice G, American Association for Thoracic S, American Society of E, American Society of Nuclear C, Heart Failure Society of A, Heart Rhythm S, Society for Cardiovascular A, Interventions and Society of Thoracic S. 2011 ACCF/AHA guideline for the diagnosis and treatment of hypertrophic cardiomyopathy: executive summary: a report of the American College of Cardiology Foundation/American Heart Association Task Force on Practice Guidelines. *Circulation*. 2011;124:2761-96.
30. van der Zwaag PA, van Rijsingen IA, Asimaki A, Jongbloed JD, van Veldhuisen DJ, Wiesfeld AC, Cox MG, van Lochem LT, de Boer RA, Hofstra RM, Christiaans I, van Spaendonck-Zwarts KY, Lekanne dit Depez RH, Judge DP, Calkins H, Suurmeijer AJ, Hauer RN, Saffitz JE, Wilde AA, van den Berg MP and van Tintelen JP. Phospholamban R14del mutation in patients diagnosed with dilated cardiomyopathy or arrhythmogenic right ventricular cardiomyopathy: evidence supporting the concept of arrhythmogenic cardiomyopathy. *Eur J Heart Fail*. 2012;14:1199-207.
31. MacLennan DH and Kranias EG. Phospholamban: a crucial regulator of cardiac contractility. *Nature reviews Molecular cell biology*. 2003;4:566-77.
32. van Rijsingen IA, van der Zwaag PA, Groeneweg JA, Nannenberg EA, Jongbloed JD, Zwinderman AH, Pinto YM, Dit Depez RH, Post JG, Tan HL, de Boer RA, Hauer RN, Christiaans I, van den Berg MP, van Tintelen JP and Wilde AA. Outcome in phospholamban R14del carriers: results of a large multicentre cohort study. *Circ Cardiovasc Genet*. 2014;7:455-65.
33. Posch MG, Perrot A, Geier C, Boldt LH, Schmidt G, Lehmkuhl HB, Hetzer R, Dietz R, Gutberlet M, Haverkamp W and Ozcelik C. Genetic deletion of arginine 14 in phospholamban causes dilated cardiomyopathy with attenuated electrocardiographic R amplitudes. *Heart Rhythm*. 2009;6:480-6.
34. Alders M, Koopmann TT, Christiaans I, Postema PG, Beekman L, Tanck MW, Zeppenfeld K, Loh P, Koch KT, Demolombe S, Mannens MM, Bezzina CR and Wilde AA. Haplotype-sharing analysis implicates chromosome 7q36 harboring DPP6 in familial idiopathic ventricular fibrillation. *Am J Hum Genet* 2009;84:468-476.

35. Postema PG, Christiaans I, Hofman N, Alders M, Koopmann TT, Bezzina CR, Loh P, Zeppenfeld K, Volders PG and Wilde AA. Founder mutations in the Netherlands: familial idiopathic ventricular fibrillation and DPP6. *Neth Heart J* 2011;19:290-296.
36. Benito B and Josephson ME. Ventricular tachycardia in coronary artery disease. *Rev Esp Cardiol (Engl Ed)*. 2012;65:939-55.
37. Mozaffarian D, Benjamin EJ, Go AS, Arnett DK, Blaha MJ, Cushman M, Das SR, de Ferranti S, Despres JP, Fullerton HJ, Howard VJ, Huffman MD, Isasi CR, Jimenez MC, Judd SE, Kissela BM, Lichtman JH, Lisabeth LD, Liu S, Mackey RH, Magid DJ, McGuire DK, Mohler ER, 3rd, Moy CS, Muntner P, Mussolino ME, Nasir K, Neumar RW, Nichol G, Palaniappan L, Pandey DK, Reeves MJ, Rodriguez CJ, Rosamond W, Sorlie PD, Stein J, Towfighi A, Turan TN, Virani SS, Woo D, Yeh RW, Turner MB, American Heart Association Statistics C and Stroke Statistics S. Heart Disease and Stroke Statistics-2016 Update: A Report From the American Heart Association. *Circulation*. 2016;133:e38-e360.
38. Weber KT, Sun Y and Katwa LC. Wound healing following myocardial infarction. *Clin Cardiol*. 1996;19:447-55.
39. de Bakker JM, van Capelle FJ, Janse MJ, Tasseron S, Vermeulen JT, de JN and Lahpor JR. Slow conduction in the infarcted human heart. 'Zigzag' course of activation. *Circulation*. 1993;88: 915-926.
40. Wilders R, Wagner MB, Golod DA, Kumar R, Wang YG, Goolsby WN, Joyner RW and Jongsma HJ. Effects of anisotropy on the development of cardiac arrhythmias associated with focal activity. *Pflugers Archiv : European journal of physiology*. 2000;441:301-12.
41. Kawara T, Derksen R, de Groot JR, Coronel R, Tasseron S, Linnenbank AC, Hauer RN, Kirkels H, Janse MJ and de Bakker JM. Activation delay after premature stimulation in chronically diseased human myocardium relates to the architecture of interstitial fibrosis. *Circulation*. 2001;104:3069-3075.
42. Derksen R, van Rijen HV, Wilders R, Tasseron S, Hauer RN, Rutten WL and de Bakker JM. Tissue discontinuities affect conduction velocity restitution: a mechanism by which structural barriers may promote wave break. *Circulation*. 2003;108:882-8.
43. Kitamura H, Ohnishi Y, Yoshida A, Okajima K, Azumi H, Ishida A, Galeano EJ, Kubo S, Hayashi Y, Itoh H and Yokoyama M. Heterogeneous loss of connexin43 protein in nonischemic dilated cardiomyopathy with ventricular tachycardia. *J Cardiovasc Electrophysiol*. 2002;13:865-70.
44. Poelzing S and Rosenbaum DS. Altered connexin43 expression produces arrhythmia substrate in heart failure. *Am J Physiol Heart Circ Physiol*. 2004;287:H1762-70.
45. Wiegerinck RF, van Veen TA, Belterman CN, Schumacher CA, Noorman M, de Bakker JM and Coronel R. Transmural dispersion of refractoriness and conduction velocity is associated with heterogeneously reduced connexin43 in a rabbit model of heart failure. *Heart Rhythm*. 2008; 5:1178-85.
46. Boulaksil M, Winckels SK, Engelen MA, Stein M, van Veen TA, Jansen JA, Linnenbank AC, Bierhuizen MF, Groenewegen WA, van Oosterhout MF, Kirkels JH, de JN, Varro A, Vos MA, de Bakker JM and van Rijen HV. Heterogeneous Connexin43 distribution in heart failure is associated with dispersed conduction and enhanced susceptibility to ventricular arrhythmias. *Eur J Heart Fail* 2010;12:913-921.
47. Pogwizd SM, Hoyt RH, Saffitz JE, Corr PB, Cox JL and Cain ME. Reentrant and focal mechanisms underlying ventricular tachycardia in the human heart. *Circulation*. 1992;86:1872-87.

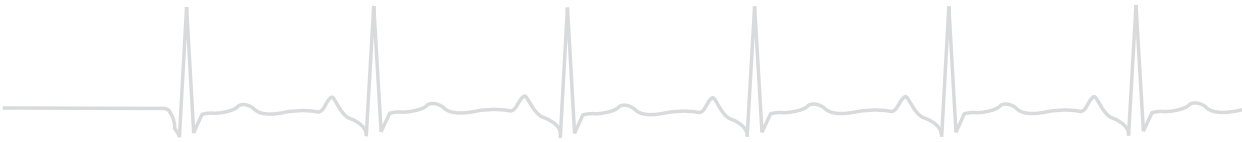
48. Pogwizd SM, McKenzie JP and Cain ME. Mechanisms underlying spontaneous and induced ventricular arrhythmias in patients with idiopathic dilated cardiomyopathy. *Circulation*. 1998; 98:2404-14.
49. Brugada P and Brugada J. Right bundle branch block, persistent ST segment elevation and sudden cardiac death: a distinct clinical and electrocardiographic syndrome. A multicenter report. *J Am Coll Cardiol* 1992;20:1391-1396.
50. Meregalli PG, Wilde AA and Tan HL. Pathophysiological mechanisms of Brugada syndrome: depolarization disorder, repolarization disorder, or more? *Cardiovasc Res* 2005;67:367-378.
51. Wilde AA, Postema PG, Di Diego JM, Viskin S, Morita H, Fish JM and Antzelevitch C. The pathophysiological mechanism underlying Brugada syndrome: depolarization versus repolarization. *J Mol Cell Cardiol* 2010;49:543-553.
52. Frustaci A, Priori SG, Pieroni M, Chimenti C, Napolitano C, Rivolta I, Sanna T, Bellocci F and Russo MA. Cardiac histological substrate in patients with clinical phenotype of Brugada syndrome. *Circulation*. 2005;112:3680-3687.
53. Coronel R, Casini S, Koopmann TT, Wilms-Schopman FJ, Verkerk AO, de Groot JR, Bhuiyan Z, Bezzina CR, Veldkamp MW, Linnenbank AC, van der Wal AC, Tan HL, Brugada P, Wilde AA and de Bakker JM. Right ventricular fibrosis and conduction delay in a patient with clinical signs of Brugada syndrome: a combined electrophysiological, genetic, histopathologic, and computational study. *Circulation*. 2005;112:2769-2777.
54. Hoogendijk MG, Potse M, Linnenbank AC, Verkerk AO, den Ruijter HM, van Amersfoort SC, Klaver EC, Beekman L, Bezzina CR, Postema PG, Tan HL, Reimer AG, van der Wal AC, Ten Harkel AD, Dalinghaus M, Vinet A, Wilde AA, de Bakker JM and Coronel R. Mechanism of right precordial ST-segment elevation in structural heart disease: excitation failure by current-to-load mismatch. *Heart Rhythm* 2010;7:238-248.
55. Go AS, Mozaffarian D, Roger VL, Benjamin EJ, Berry JD, Blaha MJ, Dai SF, Ford ES, Fox CS, Franco S, Fullerton HJ, Gillespie C, Hailpern SM, Heit JA, Howard VJ, Huffman MD, Judd SE, Kissela BM, Kittner SJ, Lackland DT, Lichtman JH, Lisabeth LD, Mackey RH, Magid DJ, Marcus GM, Marelli A, Matchar DB, McGuire DK, Mohler ER, Moy CS, Mussolino ME, Neumar RW, Nichol G, Pandey DK, Paynter NP, Reeves MJ, Sorlie PD, Stein J, Towfighi A, Turan TN, Virani SS, Wong ND, Woo D, Turner MB, Stat AHAS and Subcomm SS. Executive Summary: Heart Disease and Stroke Statistics-2014 Update A Report From the American Heart Association. *Circulation*. 2014;129:399-410.
56. Wollert KC, Meyer GP, Lotz J, Ringes-Lichtenberg S, Lippolt P, Breidenbach C, Fichtner S, Korte T, Hornig B, Messinger D, Arseniev L, Hertenstein B, Ganser A and Drexler H. Intracoronary autologous bone-marrow cell transfer after myocardial infarction: the BOOST randomised controlled clinical trial. *Lancet*. 2004;364:141-8.
57. Bolli R, Chugh AR, D'Amario D, Loughran JH, Stoddard MF, Ikram S, Beache GM, Wagner SG, Leri A, Hosoda T, Sanada F, Elmore JB, Goichberg P, Cappetta D, Solankhi NK, Fahsah I, Rokosh DG, Slaughter MS, Kajstura J and Anversa P. Cardiac stem cells in patients with ischaemic cardiomyopathy (SCIPIO): initial results of a randomised phase 1 trial. *Lancet*. 2011;378:1847-1857.
58. Makkar RR, Smith RR, Cheng K, Malliaras K, Thomson LE, Berman D, Czer LS, Marban L, Mendizabal A, Johnston PV, Russell SD, Schuleri KH, Lardo AC, Gerstenblith G and Marban E. Intracoronary cardiosphere-derived cells for heart regeneration after myocardial infarction (CADUCEUS): a prospective, randomised phase 1 trial. *Lancet*. 2012;379:895-904.

59. Askar SF, Ramkisoensing AA, Atsma DE, SchaliJ MJ, de Vries AA and Pijnappels DA. Engraftment patterns of human adult mesenchymal stem cells expose electrotonic and paracrine proarrhythmic mechanisms in myocardial cell cultures. *Circ Arrhythm Electrophysiol* 2013;6: 380-391.
60. Chang MG, Tung L, Sekar RB, Chang CY, Cysyk J, Dong P, Marban E and Abraham MR. Proarrhythmic potential of mesenchymal stem cell transplantation revealed in an in vitro coculture model. *Circulation*. 2006;113:1832-1841.



# **PART I**

## **Markers of Vulnerability for Ventricular Arrhythmias**





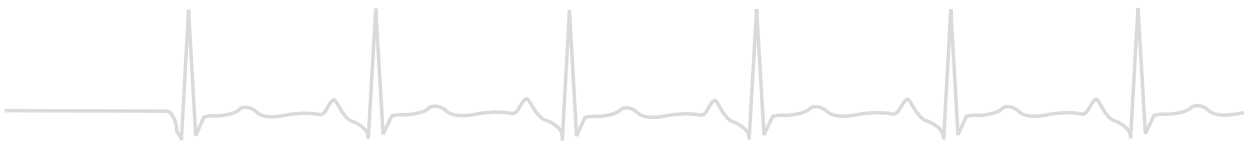


# CHAPTER 2

## **Value of serial heart rate variability measurement for prediction of appropriate ICD discharge in patients with heart failure**

Judith N. ten Sande, Peter Damman, Jan G.P. Tijssen, Joris R. de Groot, Reinoud E. Knops,  
Arthur A.M. Wilde, Pascal F.H.M. van Dessel

*Journal of Cardiovascular Electrophysiology 2014 Jan;25(1):60-5*



## ABSTRACT

### Introduction

Decreased heart rate variability (HRV) is associated with adverse outcomes in patients with heart failure. Our objective was to examine whether decreased HRV predicts appropriate implantable cardioverter defibrillator (ICD) shocks.

### Methods and Results

In 105 patients with a Boston Scientific Contak Renewal, Cognis or Energen device implanted for either primary (73.3%) or secondary prevention (26.7%), time domain HRV variables standard deviation of averages of normal beat-to-beat interval (SDANN) and footprint percentage (FFP) were collected at baseline and during follow-up. In case of appropriate shock, HRV before shock was assessed. Using time-dependent Cox regression models, the relation between median-based dichotomized SDANN or FFP and appropriate shock was investigated. Baseline characteristics between patients with or without shocks were similar, with exception of secondary prevention patients using more often antiarrhythmic drugs. During follow-up (median 451, IQR 202–1,460 days), appropriate shocks occurred in 20 (19%) patients. SDANN and FFP did not differ significantly at baseline between patients with or without shocks (respectively,  $P = 0.18$  and  $P = 0.78$ ). However, time-dependent Cox regression analysis showed a trend that patients were at lower risk for appropriate shock (SDANN: HR 0.43, 95% CI [0.18–1.05],  $P = 0.06$  and FFP: HR 0.49, 95% CI [0.20–1.20],  $P = 0.12$ ) when HRV values were above median baseline value during follow-up.

### Conclusions

These results imply that HRV could be an independent predictor for appropriate shocks. Therefore, low HRV could be of additional use in predicting imminent appropriate shocks and could possibly guide concomitant medical therapy.

## INTRODUCTION

The risk of sudden cardiac death (SCD) is increased among patients with congestive heart failure (CHF). Major trials have shown that the implantable cardioverter defibrillator (ICD) reduces mortality in patients with chronic heart failure<sup>1-5</sup>. Unfortunately, implantation of an ICD is not without risks<sup>6</sup> and some trials found an association between shocks and increased mortality<sup>7, 8</sup>.

Several studies have evaluated possible new indicators of SCD risk including autonomic cardiac activity, heart rate turbulence, microvolt T-wave alternans and programmed electrical stimulation<sup>9-14</sup> but although these tests appear to have reasonable negative predictive value, their role in predicting appropriate ICD therapy is less well established. Even less is known whether changes in these parameters might predict appropriate ICD therapy in people who already had an ICD implanted.

Autonomic activity in patients with CHF is often impaired and dysfunction can be measured by analysis of heart rate variability (HRV). HRV is assessed by continuous measurement of beat-to-beat intervals which are influenced by the balance in parasympathetic and sympathetic tone and varying activity. HRV can be expressed as long term HRV (analysis of the total electrocardiographic recording, usually 24hours) or as short-term HRV (measuring time usually 5 minutes)<sup>15</sup>. In patients with CHF chronic enhanced activation of the adrenergic system - which is thought to facilitate the occurrence of life threatening arrhythmias - can be made apparent by decreased long-term HRV.

There is compelling evidence that impaired HRV plays an important role in the pathophysiology of SCD<sup>16, 17</sup>. HRV has also been found to be of value in predicting adverse outcome in cardiovascular diseases<sup>18-21</sup>. A recent study by Battipaglia et al.<sup>22</sup> showed that HRV parameters in heart failure patients were significantly depressed following ICD shocks and this again suggests an association between HRV and the occurrence of life threatening ventricular tachyarrhythmias.

We hypothesized that HRV is a potential predictor of risk for ventricular arrhythmias, and therefore we analyzed HRV data at implantation, prior to ICD discharge and during follow-up as well as the course of events during follow-up in patients with heart failure. Aim of this study was to investigate whether decreased HRV precedes subsequent occurrence of life threatening ventricular tachyarrhythmia.

## METHODS

### Source population

Between July 2002 and June 2012 all ICD recipients in our institution, aged 18 years or older, who (1) were referred for primary prevention ICD implantation, secondary prevention

or cardiac resynchronization therapy with defibrillator function, and (2) received a Boston Scientific® Contak Renewal, Cognis or Energen series ICD, with or without left ventricular lead were included in the study. Patients were not specifically selected to receive Boston Scientific devices. All primary prevention ICDs were programmed uniformly, resembling ICD settings published recently by Moss et al.<sup>23</sup>, including high VF cut-off rates and extended detection duration. Individual programming decisions were left to the discretion of the attending physicians. Patient and device data were stored in a research electronic medical record database. The institutional review board gave a waiver for obtaining informed consent for this study.

### ICD parameters

Boston Scientific® Contak Renewal, Cognis or Energen series ICD are capable of automatic assessment of HRV parameters and HRV data are automatically stored in the device. During device interrogation the HRV values of the preceding 24 hour can be obtained. HRV parameters can only be obtained by the device when ventricular activation follows intrinsic atrial activation for at least 67% of the 24-hour measurement. Therefore HRV cannot be obtained when there is frequent ectopic activity, atrial fibrillation or when the device is programmed to rate-responsive tracking modes. These limits and other aspects of the HRV analysis algorithm in the device are preset by Boston Scientific® and are nonprogrammable. We obtained the first available HRV parameters after implantation (baseline HRV with a maximum of 180 days between implantation and first available HRV) and all subsequent HRV parameters retrieved during device interrogation until latest available follow-up in all patients. If the patient experienced appropriate shocks, latest HRV parameters before shock (with a maximum of 180 days between measurement and shock) were retrieved. We collected the following long-term time domain variables; standard deviation of the averages of normal beat-to-beat intervals in the 288 five-minute segments of a day (SDANN) and footprint percentage (FPP: distribution of the R-R variability versus heart rate). These parameters were routinely available at each ICD interrogation if HRV was successfully measured and represent the most recent HRV measured in the preceding 24 hours. Recorded episodes of ICD therapies were also collected for analysis.

### Study population

For purpose of this study, we retrieved specific data including drug therapy from the patients' medical files. Patients with at least 2 HRV measurements (baseline and during follow-up) minimally 7 days apart were considered eligible for the study. Patients in whom HRV analysis by the device was technically not feasible, e.g. due to atrial fibrillation or because of frequent premature atrial or ventricular complexes or sensor driven atrial rate, were excluded.

In total we selected 182 patients who received an implantable device capable of assessing HRV. Sixty-seven patients were excluded because HRV could not be obtained mainly because of sensor driven atrial rates or atrial fibrillation. Five patients had more than 180 days between implantation and first measured or last available HRV before shock and these patients were excluded as well. Finally, five patients had less than 7 days between first and last measured HRV and were therefore not eligible for the study. In total, 105 patients with recorded HRV data were included in the study.

### Clinical endpoints

The primary endpoint was the occurrence of appropriate ICD shocks for episodes of sustained ventricular tachycardia (VT) or ventricular fibrillation (VF) related to the most recent HRV before shock. To prevent analysis of possible appropriate but unnecessary therapy, anti tachycardia pacing (ATP) *only* was not considered as an endpoint since ATP might also have been given for non-sustained ventricular tachycardia, which might have terminated spontaneously without ICD intervention as well. Episodes where ATP deteriorated VT into VF or where ATP accelerated VT into the VF zone necessitating shock therapy were considered as appropriate shock. All ICD episodes including electrograms (EGMs) retrieved by ICD interrogation were evaluated for appropriateness of therapy by two independent investigators.

### Statistical analysis

ROC analysis was performed to determine cut-off values of HRV parameters, which appeared to be the median value for both parameters. Baseline HRV values were dichotomized based on median value and their relation with appropriate shocks was investigated. Cumulative event rates were estimated using the Kaplan Meier method and compared with the log-rank test. Follow-up was calculated from the date of the first measured HRV and was censored on the date of last available HRV or 1460 days (4 years) whichever came first.

Because multiple HRV measurements with different time intervals per patient were available we performed a time-dependent Cox proportional hazard analysis to evaluate the dynamics of HRV parameters over time and their relation with appropriate shocks. Both univariable (including HRV), as well as multivariable adjusted Cox analyses were performed. Adjustments were made for independent predictors for appropriate shock that were identified as follows: First, baseline variables with a P value <0.10 in univariable regression were simultaneously entered in the multivariable model. Variables with a P value above 0.10 in multivariable regression analysis were excluded from the model.

Continuous variables are presented as mean with standard deviation (SD) and compared with the unpaired t-test in case of a normal distribution, and presented as the median with inter-quartile range (IQR) in case of a skewed distribution. Categorical variables were presented as frequencies with percentages and analyzed by the Fisher exact test.

## RESULTS

### Baseline measurements

During follow-up (median 451; IQR 202-1460 days), appropriate shocks occurred in 20 (19%) of 105 patients of whom 6 (5.7%) of 105 patients had multiple shocks. Of the 20 appropriate shocks, 7 (35%) shocks were preceded by ATP therapy. Five (71.4%) of these ATP therapies accelerated the VT or deteriorated the VT to VF necessitating a defibrillation shock. There were no differences in HRV values in this small subset of patients where ATP therapy influenced the arrhythmia or not. Inappropriate shocks occurred in 5 of 105 (4.8%) patients. Six of 105 patients (5.7%) received ATP only for termination of VT and no other therapy during follow-up. Seven of 105 (6.7%) patients received also ATP therapy only, but experienced later during follow-up an episode requiring ATP and shock or shock only. No differences in HRV values were seen whether inappropriate shocks or successful ATP were considered as grouping variable. Median time from implantation to first measured HRV was 2 (IQR 2-3) days. Median time from last available HRV before shock to shock occurrence was 17 (IQR 4-55) days. HRV at baseline did not differ significantly between patients with or without shocks: SDANN  $64 \pm 21$  vs.  $73 \pm 27$  ms;  $P=0.18$  and FPP  $31 \pm 12$  vs.  $32 \pm 11$  %;  $P=0.78$ . LVEF, QRS width, renal function and medication use were similar in patients with or without shocks. The only significant differences in baseline characteristics between patients were type of prevention (80% primary prevention in patients without shocks vs. 45% in patients with shocks) and antiarrhythmic drug (AAD) use (Table 1). AAD were more frequently used in patients with shocks and those who received an ICD for secondary prevention. Patients received only class III AAD (amiodarone (78.9%) or sotalol (21.1%)), mostly because of prior ventricular arrhythmias (79%). All patients were intentionally treated with optimal heart failure medication according the current heart failure guidelines.

### Primary endpoint

Median baseline SDANN was 68ms (IQR 54-87) for the entire population. Event free survival was 79% in patients with a SDANN above 68ms at baseline versus 61% in patients with a SDANN below 68ms (log rank  $P=0.10$ ) (Figure 1). Median baseline FPP was 31% (IQR 24-38) for the entire population. Event free survival was 75% in patients with FPP above the median at baseline versus 64% in patients with a FPP below the median (log rank  $P=0.39$ ) (Figure 1).

In time-dependent Cox analysis, SDANN above median value during follow-up was associated with a lower risk of appropriate ICD discharge (HR 0.43 (0.18–1.05)  $P=0.06$ ) (Table 2). Time-dependent Cox analysis showed that FPP above the baseline median value during follow-up was associated with a reduced incidence of appropriate shocks (HR 0.49 95%CI (0.20 – 1.20)  $P=0.12$ ). Adjusting for possible other baseline predictors (type of prevention) only marginally affected hazard ratios for both SDANN as well as FPP (Table 2).

Table 1. Baseline characteristics.

	Patients with shocks (n=20)	Patients without shocks (n=85)	All patients (n=105)	P value	Univariate HR 95%CI	Multivariate HR 95%CI P value
Age in years	68±10	69±10	69±10	0.63		
Male	13 (65%)	59 (69.4%)	72 (68.6%)	0.79		
Etiology heart failure						
Ischemic	14 (70%)	38 (44.7%)	52 (49.5%)	0.05	0.4 (0.12–0.99)	0.5 (0.17–1.33) P=0.16
Non-ischemic	6 (30%)	47 (55.3%)	53 (50.5%)			
NYHA (New York Heart Association class)				0.79		
I/II	6 (31.6%)	31 (36.5%)	37 (35.2%)			
III	13 (68.4%)	52 (61.2%)	65 (61.9%)			
LVEF before implantation in %	20 (15–26)	20 (15–25)	20 (15–25)	0.68		
Primary prevention	9 (45%)	68 (80%)	77 (73.3%)	<0.01	4.9 (1.75–13.68)	3.6 (1.37–9.39) P<0.01
CRT	19 (95%)	82 (96.5%)	101 (96.2%)	0.58		
QRS width in ms	168±27	162±26	163±26	0.38		
Creatinin in µmol/L	98±24	103±32	102±30	0.50		
<b>HRV parameters</b>						
SDANN in ms	64±21	73±27	72±26	0.18		
FPP in %	31±12	32±11	31±11	0.78		
<b>Medication</b>						
AAD	7 (35%)	12 (14.1%)	19 (18.1%)	0.05	3.3 (1.09–9.72)	1.1 (0.36–3.56) P=0.83
Diuretics	19 (95%)	70 (82.4%)	89 (84.8%)	0.23		
Digoxin	4 (20%)	10 (11.8%)	14 (13.3%)	0.46		
ACE inhibitor/ARB	18 (90%)	79 (92.9%)	97 (92.4%)	1.00		



Table 1. Baseline characteristics. (continued)

	Patients with shocks (n=20)	Patients without shocks (n=85)	All patients (n=105)	P value	Univariate HR 95%CI	Multivariate HR 95%CI P value
Calcium antagonist	3 (15%)	8 (9.4%)	11 (10.5%)	0.44		
Beta-blocker	14 (70%)	68 (80%)	82 (78.1%)	0.37		
Spironolactone/epplerenone	9 (45%)	37 (43.5%)	46 (43.8%)	1.00		
Anticoagulant	13 (65%)	36 (42.4%)	49 (46.7%)	0.08	2.5 (0.92–6.79)	1.7 (0.61–4.67) P=0.31
Antiplatelet therapy	6 (30%)	32 (37.6%)	38 (36.2%)	0.61		

AAD: anti arrhythmic drugs, ARB: angiotensin receptor blocker, CI: confidence interval, CRT: cardiac resynchronization therapy, FPP: footprint percentage, HF: heart failure, HR: hazard ratio, LVEF: left ventricular ejection fraction, SDANN: standard deviation of the averages of normal beat-to-beat intervals in the 288 five-minutes segments of a day. Data are presented as mean with standard deviation or as median with inter-quartile range or as frequencies with percentages.

**Table 2.** Four-year risk of appropriate shock according to the median values of SDANN and FPP.

	Hazard ratio (95%CI)	P value
<b>SDANN</b>		
Baseline SDANN lower than 68ms	Reference	
Baseline SDANN higher than 68ms	0.47 (0.19–1.17)	0.10
Time-dependent Cox model <i>unadjusted</i>		
SDANN lower than 68ms	Reference	
SDANN higher than 68ms	0.43 (0.18–1.05)	0.06
Time-dependent Cox model <i>adjusted</i> *		
SDANN lower than 68ms	Reference	
SDANN higher than 68ms	0.44 (0.18–1.10)	0.07
<b>FPP</b>		
Baseline FPP lower than 31%	Reference	
Baseline FPP higher than 31%	0.68 (0.28–1.64)	0.39
Time-dependent Cox model <i>unadjusted</i>		
FPP lower than 31%	Reference	
FPP higher than 31%	0.49 (0.20–1.20)	0.12
Time-dependent Cox model <i>adjusted</i> *		
FPP lower than 31%	Reference	
FPP higher than 31%	0.50 (0.21–1.21)	0.13

\* Type of prevention. Univariate and time-dependent Cox analysis unadjusted and adjusted for identified baseline characteristics. CI: confidence interval, ms: milliseconds.

## DISCUSSION

Our current study shows that HRV, especially SDANN, is low prior to appropriate shock. Low HRV values can therefore be considered to be a possible independent predictor for appropriate ICD therapy, even after adjustments for type of prevention which was the only identified other baseline predictor. This can be explained by the equal distribution of indication for device implantation in patients with HRV indices above or below median baseline value. At baseline, there was no significant difference in HRV parameters between the patients with or without event free survival but time-dependent Cox analysis showed a trend between decrease of SDANN during follow-up and subsequent appropriate ICD discharge. These results suggest that in patients with CHF decrease of HRV during follow-up increases risk of appropriate device discharge.

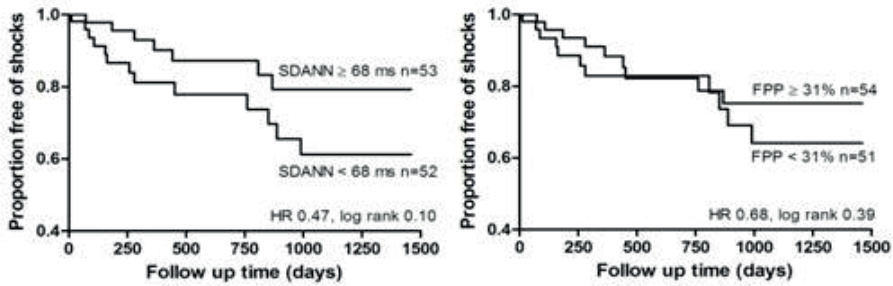


Figure 1. Kaplan-Meier cumulative proportional freedom of appropriate shocks for SDANN (left) and FPP at baseline below and above median value. Zero time point is the first measured HRV parameter after device implantation.

### Previous studies

A cross sectional study conducted by Battipaglia et al.<sup>22</sup> reported that depressed HRV indices were observed significantly more often following appropriate ICD discharge in the preceding six months in 42 patients with either idiopathic or ischemic dilated cardiomyopathy and ICD implantation for either primary or secondary prevention. They stated that SDANN was the most significant time domain variable. These findings are in agreement with our study. In contrast to our study, no conclusions can be drawn in their study about the temporal relationship between HRV and ICD therapy because HRV parameters were only obtained after appropriate device therapy. Our study demonstrates however that low HRV tends to precede appropriate ICD therapy.

Kleiger et al.<sup>18</sup> were the first to show the validity of HRV parameters as correlate of autonomic cardiac regulation. They demonstrated that decreased HRV after myocardial infarction predicts all-cause mortality. Several other studies followed to analyze the role of HRV in different cardiovascular diseases with respect to cardiovascular mortality and SCD<sup>24, 25</sup>. Among other studies, the UK-Heart trial<sup>26</sup> analyzed the predictive value of HRV measured by 24-hour ambulatory ECG monitoring in a prospective study of 433 outpatients with NYHA class I to III and LVEF<45%. They demonstrated that severely reduced HRV was an independent predictor of death.

Similar to our study, Hohnloser et al.<sup>27</sup> reported a prospective observational study of 137 non-ischemic dilated cardiomyopathy patients in whom HRV at baseline did not predict ventricular tachyarrhythmic events during a mean follow-up of 14 months. This study is still consistent with our results where HRV was also not significantly different at baseline but was depressed over time in patients who experienced appropriate shocks. These findings support our view that HRV should not be measured at baseline only, but should be measured more frequently to evaluate the course of arrhythmic risk over time.

The relationship of HRV, obtained by integrated algorithms in CRT-D devices as in our study, and the risk of mortality was analyzed earlier<sup>28-30</sup>. Gilliam III et al.<sup>30</sup> reported that HRV

indices at baseline such as SDANN and FPP retrieved from the device were of predictive value with respect to all-cause mortality in a prospective cohort study of 842 patients with NYHA class III and IV heart failure selected for CRT-D implantation. They showed that a higher SDANN and FPP were significantly associated with a lower risk of death. Furthermore they state that patients with low HRV at baseline and small changes in HRV during follow-up tended to have the highest risk for death. Whether changes in HRV during follow-up predict appropriate ICD therapy cannot be concluded from that study. However, these results corroborate our findings that changes in HRV are associated with altered risk of appropriate shock and therefore the risk of SCD in patients CHF.

### Clinical implication

CHF is a progressive disease and patients with impaired HRV could be in more advanced heart failure<sup>31, 32</sup> and therefore at higher risk for appropriate shocks. Although our data only showed a trend between HRV and appropriate ICD shocks, these data still suggest that monitoring HRV dynamics may identify patients at risk for appropriate shocks and may warrant changes in anti-arrhythmic, heart failure therapy or intensity of outpatient follow-up to prevent appropriate shock occurrence. Also anecdotically up to now, autonomic modulation has been shown to have potential benefit in reducing the number of ventricular arrhythmia episodes triggering ICD therapy<sup>32</sup>. HRV data can easily be obtained during ICD interrogation. These results could plea for routinely remote monitoring of HRV on a regular basis.

### Limitations

HRV measurements were available from irregular intervals determined by timing of outpatient clinic visits and subsequent ICD interrogation. This may have led to underestimation of the effect of the HRV parameters. Nevertheless we found a suggestive association between low HRV and subsequent appropriate shocks. Unfortunately, we could not perform valid subgroup analysis with respect to different ICD therapies due to the limited number of patients. However, separate analyses did not reveal any differences between HRV parameters among different ICD therapy groups. Baseline characteristics between patients with or without shocks were similar, with exception of implantation indication and AAD use. However, adjustment for device indication only marginally affected the hazard ratio and the equal distribution of device indication and AAD use in patients with values above or below median for both indices further suggests a limited influence of AAD on HRV parameters. Finally, as a result of the number of patients and the small amount of events these data should be confirmed in a larger prospective population.

## CONCLUSION

These results imply that HRV could be an independent predictor for imminent appropriate shocks since indices are low prior to appropriate shock, but larger studies are necessary to corroborate our data. Low HRV may identify patients at risk for appropriate ICD therapy. Preserved HRV tends to be associated with a reduced risk of appropriate therapy. Therefore, HRV may be of additional use in predicting risk for appropriate shocks.

## REFERENCES

1. Moss AJ, Hall WJ, Cannom DS, Daubert JP, Higgins SL, Klein H, Levine JH, Saksena S, Waldo AL, Wilber D, Brown MW and Heo M. Improved survival with an implanted defibrillator in patients with coronary disease at high risk for ventricular arrhythmia. Multicenter Automatic Defibrillator Implantation Trial Investigators. *The New England journal of medicine*. 1996;335: 1933-40.
2. Buxton AE, Lee KL, Fisher JD, Josephson ME, Prystowsky EN and Hafley G. A randomized study of the prevention of sudden death in patients with coronary artery disease. Multicenter Unsustained Tachycardia Trial Investigators. *The New England journal of medicine*. 1999;341: 1882-1890.
3. Moss AJ, Zareba W, Hall WJ, Klein H, Wilber DJ, Cannom DS, Daubert JP, Higgins SL, Brown MW and Andrews ML. Prophylactic implantation of a defibrillator in patients with myocardial infarction and reduced ejection fraction. *The New England journal of medicine*. 2002;346: 877-883.
4. Kadish A, Dyer A, Daubert JP, Quigg R, Estes NA, Anderson KP, Calkins H, Hoch D, Goldberger J, Shalaby A, Sanders WE, Schaechter A and Levine JH. Prophylactic defibrillator implantation in patients with nonischemic dilated cardiomyopathy. *The New England journal of medicine*. 2004;350:2151-2158.
5. Bardy GH, Lee KL, Mark DB, Poole JE, Packer DL, Boineau R, Domanski M, Troutman C, Anderson J, Johnson G, McNulty SE, Clapp-Channing N, Davidson-Ray LD, Fraulo ES, Fishbein DP, Luceri RM and Ip JH. Amiodarone or an implantable cardioverter-defibrillator for congestive heart failure. *The New England journal of medicine*. 2005;352:225-237.
6. van Rees JB, de Bie MK, Thijssen J, Borleffs CJ, Schalijs MJ and van EL. Implantation-related complications of implantable cardioverter-defibrillators and cardiac resynchronization therapy devices: a systematic review of randomized clinical trials. *J Am Coll Cardiol* 2011;58:995-1000.
7. Daubert JP, Zareba W, Cannom DS, McNitt S, Rosero SZ, Wang P, Schuger C, Steinberg JS, Higgins SL, Wilber DJ, Klein H, Andrews ML, Hall WJ and Moss AJ. Inappropriate implantable cardioverter-defibrillator shocks in MADIT II: frequency, mechanisms, predictors, and survival impact. *J Am Coll Cardiol* 2008;51:1357-1365.
8. Poole JE, Johnson GW, Hellkamp AS, Anderson J, Callans DJ, Raitt MH, Reddy RK, Marchlinski FE, Yee R, Guarnieri T, Talajic M, Wilber DJ, Fishbein DP, Packer DL, Mark DB, Lee KL and Bardy GH. Prognostic importance of defibrillator shocks in patients with heart failure. *The New England journal of medicine*. 2008;359:1009-1017.
9. Hartikainen JE, Malik M, Staunton A, Poloniecki J and Camm AJ. Distinction between arrhythmic and nonarrhythmic death after acute myocardial infarction based on heart rate variability, signal-averaged electrocardiogram, ventricular arrhythmias and left ventricular ejection fraction. *J Am Coll Cardiol* 1996;28:296-304.
10. Stein PK and Barzilay JI. Relationship of abnormal heart rate turbulence and elevated CRP to cardiac mortality in low, intermediate, and high-risk older adults. *J Cardiovasc Electrophysiol* 2011;22:122-127.
11. Gold MR, Bloomfield DM, Anderson KP, El-Sherif NE, Wilber DJ, Groh WJ, Estes NA, 3rd, Kaufman ES, Greenberg ML and Rosenbaum DS. A comparison of T-wave alternans, signal averaged electrocardiography and programmed ventricular stimulation for arrhythmia risk stratification. *J Am Coll Cardiol*. 2000;36:2247-53.

12. Rashba EJ, Osman AF, Macmurdy K, Kirk MM, Sarang SE, Peters RW, Shorofsky SR and Gold MR. Enhanced detection of arrhythmia vulnerability using T wave alternans, left ventricular ejection fraction, and programmed ventricular stimulation: a prospective study in subjects with chronic ischemic heart disease. *J Cardiovasc Electrophysiol* 2004;15:170-176.
13. Chow T, Kereiakes DJ, Onufer J, Woelfel A, Gursoy S, Peterson BJ, Brown ML, Pu W, Benditt DG and Investigators MT. Does microvolt T-wave alternans testing predict ventricular tachyarrhythmias in patients with ischemic cardiomyopathy and prophylactic defibrillators? The MASTER (Microvolt T Wave Alternans Testing for Risk Stratification of Post-Myocardial Infarction Patients) trial. *J Am Coll Cardiol*. 2008;52:1607-15.
14. Lahiri MK, Kannankeril PJ and Goldberger JJ. Assessment of autonomic function in cardiovascular disease: physiological basis and prognostic implications. *J Am Coll Cardiol* 2008;51:1725-1733.
15. Heart rate variability. Standards of measurement, physiological interpretation, and clinical use. Task Force of the European Society of Cardiology and the North American Society of Pacing and Electrophysiology. *Eur Heart J* 1996;17:354-381.
16. Fauchier L, Babuty D, Cosnay P and Fauchier JP. Prognostic value of heart rate variability for sudden death and major arrhythmic events in patients with idiopathic dilated cardiomyopathy. *J Am Coll Cardiol* 1999;33:1203-1207.
17. La Rovere MT, Pinna GD, Maestri R, Mortara A, Capomolla S, Febo O, Ferrari R, Franchini M, Gnemmi M, Opasich C, Riccardi PG, Traversi E and Cobelli F. Short-term heart rate variability strongly predicts sudden cardiac death in chronic heart failure patients. *Circulation*. 2003;107:565-570.
18. Kleiger RE, Miller JP, Bigger JT, Jr. and Moss AJ. Decreased heart rate variability and its association with increased mortality after acute myocardial infarction. *Am J Cardiol* 1987;59:256-262.
19. Ponikowski P, Anker SD, Chua TP, Szelemez R, Piepoli M, Adamopoulos S, Webb-Peploe K, Harrington D, Banasiak W, Wrabec K and Coats AJ. Depressed heart rate variability as an independent predictor of death in chronic congestive heart failure secondary to ischemic or idiopathic dilated cardiomyopathy. *Am J Cardiol* 1997;79:1645-1650.
20. La Rovere MT, Bigger JT, Jr., Marcus FI, Mortara A and Schwartz PJ. Baroreflex sensitivity and heart-rate variability in prediction of total cardiac mortality after myocardial infarction. ATRAMI (Autonomic Tone and Reflexes After Myocardial Infarction) Investigators. *Lancet*. 1998;351:478-484.
21. Boveda S, Galinier M, Pathak A, Fourcade J, Dongay B, Benchendikh D, Massabuau P, Fauvel JM, Senard JM and Bounhoure JP. Prognostic value of heart rate variability in time domain analysis in congestive heart failure. *J Interv Card Electrophysiol* 2001;5:181-187.
22. Battipaglia I, Barone L, Mariani L, Infusino F, Remoli R, Careri G, Pinnacchio G, Tarzia P, Lanza GA and Crea F. Relationship between cardiac autonomic function and sustained ventricular tachyarrhythmias in patients with an implantable cardioverter defibrillators. *Europace : European pacing, arrhythmias, and cardiac electrophysiology : journal of the working groups on cardiac pacing, arrhythmias, and cardiac cellular electrophysiology of the European Society of Cardiology*. 2010;12:1725-1731.
23. Moss AJ, Schuger C, Beck CA, Brown MW, Cannom DS, Daubert JP, Estes NA, III, Greenberg H, Hall WJ, Huang DT, Kautzner J, Klein H, McNitt S, Olshansky B, Shoda M, Wilber D and Zareba W. Reduction in inappropriate therapy and mortality through ICD programming. *The New England journal of medicine*. 2012;367:2275-2283.

24. La Rovere MT, Pinna GD, Hohnloser SH, Marcus FI, Mortara A, Nohara R, Bigger JT, Jr., Camm AJ and Schwartz PJ. Baroreflex sensitivity and heart rate variability in the identification of patients at risk for life-threatening arrhythmias: implications for clinical trials. *Circulation*. 2001; 103:2072-2077.
25. Huikuri HV, Raatikainen MJ, Moerch-Joergensen R, Hartikainen J, Virtanen V, Boland J, Anttonen O, Hoest N, Boersma LV, Platou ES, Messier MD and Bloch-Thomsen PE. Prediction of fatal or near-fatal cardiac arrhythmia events in patients with depressed left ventricular function after an acute myocardial infarction. *Eur Heart J* 2009;30:689-698.
26. Nolan J, Batin PD, Andrews R, Lindsay SJ, Brooksby P, Mullen M, Baig W, Flapan AD, Cowley A, Prescott RJ, Neilson JM and Fox KA. Prospective study of heart rate variability and mortality in chronic heart failure: results of the United Kingdom heart failure evaluation and assessment of risk trial (UK-heart). *Circulation*. 1998;98:1510-1516.
27. Hohnloser SH, Klingenhoben T, Bloomfield D, Dabbous O and Cohen RJ. Usefulness of microvolt T-wave alternans for prediction of ventricular tachyarrhythmic events in patients with dilated cardiomyopathy: results from a prospective observational study. *J Am Coll Cardiol* 2003; 41:2220-2224.
28. Adamson PB, Smith AL, Abraham WT, Kleckner KJ, Stadler RW, Shih A and Rhodes MM. Continuous autonomic assessment in patients with symptomatic heart failure: prognostic value of heart rate variability measured by an implanted cardiac resynchronization device. *Circulation*. 2004;110:2389-2394.
29. Molon G, Solimene F, Melissano D, Curnis A, Belotti G, Marrazzo N, Marczyk J, Accardi F, Raciti G and Zecchi P. Baseline heart rate variability predicts clinical events in heart failure patients implanted with cardiac resynchronization therapy: validation by means of related complexity index. *Ann Noninvasive Electrocardiol* 2010;15:301-307.
30. Gilliam FR, III, Singh JP, Mullin CM, McGuire M and Chase KJ. Prognostic value of heart rate variability footprint and standard deviation of average 5-minute intrinsic R-R intervals for mortality in cardiac resynchronization therapy patients. *J Electrocardiol* 2007;40:336-342.
31. Casolo GC, Stroder P, Sulla A, Chelucci A, Freni A and Zeraushek M. Heart rate variability and functional severity of congestive heart failure secondary to coronary artery disease. *Eur Heart J* 1995;16:360-367.
32. Hayase J, Patel J, Narayan SM and Krummen DE. Percutaneous Stellate Ganglion Block Suppressing VT and VF in a Patient Refractory to VT Ablation. *J Cardiovasc Electrophysiol* 2013.





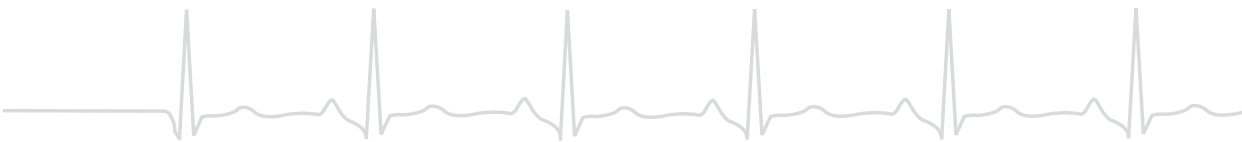
# CHAPTER 3

## Myocardial Fibrosis as an early feature in Phospholamban p.Arg14del mutation carriers: Phenotypical insights using Cardiovascular Magnetic Resonance Imaging

Judith N. ten Sande<sup>#</sup>, Wouter P. te Rijdt<sup>#</sup>, Thomas M. Gorter<sup>#</sup>, Paul A. van der Zwaag, Ingrid A. van Rijsingen, S. Matthijs Boekholdt, J. Peter van Tintelen, Paul L. van Haelst, R. Nils Planken, Rudolf A. de Boer, Dirk J. van Veldhuisen, Arthur A.W. Wilde, Tineke P. Willems, Pascal F.H.M. van Dessel, Maarten P. van den Berg

*<sup>#</sup> contributed equally*

*Submitted*



## ABSTRACT

### Background

The p.Arg14del founder mutation in the gene encoding phospholamban (PLN) is associated with increased risk of ventricular arrhythmias (VA) and heart failure. This mutation has been shown to lead to calcium overload, cardiomyocyte damage and eventually myocardial fibrosis. In PLN p.Arg14del mutation carriers, the electrocardiographic hallmarks are the gradual attenuation of QRS complex amplitude and repolarization abnormalities which are often the first clinical signs of disease development observed. We aimed to study ventricular function, extent, and localization of myocardial fibrosis measured by cardiac magnetic resonance imaging (CMR) with late gadolinium enhancement (LGE) and determined the associations with ECG features and VA.

### Methods

CMR studies of 150 mutation carriers were retrospectively analyzed. Left ventricular (LV) and right ventricular (RV) volumes, mass and ejection fraction (EF) were measured. The extent of LGE was expressed as percentage of myocardial mass. All standard ECG parameters were measured including conduction and repolarization parameters, R-wave amplitude and T-wave morphology. Occurrence of VA was analyzed on ambulatory (Holter) and/or exercise electrocardiography, if available.

### Results

Mean age was  $40 \pm 15$  years; 42% males; 7% index patients, the other subjects were pre-symptomatic carriers identified after cascade screening. Mean LVEF and RVEF were  $58 \pm 9\%$  and  $55 \pm 9\%$ , respectively. There was a significant correlation between LVEF and RVEF ( $r=0.78$ ,  $p<0.01$ ). LV-LGE was present in 91% of the mutation-carriers with reduced LVEF ( $<45\%$ ) and in 30% of mutation carriers with preserved LVEF. In carriers with positive LGE, the median extent of LGE was 5.9% (interquartile range 3.2-12.7). LGE was most commonly observed in the inferolateral wall. As expected, index patients showed more extensive structural and functional signs of disease. Carriers with inverted T-waves in the lateral ECG leads more often showed LV-LGE on CMR ( $p<0.01$ ) than carriers without. Finally, presence of LV-LGE and inverted lateral T waves, but not attenuated R waves, were independently associated with VA.

### Conclusions

LV myocardial fibrosis can already be found in many PLN p.Arg14del mutation carriers with still preserved LVEF. It is present predominantly in the inferolateral wall and corresponds with electrocardiographic repolarization abnormalities. Moreover, myocardial fibrosis was independently associated with VA. Our findings support the use of CMR, with LGE early in the diagnostic work-up.

## INTRODUCTION

In the Netherlands, the pathogenic p.Arg14del mutation in phospholamban (PLN), can be found in up to 10-15% of patients diagnosed with dilated cardiomyopathy (DCM) and/or arrhythmogenic cardiomyopathy (ACM)<sup>1-3</sup>. PLN is a transmembrane sarcoplasmic reticulum (SR) phosphoprotein that regulates sarcoplasmic reticulum Ca<sup>2+</sup>-ATPase (SERCA) activity and the p.Arg14del mutation has been shown to lead to calcium overload and consequently cardiomyocyte damage and eventually myocardial fibrosis<sup>4,5</sup>. Indeed, examination of 20 complete heart specimens (autopsies and explants) of PLN p.Arg14del mutation carriers revealed extensive myocardial fibrosis in all cases<sup>6,7</sup>. A striking clinical manifestation of PLN p.Arg14del mutation related cardiomyopathy is the development of low amplitude QRS complexes on the surface ECG<sup>1,8</sup> and it is readily conceivable that this is a reflection of underlying fibrosis but this is yet unproven. In addition, repolarization changes on the ECG are an early manifestation in mutation carriers, in particular negative T-waves in the lateral leads.

Late gadolinium-enhanced (LGE) cardiovascular magnetic resonance imaging (CMR) has become the gold standard for noninvasive *in vivo* assessment of ventricular myocardial fibrosis and allows (early) identification and evaluation of both extent and localization of myocardial fibrosis in different forms of cardiomyopathy *in vivo*<sup>9-11</sup>. Indeed, LGE has consistently been shown to be a strong risk factor for sudden cardiac death (SCD) and overall mortality in a wide range of cardiomyopathies, e.g. DCM<sup>12-16</sup>.

We hypothesized, based on these previous electrocardiographical and histopathological findings, that LGE is present in PLN p.Arg14del mutation carriers and is a reflection of fibrosis. Moreover, we hypothesized that the ECG changes are a reflection of fibrosis and that, assuming that fibrosis is a substrate for ventricular arrhythmias (VA) in mutation carriers, therefore the presence of LGE is associated with VA.

In the present study, we investigated CMR- and ECG parameters and VA occurrence in a large cohort of mutation carriers to test these hypotheses. In particular, we analyzed CMR LGE extent and localization together with ECG parameters to investigate whether the development of low voltage QRS amplitude and/or repolarization changes is associated with LV-LGE. In addition, we investigated whether these ECG and/or CMR findings are associated with VA.

## METHODS

### Source population

Demographic and clinical parameters at the time of CMR were collected retrospectively in three Dutch hospitals (University Medical Center Groningen, Academic Medical Center

Amsterdam and Antonius Hospital Sneek) from adult (>18 years) PLN p.Arg14del mutation carriers. This group comprised both index patients and their relatives referred to a cardiogenetics outpatient clinic for family cascade screening. Index patients in the cohort were not known to be related to each other.

The study conformed to principles defined in the Helsinki Declaration and the medical ethics committee of the University Medical Center Groningen. Because the data were collected retro-spectively, no standardized diagnostic and therapeutic protocols were used. Clinical evaluations were performed as standard clinical care.

### Cardiac magnetic resonance imaging protocol

CMR studies in all three centers were performed on a 1.5 Tesla whole-body CMR scanner (Magnetom Avanto, Siemens, Erlangen, Germany) using a phased array cardiac receiver coil. ECG-gated steady state, free precession cine loops were acquired during repeated breath holds in contiguous short-axis slices (6 – 8 mm per slice) covering the entire left and right ventricle.

Using identical slice locations, LGE images were acquired 10 minutes after intravenous administration of a gadolinium-based contrast agent (Dotarem, Gorinchem, the Netherlands; 0.2 mmol/kg) with an inversion-recovery, gradient-echo pulse sequence. The inversion time was individually set to null the signal of viable myocardium. All procedures were performed according to the standardized Society for Cardiovascular Magnetic Resonance recommended protocols<sup>17</sup>.

### Cardiac magnetic resonance imaging analysis

All CMR analyses were performed using QMass 7.6 (Medis, Leiden, The Netherlands). The endo- and epicardial contours of the left and right ventricle were manually traced on the short-axis slices in the end-diastolic and end-systolic phase by a single experienced observer (T.G.) who was blinded for clinical patient data. Papillary muscle and trabeculae were included in the blood volume. End-systolic and end-diastolic volumes were calculated using the summation of slice multiplied by slice thickness method and were indexed to body surface area (BSA) and compared to reference values<sup>18</sup>. LV dilatation was dichotomized based on reference values<sup>18</sup> into dilated (>112 ml/m<sup>2</sup> for males and >99 ml/m<sup>2</sup> for females) or non-dilated.

For LGE imaging, the presence of delayed-enhanced signal intensity was determined by two independent observers who were blinded for clinical patient data (T.G. and T.W.). The amount of LV-LGE was quantified using the full width at half maximum technique and was expressed as percentage of total LV mass. LV-LGE location was determined using the 17-segment model<sup>19</sup>. The amount of RV LGE was quantified using the 12-segment model of the RV and classified as small ( $\leq 4$  segments involved) or large (>4 segments involved)<sup>20</sup>.

## ECG analysis

Standard 12-lead resting ECGs, recorded around the time of CMR, were analyzed after digitization using ImageJ (<http://rsb.info.nih.gov/ij/>). Each ECG was time calibrated and conduction and repolarization parameters during sinus rhythm were determined. Measurements of time related parameters (heart rate, PQ-interval, QRS-duration and QT-interval) were performed manually on-screen, in lead II whenever possible. Parameters were averaged from up to 3 consecutive beats with similar preceding RR-intervals. For the QT and heart-rate corrected QT- interval (QTc), the tangent method with Bazett's correction was used<sup>21</sup>. R waves of all 12 leads were summed and dichotomized based on the median value (5.3mm) into "normal voltage" or "low voltage". Inverted T-waves were determined and considered present if inverted in the right precordial leads (V1 as well as V2) and/or in at least in two adjacent lateral leads (V4, V5 or V6). ECGs were not analyzed in case of a left or right bundle branch block or bifascicular block.

## Ventricular arrhythmias

To determine the association between ECG parameters, fibrosis and VA, occurrence of VA was analyzed on ambulatory (Holter) and/or exercise electrocardiography, if available. Non sustained ventricular tachycardia (VT) was defined as at least three consecutive ventricular complexes at a heart rate >100 beats/min with a duration of less than 30 seconds. Sustained VT was defined as an arrhythmia at a heart rate >100 beats/min that lasted  $\geq 30$  seconds and/or requiring termination because of hemodynamic compromise in <30 seconds.

## Statistical analysis

Statistical analyses were performed using the SPSS software, version 24.0 (SPSS for Windows, 2016 release 24.0.0.0, Chicago, Ill, USA). Continuous variables are presented as mean with standard deviation (SD) and compared with the unpaired t-test in case of a normal distribution, or presented as median with interquartile range in case of a skewed distribution, as determined by the Kolmogorov-Smirnov Goodness- of-Fit test. Categorical variables are presented as frequencies with percentages and analyzed using Fisher exact test. Associations between demographic-, ECG- and CMR variables were first analyzed using univariable regression. All variables that were statistically significantly associated with LGE presence in the univariable analysis were subsequently included in a multivariable regression model. Also the association with VA was analyzed. Odd's ratios and 95% confidence intervals were calculated. A p-value of less than 0.05 was considered statistically significant.

## RESULTS

### Patient characteristics

In total, 194 mutation carriers who underwent CMR imaging in the three centers were identified. For 28 patients clinical ECG data and/or CMR LGE were unavailable and in 6 patients LGE could not be evaluated due to insufficient CMR image quality. Ten patients were excluded based on their ECG (3 bifascicular block, 4 right bundle branch block, 1 left bundle branch block, 1 atrial fibrillation and 1 Wolff Parkinson White syndrome). The final study group thus consisted of 150 mutation carriers (table 1). Mean age was  $40 \pm 15$  years and 42% was male. Ten of them (7%) were index patients (mean age  $44 \pm 10$  years) while the remaining 140 participants were relatives identified by family cascade screening (mean age  $40 \pm 15$  years). The large majority (93%) of participants were in NYHA functional class I and did not receive heart failure medication. Prescription of beta-blockers, ACE-inhibitors/ARBs, aldosterone-blocking agents (spironolactone/eplerenone) and diuretics was significantly higher ( $p < 0.05$ ) in index patients.

### CMR findings

On CMR, mean end-diastolic LV and RV volumes, LVEF and RVEF were on average normal (table 2) but we observed significant differences between index patients and their relatives for LVEDV ( $240 \pm 105$  vs.  $174 \pm 35$  ms,  $p < 0.05$ ), LVEDVi ( $119 \pm 43$  vs.  $91 \pm 15$  ms,  $p < 0.05$ ), LVEF ( $40 \pm 14$  vs.  $59 \pm 7$  ms,  $p < 0.05$ ), and RVEF ( $45 \pm 11$  vs.  $56 \pm 9$  ms,  $p < 0.05$ ). Eleven (7%) mutation carriers had reduced LVEF (i.e.  $< 45\%$ ), of whom 5 were index patients (index 5/10 vs. relatives 6/140,  $p < 0.05$ ). There was a significant correlation between LVEF and RVEF ( $r = 0.78$ ,  $p < 0.001$ ) (figure 1).

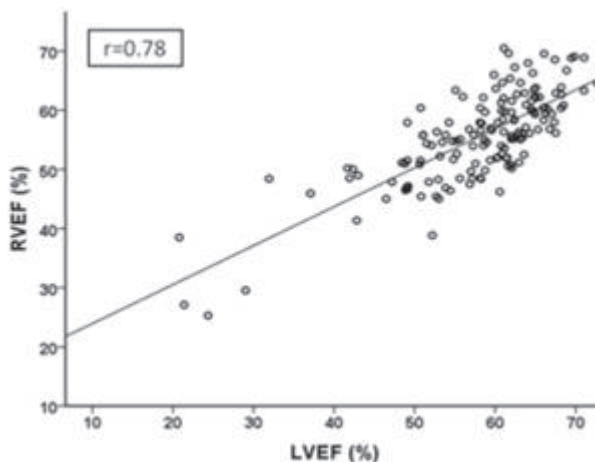


Figure 1. Scatterplot depicting the relationship between LVEF and RVEF ( $n = 150$ ;  $p < 0.01$ ).

LV-LGE was present in 50 mutation carriers (index 9/10 vs. relatives 41/140,  $p<0.05$ ). Mutation carriers with LV-LGE were significantly older ( $47\pm 15$  vs.  $36\pm 14$  years,  $p<0.01$ ) than those without. LV-LGE was present in almost all mutation-carriers with reduced LVEF (9/11; 81%) but it was also present in 30% (42/139) of mutation carriers with preserved LVEF (figure 2).

In carriers with LGE, the median volume of enhanced LV myocardium was 5.9% (3.2-12.7), index patients show higher volumes than relatives (18.0% (8.1-30.2) vs. 4.6% (3.0-8.3),  $p<0.05$ ). Delayed enhancement was predominantly present in the basal inferolateral wall of the LV (most abundant in segments 5 and 11) whereas segments 1-3, 7-9 and 14 were least affected (figure 3). In the RV we observed LGE in only 8 (5%) of mutation carriers (index 2/10 vs. relatives 6/140,  $p<0.05$ ).

### ECG findings and arrhythmia occurrence

ECG conduction and repolarization parameters were on average within the normal range (table 1). Median R-wave amplitude was 5.3mm (index 3.4mV vs. relatives 5.5mV,  $p<0.05$ ). Carriers with a low voltage (mean R-value below median) were significantly older than carriers with normal voltages ( $44\pm 15$  vs.  $36\pm 14$  years,  $p<0.01$ ).

Inverted T waves in the right precordial leads were present in 17 (11%) carriers and inverted T waves in the lateral leads were present in 43 (29%) of 150 carriers (index 8/10 vs. relatives 36/140,  $p<0.05$ ).

In 23 of 150 carriers (15%), either (non-)sustained ventricular tachycardia or ventricular fibrillation was documented (index 6/10 vs. relatives 17/140,  $p<0.05$ ).

### Association between ECG findings and CMR LGE

In univariable analysis, the presence of low voltage on the surface ECG was associated with presence of LV-LGE on CMR (OR=3.06,  $p<0.01$ ) (Table 3). If the surface ECG showed inverted T-waves in the lateral leads (V4-6), LV-LGE was also more often present on CMR (OR=8.48,  $p<0.01$ ).

In a multivariable regression model including age, low voltage ECG, inverted lateral T-waves, LVEF, LV dilatation and RVEF (all  $P<0.05$  in univariable analysis), only age (OR=1.05,  $p<0.01$ ) and inverted lateral T-waves (OR=5.70,  $p<0.01$ ) were independently associated with the presence of LV-LGE.

### Association between ECG findings, CMR LGE and occurrence of ventricular arrhythmias

In the univariable analysis, inverted lateral T-waves, low voltage ECG and LVEF<45% were associated with the occurrence of VA. In addition, we found that the presence of CMR LGE was also significantly associated with the occurrence of VA (OR=10.7,  $p<0.01$ ) (table



Table 1. Patient characteristics

	All patients (n=150)	Index (n=10)	Relatives (n=140)
Age (years)	40±15	44±10	40±15
Male	63 (42%)	5 (50%)	58 (41%)
Body surface area (m <sup>2</sup> )	1.92±0.16	1.99±0.26	1.91±0.17
NYHA functional			
I	139 (93%)	8 (80%)	131 (94%)
II	11 (7%)	2 (20%)	9 (6%)
III/IV	0 (0%)	0 (0%)	0 (0%)
Ventricular Arrhythmias (ns)VT+VF	23 (15%)	6 (60%)	17 (12%) *
ECG parameters			
PR interval (ms)	150±21	151±10	150±21
QRS width (ms)	85±11	91±15	85±11
QTc (ms)	408±23	411±29	409±23
R wave amplitude (mV; median)	5.3 (1.4-17.0)	3.4 (1.6-6.1)	5.5 (1.4-17.0) *
Inverted right precordial T waves (V1 and V2)	17 (11%)	0 (0%)	17 (12%)
Inverted lateral T waves (V4, 5 or 6)	43 (23%)	8 (80%)	35 (25%) *
Medication			
Anti-arrhythmic	6 (4%)	2 (20%)	4 (3%)
Beta-blocker	22 (15%)	7 (70%)	15 (11%) *
ACE inhibitor/ARB	15 (10%)	6 (60%)	9 (7%) *
Spirolactone/Eplerenone	2 (1%)	2 (20%)	0 (0%) *
Diuretics	9 (6%)	4 (40%)	5 (4%) *
Anticoagulant	7 (5%)	2 (20%)	5 (4%)
Antiplatelet therapy	4 (3%)	1 (10%)	3 (2%)

(\*p<0.05) ARB: angiotensin-renin blocker, ms: milliseconds, mV: millivolt, NYHA: New York Heart Association, VF: ventricular fibrillation, VT: ventricular tachycardia

4). The distribution of PLN p.Arg14del carriers with or without VA, in relation to LVEF and percentage LGE of LV myocardium, is shown in figures 4 and 5.

Due to the low prevalence of VA we had to limit our selection of variables for the corresponding multivariable analysis (table 4). Variables were therefore selected based on clinical relevance and prevalence. Included variables in the multivariable analysis were low voltage ECG, inverted lateral T-waves, LVEF and LV-LGE. The presence of inverted T-waves (OR 3.93, p=0.03) and especially LV-LGE (OR 5.17, p<0.01) remained independently associated with the occurrence of VA. Low voltage and LVEF<45% were not independently associated with VA occurrence.

Table 2. CMR parameters

	All patients	Index (n=10)	Relative (n=140)
<b>Left ventricle</b>			
LVEDV (ml)	179±46	240±105	174±35 *
LVEDVi (ml/m <sup>2</sup> )	93±19	119±43	91±15 *
LVEF (%)	58±9	40±14	59±7 *
LVEF <45%	11 (7%)	5 (50%)	6 (4%) *
LV-LGE present (%)	50 (33%)	9 (90%)	41 (29%) *
LGE % LV mass (median; IQR), if present	5.9 (3.2-12.7)	18 (8,1-30.2)	4.6 (3.0-8.3) *
<b>Right ventricle</b>			
RVEDV (ml)	186±42	203±78	185±38
RVEDVi (ml/m <sup>2</sup> )	97±17	100±28	97±16
RVEF (%)	55±8	45±11	56±9 *
RV-LGE present (%)	8 (5%)	2 (20%)	6 (4%) *

(\*p<0.05). EDV(i): end-diastolic volume (index), EF: ejection fraction, IQR: interquartile range, LGE: late gadolinium enhancement, LV: left ventricle, ml: milliliter, RV: right ventricle

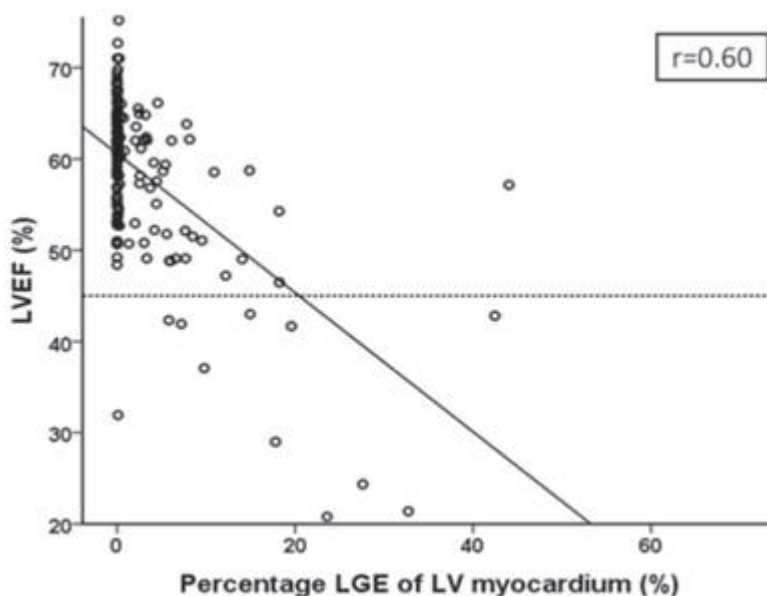
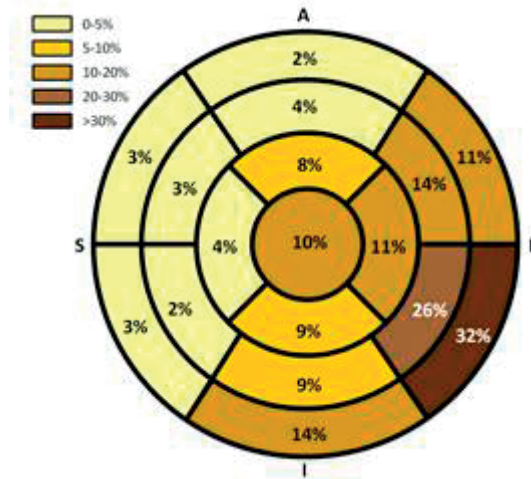


Figure 2. Scatterplot depicting relationship between the extent of LV myocardial fibrosis (%) and LVEF (%) in phospholamban p.Arg14del mutation carriers (n=150; p<0.01). The dotted line represents LVEF of 45%.

## DISCUSSION



**Figure 3.** Bull's eye plot (17 left ventricular segments model) depicting the presence and localization of myocardial fibrosis in PLN p.Arg14del mutation carriers (n=150; % per segment represents the mutation carriers with CMR LGE in that segment).

PLN p.Arg14del cardiomyopathy is characterized by early changes on the ECG, i.e. low voltage and repolarization changes, and a high risk for VA. The present study demonstrated that among PLN p.Arg14del mutation carriers, both the presence of low voltage and inverted T-waves in the lateral precordial leads are associated with LV-LGE. LV-LGE was most abundant in the LV inferolateral wall where we observed the highest prevalence of negative T waves. These findings suggest that these ECG changes are a reflection of myocardial fibrosis.

In line with this, we demonstrated that LV-LGE on CMR is independently associated with the occurrence of VA, again attesting to the importance of fibrosis in this disease. As expected, index patients showed more extensive structural and functional evidence of disease progress. Interestingly, LV-LGE on CMR was observed in many subjects with still preserved LV systolic function (LVEF >45%), indicating that fibrosis in PLN p.Arg14del cardiomyopathy not necessarily impacts LV function, but often develops as an early feature of the disease. Finally, in line with previous clinical and histopathological findings<sup>6</sup>, the present data support the notion of biventricular involvement in PLN p.Arg14del cardiomyopathy given the strong correlation between LV and RV systolic function on CMR.

Current guidelines for primary prevention of SCD in patients with DCM recommend defibrillator implantation in patients with New York Heart Association functional class II/III and a LVEF of less than 35%<sup>22-24</sup>. However, previous studies suggest that LGE on CMR imaging is a helpful independent prognostic factor in patients<sup>12-16</sup>. In our previous study in PLN p.Arg14del mutation carriers, we showed that an LVEF of less than 45% (rather than 35%) is an independent predictor for VA<sup>3</sup>. Taken together, these studies show that besides

**Table 3.** Univariable and multivariable analysis of the association between demographic-, ECG- and CMR variables and presence or absence of LGE.

	<b>LV-LGE (n=50)</b>	<b>No LV-LGE (n=100)</b>	<b>Univariable OR 95%CI</b>	<b>Multivariable OR 95%CI</b>
Age	47±15	36±14	1.04(1.02-1.07) P<0.05	1.05(1.01-1.08) P<0.01*
Sex	25(50%)	38(38%)	1.63(0.82-3.24)	
Male	25(50%)	62(62%)	P=0.16	
Female				
NYHA functional class (≥2)	6(12%)	5(5%)	2.59(0.75-8.95) P=0.13	
Low voltages (present)	34(68%)	41(41%)	3.06(1.50-6.25) P<0.05	1.09(0.45-2.62) P=0.85
Inverted lateral T wave (present)	29(58%)	14(14%)	8.48(3.83-18.8) P<0.05	5.70(2.28-14.26) P<0.01*
LV dilatation (present)	16(32%)	13(13%)	3.15(1.37-7.24) P<0.05	2.51(0.83-7.61) P=0.10
LVEF <45% (present)	10 (20%)	1(1%)	24.8(3.07-199) P<0.05	5.34(0.52-54.8) P=0.16
RVEF <45% (present)	6 (12%)	1 (1%)	13.5(1.58-116) P<0.05	2.11(0.12-37.59) P=0.61

CMR: cardiac magnetic resonance, ECG: electrocardiogram, EF: ejection fraction LGE: late gadolinium enhancement, LV: left ventricle, NYHA: New York Heart Association, OR: odds ratio, RV: right ventricle.

**Table 4.** Univariable and multivariable analysis of the association between ECG- and CMR variables and occurrence of VA

	<b>VA(n=23)</b>	<b>No VA(n=127)</b>	<b>Univariable OR 95%CI</b>	<b>Multivariable OR 95%CI</b>
Low voltages (present)	16(70%)	59(46%)	2.63(1.02-6.84) P<0.05	0.69(0.19-2.45) P=0.56
Inverted lateral T wave (present)	18(78%)	32(25%)	10.7(3.67-31.12) P<0.05	3.93(1.14-13.60) P<0.05*
LVEF<45% (present)	7(30%)	4(3%)	12.7(3.35-47.83) P<0.05	4.18(0.91-19.27) P=0.07
LV-LGE (present)	18(78%)	32(25%)	10.7(3.67-31.12) P<0.05	5.17(1.52-17.50) P<0.01*

CMR: cardiac magnetic resonance, ECG: electrocardiogram, EF: ejection fraction LGE: late gadolinium enhancement, LV: left ventricle, OR: odds ratio, RV: right ventricle, VA: ventricular arrhythmia.

a more reliable risk stratification in DCM patients with severe left ventricular impairment, LGE-CMR may also facilitate identification of high-risk patients with milder degrees of left ventricular dysfunction.

In previous studies<sup>1, 8</sup> attenuation of R-waves on the surface ECG in PLN p.Arg14del mutation carriers was shown to be an early manifestation of PLN cardiomyopathy irrespective of cardiac function compared to their family members without PLN p.Arg14del

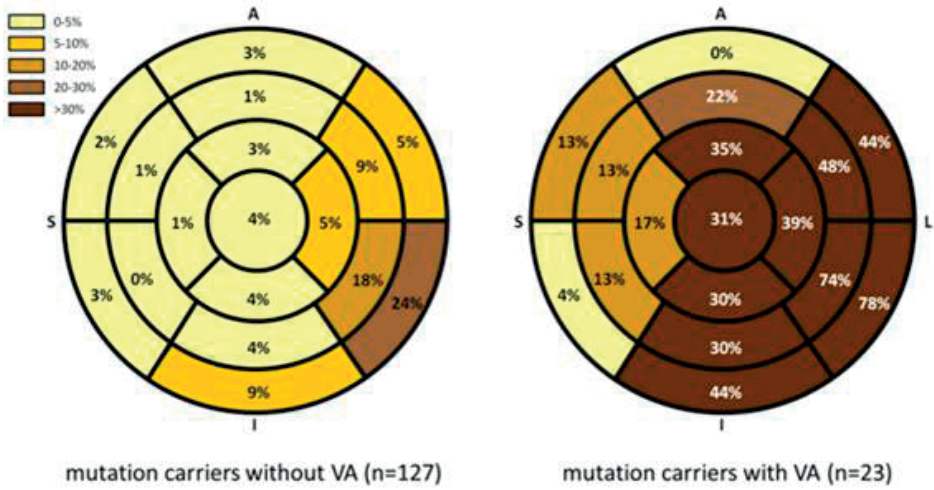


Figure 4. Bull's eye plot (17 left ventricular segments model) showing localization and amount (% per segment represents the mutation carriers with CMR LGE in that segment) of LGE in PLN p.Arg14del mutation carriers who experienced (non)-sustained ventricular tachycardia/ventricular fibrillation (n=23; right figure) versus no ventricular tachycardia/ventricular (n=127; left figure). VA: ventricular arrhythmias.

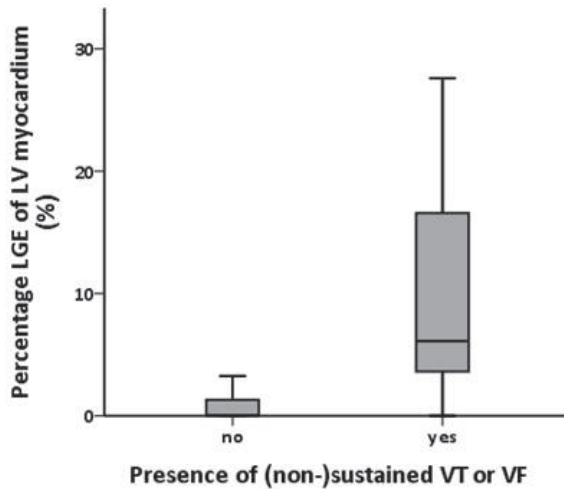


Figure 5. Boxplot depiction of the distribution of LGE (%) among mutation carriers with or without (non)-sustained VT of VF. Boxes represent the middle one-half of the distribution (25th to 75th percentile). Horizontal lint in the box is the median. The error bars represent 95% CI.

mutation. The study by Posch et al. showed that the presence of attenuated R-waves was indeed related to fibrosis on CMR and that fibrosis was already present even with a preserved cardiac function but CMR studies were conducted only in a single family (n=6)<sup>8</sup>.

Our present findings in a much larger cohort of PLN p.Arg14del mutation carriers extend this observation.

### Considerations

CMR (including LGE) imaging was only performed in PLN p.Arg14del mutation carriers without pacemaker or ICD, leading to preferential inclusion of patients with earlier stage disease. However, this provided us with the unique opportunity to study early-stage disease.

The main limitation of the LGE technique is the inability to evaluate diffuse myocardial fibrosis. The enhanced area is defined on the basis of the difference in signal intensity relative to that of the normal myocardium. If there is diffuse instead of focal myocardial fibrosis, no differences in signal intensity will be observed. T1 mapping, a novel CMR sequence to visualize and quantify diffuse myocardial interstitial fibrosis in the whole heart, truly reflecting the global myocardial fibrosis burden<sup>25</sup>, has only recently been routinely performed at our centers.

We speculate that the presence of RV myocardial fibrosis is underestimated in the present cohort. We believe the observed low prevalence of RV-LGE is mainly due to the thin wall of the RV because of which the RV is much harder to visualize.

The occurrence of VA was determined on ambulatory (Holter) and/or (exercise) electrocardiography and was not available in every patient, this may have underestimated the VA burden in this study population. Finally, this was a retrospective study with inherent limitations, in particular regarding collection of the data. Although this does not negate the observed associations between ECG and CMR findings, caution is definitely warranted regarding the findings on prognostication.

## CONCLUSIONS

Ours is the largest CMR study in a genetically homogeneous cardiomyopathy cohort worldwide. Moreover, we also investigated the association between CMR findings and ECG findings and VA. In PLN p.Arg14del mutation carriers LV myocardial fibrosis may be observed even in the presence of preserved LVEF, which suggests an extensive remodeling process preceding ventricular dysfunction. This can be observed non-invasively using CMR imaging and ECG. The presence of LV-LGE was independently associated with VA. Given the associations it seems plausible to integrate CMR findings in clinical decision making.

### Acknowledgement

We acknowledge the support from the Netherlands Cardiovascular Research Initiative, an initiative with support of the Dutch Heart Foundation: CVON2012-10 PREDICT and CVON2014-40 DOSIS projects.

## REFERENCES

1. van der Zwaag PA, van Rijsingen IA, Asimaki A, Jongbloed JD, van Veldhuisen DJ, Wiesfeld AC, Cox MG, van Lochem LT, de Boer RA, Hofstra RM, Christiaans I, van Spaendonck-Zwarts KY, Lekanne dit Deprez RH, Judge DP, Calkins H, Suurmeijer AJ, Hauer RN, Saffitz JE, Wilde AA, van den Berg MP and van Tintelen JP. Phospholamban R14del mutation in patients diagnosed with dilated cardiomyopathy or arrhythmogenic right ventricular cardiomyopathy: evidence supporting the concept of arrhythmogenic cardiomyopathy. *European journal of heart failure*. 2012;14:1199-207.
2. van der Zwaag PA, van Rijsingen IA, de Ruiter R, Nannenberg EA, Groeneweg JA, Post JG, Hauer RN, van Gelder IC, van den Berg MP, van der Harst P, Wilde AA and van Tintelen JP. Recurrent and founder mutations in the Netherlands-Phospholamban p.Arg14del mutation causes arrhythmogenic cardiomyopathy. *Neth Heart J*. 2013;21:286-93.
3. van Rijsingen IA, van der Zwaag PA, Groeneweg JA, Nannenberg EA, Jongbloed JD, Zwinderman AH, Pinto YM, Dit Deprez RH, Post JG, Tan HL, de Boer RA, Hauer RN, Christiaans I, van den Berg MP, van Tintelen JP and Wilde AA. Outcome in phospholamban R14del carriers: results of a large multicentre cohort study. *Circ Cardiovasc Genet*. 2014;7:455-65.
4. MacLennan DH and Kranias EG. Phospholamban: a crucial regulator of cardiac contractility. *Nature reviews Molecular cell biology*. 2003;4:566-77.
5. Haghghi K, Kolokathis F, Gramolini AO, Waggoner JR, Pater L, Lynch RA, Fan GC, Tsiapras D, Parekh RR, Dorn GW, 2nd, MacLennan DH, Kremastinos DT and Kranias EG. A mutation in the human phospholamban gene, deleting arginine 14, results in lethal, hereditary cardiomyopathy. *Proceedings of the National Academy of Sciences of the United States of America*. 2006; 103:1388-93.
6. Te Rijdt WP, van Tintelen JP, Vink A, van der Wal AC, de Boer RA, van den Berg MP and Suurmeijer AJ. Phospholamban p.Arg14del cardiomyopathy is characterized by phospholamban aggregates, aggresomes and autophagic degradation. *Histopathology*. 2016.
7. Gho JM, van Es R, Stathonikos N, Harakalova M, te Rijdt WP, Suurmeijer AJ, van der Heijden JF, de Jonge N, Chamuleau SA, de Weger RA, Asselbergs FW and Vink A. High resolution systematic digital histological quantification of cardiac fibrosis and adipose tissue in phospholamban p.Arg14del mutation associated cardiomyopathy. *PLoS One*. 2014;9:e94820.
8. Posch MG, Perrot A, Geier C, Boldt LH, Schmidt G, Lehmkuhl HB, Hetzer R, Dietz R, Gutberlet M, Haverkamp W and Ozcelik C. Genetic deletion of arginine 14 in phospholamban causes dilated cardiomyopathy with attenuated electrocardiographic R amplitudes. *Heart Rhythm*. 2009;6:480-6.
9. McCrohon JA, Moon JC, Prasad SK, McKenna WJ, Lorenz CH, Coats AJ and Pennell DJ. Differentiation of heart failure related to dilated cardiomyopathy and coronary artery disease using gadolinium-enhanced cardiovascular magnetic resonance. *Circulation*. 2003;108:54-9.
10. Holmstrom M, Kivisto S, Helio T, Jurkko R, Kaartinen M, Antila M, Reissell E, Kuusisto J, Karkkainen S, Peuhkurinen K, Koikkalainen J, Lotjonen J and Lauerma K. Late gadolinium enhanced cardiovascular magnetic resonance of lamin A/C gene mutation related dilated cardiomyopathy. *J Cardiovasc Magn Reson*. 2011;13:30.
11. Almaas VM, Haugaa KH, Strom EH, Scott H, Smith HJ, Dahl CP, Geiran OR, Endresen K, Aakhus S, Amlie JP and Edvardsen T. Noninvasive assessment of myocardial fibrosis in patients with obstructive hypertrophic cardiomyopathy. *Heart*. 2014;100:631-8.

12. Assomull RG, Prasad SK, Lyne J, Smith G, Burman ED, Khan M, Sheppard MN, Poole-Wilson PA and Pennell DJ. Cardiovascular magnetic resonance, fibrosis, and prognosis in dilated cardiomyopathy. *J Am Coll Cardiol*. 2006;48:1977-85.
13. Wu KC, Weiss RG, Thiemann DR, Kitagawa K, Schmidt A, Dalal D, Lai S, Bluemke DA, Gerstenblith G, Marban E, Tomaselli GF and Lima JA. Late gadolinium enhancement by cardiovascular magnetic resonance heralds an adverse prognosis in nonischemic cardiomyopathy. *J Am Coll Cardiol*. 2008;51:2414-21.
14. Lehrke S, Lossnitzer D, Schob M, Steen H, Merten C, Kemmling H, Pribe R, Ehlermann P, Zugck C, Korosoglou G, Giannitsis E and Katus HA. Use of cardiovascular magnetic resonance for risk stratification in chronic heart failure: prognostic value of late gadolinium enhancement in patients with non-ischaemic dilated cardiomyopathy. *Heart*. 2011;97:727-32.
15. Gulati A, Jabbour A, Ismail TF, Guha K, Khwaja J, Raza S, Morarji K, Brown TD, Ismail NA, Dweck MR, Di Pietro E, Roughton M, Wage R, Daryani Y, O'Hanlon R, Sheppard MN, Alpendurada F, Lyon AR, Cook SA, Cowie MR, Assomull RG, Pennell DJ and Prasad SK. Association of fibrosis with mortality and sudden cardiac death in patients with nonischemic dilated cardiomyopathy. *JAMA*. 2013;309:896-908.
16. Disertori M, Rigoni M, Pace N, Casolo G, Mase M, Gonzini L, Lucci D, Nollo G and Ravelli F. Myocardial Fibrosis Assessment by LGE Is a Powerful Predictor of Ventricular Tachyarrhythmias in Ischemic and Nonischemic LV Dysfunction: A Meta-Analysis. *JACC Cardiovascular imaging*. 2016;9:1046-55.
17. Kramer CM, Barkhausen J, Flamm SD, Kim RJ, Nagel E and Society for Cardiovascular Magnetic Resonance Board of Trustees Task Force on Standardized P. Standardized cardiovascular magnetic resonance (CMR) protocols 2013 update. *J Cardiovasc Magn Reson*. 2013;15:91.
18. Alfakih K, Plein S, Thiele H, Jones T, Ridgway JP and Sivananthan MU. Normal human left and right ventricular dimensions for MRI as assessed by turbo gradient echo and steady-state free precession imaging sequences. *J Magn Reson Imaging*. 2003;17:323-329.
19. Cerqueira MD, Weissman NJ, Dilsizian V, Jacobs AK, Kaul S, Laskey WK, Pennell DJ, Rumberger JA, Ryan T, Verani MS, American Heart Association Writing Group on Myocardial S and Registration for Cardiac I. Standardized myocardial segmentation and nomenclature for tomographic imaging of the heart. A statement for healthcare professionals from the Cardiac Imaging Committee of the Council on Clinical Cardiology of the American Heart Association. *Circulation*. 2002;105:539-42.
20. Kumar A, Abdel-Aty H, Kriedemann I, Schulz-Menger J, Gross CM, Dietz R and Friedrich MG. Contrast-enhanced cardiovascular magnetic resonance imaging of right ventricular infarction. *J Am Coll Cardiol*. 2006;48:1969-76.
21. Postema PG, De Jong JS, Van der Bilt IA and Wilde AA. Accurate electrocardiographic assessment of the QT interval: teach the tangent. *Heart Rhythm* 2008;5:1015-1018.
22. Epstein AE, DiMarco JP, Ellenbogen KA, Estes NA, 3rd, Freedman RA, Gettes LS, Gillinov AM, Gregoratos G, Hammill SC, Hayes DL, Hlatky MA, Newby LK, Page RL, Schoenfeld MH, Silka MJ, Stevenson LW, Sweeney MO, American College of Cardiology F, American Heart Association Task Force on Practice G and Heart Rhythm S. 2012 ACCF/AHA/HRS focused update incorporated into the ACCF/AHA/HRS 2008 guidelines for device-based therapy of cardiac rhythm abnormalities: a report of the American College of Cardiology Foundation/American Heart Association Task Force on Practice Guidelines and the Heart Rhythm Society. *Circulation*. 2013;127:e283-352.



23. Priori SG, Blomstrom-Lundqvist C, Mazzanti A, Blom N, Borggrefe M, Camm J, Elliott PM, Fitzsimons D, Hatala R, Hindricks G, Kirchhof P, Kjeldsen K, Kuck KH, Hernandez-Madrid A, Nikolaou N, Norekval TM, Spaulding C and Van Veldhuisen DJ. 2015 ESC Guidelines for the management of patients with ventricular arrhythmias and the prevention of sudden cardiac death: The Task Force for the Management of Patients with Ventricular Arrhythmias and the Prevention of Sudden Cardiac Death of the European Society of Cardiology (ESC). Endorsed by: Association for European Paediatric and Congenital Cardiology (AEPC). *Eur Heart J*. 2015; 36:2793-867.
24. Ponikowski P, Voors AA, Anker SD, Bueno H, Cleland JG, Coats AJ, Falk V, Gonzalez-Juanatey JR, Harjola VP, Jankowska EA, Jessup M, Linde C, Nihoyannopoulos P, Parissis JT, Pieske B, Riley JP, Rosano GM, Ruilope LM, Ruschitzka F, Rutten FH, van der Meer P and Authors/Task Force M. 2016 ESC Guidelines for the diagnosis and treatment of acute and chronic heart failure: The Task Force for the diagnosis and treatment of acute and chronic heart failure of the European Society of Cardiology (ESC) Developed with the special contribution of the Heart Failure Association (HFA) of the ESC. *Eur Heart J*. 2016;37:2129-200.
25. Jellis CL and Kwon DH. Myocardial T1 mapping: modalities and clinical applications. *Cardiovascular diagnosis and therapy*. 2014;4:126-37.





# CHAPTER 4

## Detailed characterization of familial idiopathic ventricular fibrillation linked to the *DPP6* locus

Judith N. ten Sande, Pieter G. Postema, S. Matthijs Boekholdt, Hanno L. Tan, Jeroen F. van der Heijden, Natasja M.S. de Groot, Paul G.A. Volders, Katja Zeppenfeld, Lucas V.A. Boersma, Eline A. Nannenbergh, Imke Christiaans, Arthur A.M. Wilde

*Heart Rhythm* 2016 Apr;13(4):905-12



## ABSTRACT

### Background

Familial idiopathic ventricular fibrillation (IVF) is a severe disease entity and is notoriously difficult to manage because there are no clinical risk indicators for premature cardiac arrest. Previously, we identified a link between familial IVF and a risk haplotype on chromosome 7q36 (involving the arrhythmia gene *DPP6*).

### Objective

The purpose of this study was to expand our knowledge of familial IVF and to discuss its (extended) clinical characteristics.

### Methods

We studied 601 family members and probands: 286 *DPP6* risk-haplotype positive (haplotype-positive) and 315 *DPP6* risk-haplotype negative (haplotype-negative) individuals. Clinical parameters, a combination of all-cause mortality and (aborted) cardiac arrest and differences between haplotype-positives and haplotype-negatives, were evaluated.

### Results

There were no differences in electrocardiographic indices between haplotype-positives and haplotype-negatives, or between haplotype-positives with or without events. Cardiac magnetic resonance documented slightly larger ventricular volumes in haplotype-positives compared to controls ( $P < .05$ ), but these were not clinically useful. Mortality and/or cardiac arrest occurred in 85 haplotype-positives (30%) and 18 haplotype-negatives (6%). Twenty-four haplotype-positives (8% male) were resuscitated from ventricular fibrillation (VF). Documented VF was always elicited by monomorphic short-coupled extrasystoles from the right ventricular apex/lower free wall. Median survival in haplotype-positives was 70 vs 93 years for haplotype-negatives ( $P < .01$ ), with a worse phenotype in males (median survival 63 vs 83 years in females,  $P < .01$ ). Implantable cardioverter-defibrillators were implanted in 99 patients (76 [77%] for primary prevention). Two arrhythmic events occurred in the primary prevention group during follow-up ( $5 \pm 3$  years).

### Conclusion

Despite our extensive analysis, the complexity in identifying asymptomatic IVF family members at risk for future arrhythmias based on clinical parameters is once more demonstrated.

## INTRODUCTION

Sudden cardiac death (SCD) is a major cause of death in developed countries and is primarily caused by ventricular fibrillation (VF)<sup>1</sup>. When VF occurs in the absence of myocardial ischemia, structural heart disease, or an inheritable arrhythmia syndrome, it is referred to as idiopathic ventricular fibrillation (IVF)<sup>2</sup>. Despite being rare, IVF may occur in families. When it does, the clinical scenario is difficult. In the absence of unprovoked or provoked risk indicators (e.g., QT prolongation, ventricular hypertrophy, type 1 Brugada ECG), identifying family members of the index patient who are also at risk for VF is impossible. Despite our earlier finding of an association between familial IVF and a risk haplotype on chromosome 7q36 (which harbors the *DPP6* gene)<sup>3</sup>, identification of patients at risk for IVF remains challenging<sup>4</sup>. Besides confirmation of the 7q36 risk haplotype, no clinical parameters to guide treatment have yet been defined<sup>5</sup>. Our current treatment strategy for asymptomatic family members carrying the risk haplotype is empirical and consists of a prophylactic implantable cardioverter-defibrillator (ICD) when the patient belongs to the age group with significantly increased risk for death in previous standardized mortality ratio (SMR) analysis. However, ICD placement is not without risk<sup>6</sup>, and in a young population the risk–benefit ratio can be unfavorable<sup>7–9</sup>. Therefore, a continued effort to achieve better risk stratification is mandatory. In this study, in order to identify risk factors for the occurrence of VF in *DPP6* risk haplotype-positive individuals (haplotype-positive), we expanded our knowledge of familial IVF linked to the *DPP6* gene and discuss its (extended) clinical characteristics. In addition, its relationship with the Purkinje network is further explored.

## METHODS

### Study population

Demographic and clinical parameters were collected from haplotype-positives and their family members referred to our cardiogenetics outpatient clinic for *DPP6* haplotype screening through December 2014. The risk haplotype is currently bordered by single nucleotide polymorphisms rs7803838 and rs10232716 in the noncoding region of the *DPP6* gene and is 548kB in length. The previously reported variant in the risk haplotype (c.1–340C4T in isoform 2) is still retained<sup>3</sup>. Cascade screening using haplotype analysis also detects obligate haplotype-positive and haplotype-negative individuals, and these were included. Individuals with otherwise unexplained SCD at age of 50 years were defined as haplotype-positive if they had a first-degree family member who carried the risk haplotype (i.e., they already had 50% chance of carrying the risk haplotype). Clinical follow-up was collected for the occurrence of all-cause mortality, aborted cardiac arrest, or unexplained SCD. Writ-

ten informed consent, approved by the institutional ethics committee, was obtained from patients referred for haplotype screening before DNA analysis.

### Resting ECG analysis

In individuals >15 years of age without signs of other heart disease (e.g., Q waves or left bundle branch block [LBBB]), the first available resting ECG with sinus rhythm in the absence of antiarrhythmic drugs was analyzed. Measurement of all parameters (heart rate, PQ interval, QRS duration, QT interval) was performed manually onscreen, in lead II whenever possible, using ImageJ (<http://rsb.info.nih.gov/ij/>). Parameters were averaged from up to three consecutive beats with similar preceding RR intervals. For QT, the tangent method with Bazett correction was used<sup>10</sup>. An early repolarization pattern was also recorded<sup>2</sup>.

### Arrhythmia analysis

To determine arrhythmias characteristics, ventricular tachycardia (VT)/VF on ICD and ECGs were collected. ICD carriers were categorized into two groups: (1) patients with previous VT/VF with a secondary prevention ICD; and (2) asymptomatic family members carrying the *DPP6* haplotype in the age range considered to be at risk who received a primary prevention ICD<sup>5</sup>.

### Cardiac magnetic resonance

Cardiac magnetic resonance (CMR) analysis was performed in *DPP6* risk haplotype-positives and in controls. Some haplotype-positive individuals already received an ICD, thus precluding additional CMR. A CMR control group of sufficient size and matched for age and gender was created using three patient groups: (1) *DPP6* family members who underwent CMR imaging performed before they were found not to carry the risk haplotype; (2) patients referred to our cardiogenetics outpatient clinic because of a family history of SCD, who had an unremarkable clinical workup, including CMR, and were found not to carry the SCD-associated familial mutation; and (3) patients with a normal ECG, without hypertension, who were referred to our outpatient clinic for thoracic complaints and underwent CMR to rule out ischemic heart disease and were found not to have ischemic heart disease. The following parameters were determined for both the left ventricle (LV) and right ventricle (RV): LV and RV end-diastolic volume, LV and RV endsystolic volume, and LV and RV stroke volume. Each was normalized for body surface area ( $0.20247 \cdot \text{length} [\text{m}]^{0.725} \cdot \text{weight} [\text{kg}]^{0.425}$ ) and LV and RV ejection fraction. In addition, LV end-diastolic wall thickness, LV and RV wall-motion abnormalities, hypertrabecularization, and presence of late enhancement after administration of gadolinium were assessed.

## Statistical analysis

Continuous variables are presented as mean $\pm$ SD and analyzed with the unpaired t-test in case of a normal distribution, or presented as the median with range in case of a skewed distribution and analyzed by the Mann-Whitney U-test. Categorical variables are presented as frequencies with percentages and comparisons between groups analyzed by the Fisher exact test. Cumulative event rates for haplotype-positive vs. haplotype-negative individuals and men vs. women are displayed in survival plots and compared with the log-rank test. Follow-up in this analysis was censored at the time of first event or at December 2014. Observed mortality of haplotype-positives was compared with the expected mortality of the Dutch general population obtained from Statistics Netherlands and standardized for age, gender, and calendar period as described in earlier studies<sup>11</sup>. The SMR is the ratio of observed-to-expected mortality and was assessed from birth until death due to all causes or end of follow-up.

## RESULTS

### Baseline characteristics

A total of 601 individuals of 26 *DPP6* distantly related families were included for demographic analysis (Table 1). Mean age was 49 $\pm$  19 years, and there were 286 (48%) haplotype-positive and 315 (52%) haplotype-negative individuals. In 20 additional patients, the risk status could not be determined with certainty because they harbored a recombination within the risk haplotype and had to be excluded from analysis (Figure 1). Successfully resuscitated patients (n=24) did not have signs of other inheritable arrhythmia syndromes after a rigorous screening protocol, which included resting ECG, exercise tests, imaging, and provocation-testing<sup>4</sup>; therefore, we have not continued with regular Holter monitoring and/or exercise testing in asymptomatic patients.

### ECG analysis

For ECG analysis, 396 individuals were included, of whom 167 (42%) haplotype-positives. In 152 individuals, no ECG was available because they were deceased while diagnosed based on family history (n=90; 78 haplotype-positive) or the ECG was not performed or could not be recovered (n=62; 19 haplotype-positive; Figure 1). Patients were excluded from ECG comparisons (n = 32) if they were <15 years of age (haplotype-positive n=15), had experienced a Q-wave myocardial infarction (haplotype-negative n=5), had right bundle branch block/LBBB (n=6; haplotype-positive n=3), arrhythmias (atrial fibrillation: haplotype-positive n=1; haplotype-negative n=2; atrial tachycardia: haplotype-negative n=1), the suggestion of a cardiomyopathy on ECG (n=5; haplotype-positive n=2), or a technically insufficient ECG (haplotype-positive n=1). ECG-parameters showed no significant



differences between haplotype-positives and haplotype-negatives (Table 1). Particularly, no distinctive ECG abnormalities such as early repolarization, right precordial ST-segment elevation, or QT prolongation were observed.

**Table 1.** Baseline characteristics

	All patients n=601	Haplotype+ n=286	Haplotype- n=315
Mean age	49±19	49±20	49±18
Male(%)	309(51)	153(53)	156(50)
Method of identification			
DNA haplotype		219(77)	309(98)
Obligate		42(15)	6(2)
SCD <50years of age and 1 <sup>st</sup> -degree family member of carrier		25(8)	0(0)
Events			
Death		85(30)	18(6)
SCD		52(62)	1(6)
Other causes		33(39)	17(94)
Resuscitated		24(8)	0(0)
ECG-characteristics	N=396	N=167(42)	N=229(58)
PQ(msec)		153±23	154±25
QRS(msec)		90±12	89±11
QTc (msec)		401±23	397±27
Heart rate(bpm)		71±13	70±14

Bpm=beats per minute, msec=milliseconds, SCD=sudden cardiac death. Data are in mean±SD or number of patients(%).

## CMR

In total, 141 CMRs were analyzed (45% male, mean age at CMR 41±16 years, 100 haplotype-positives and 41 controls [haplotype-negative n=7, healthy control n=34]). Sex and age at time of CMR were not correlated with LV/RV values. Left ventricular end-diastolic wall thickness of the basal septum averaged 8±2 mm for the entire group. RV/LV end-diastolic and end-systolic volumes were larger in haplotype-positives compared to controls ( $P<0.05$ ; Table 2), except for LV end-systolic volume. One haplotype-positive had diffuse hypokinesia of the LV wall. One haplotype-positive had moderate LV hypertrabecularization in addition to mildly dilated LV. Three other haplotype-positive individuals also showed moderate LV hypertrabecularization. In 5 haplotype-positives, RV contractility was moderately reduced. Otherwise, RV systolic function was normal. Thirteen haplotype-positives and 1 control showed RV wall-motion abnormalities, and 1 haplotype-positive had a RV aneurysm. Seventeen patients, all haplotype-positive, had RV dilation. Four of these patients and 8 other patients (7 haplotype-positive) had RV hypertrabecularization.

Five patients (4 haplotype-positive) showed delayed enhancement (predominantly septal). Haplotype-positives who experienced an aborted sudden cardiac arrest (aSCA) had no statistical differences in CMR parameters compared to haplotype-positives without events, and the LV/RV volumes of those with aSCA were distributed throughout the whole range of RV/LV volumes (Figure 2).

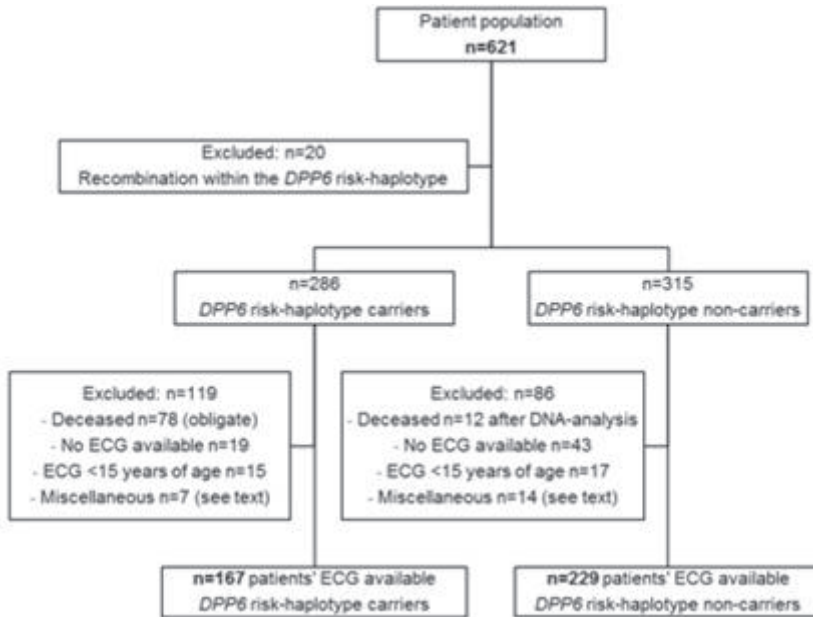
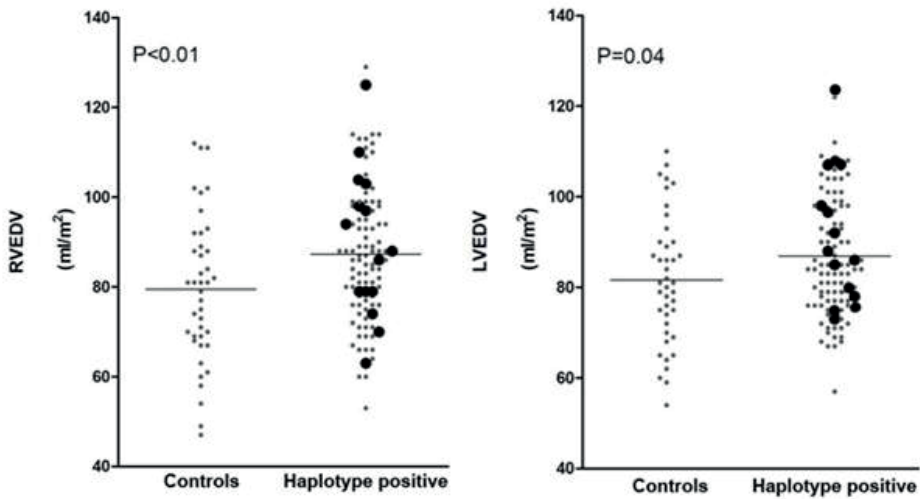


Figure 1. Flow chart of ECG analysis.

Table 2. CMR diagnostics of all individuals and DPP6 risk-haplotype+ with or without an event.

	All patients n=141	Haplotype+, n=100	Controls n=41	P-value	Haplotype+, no event n=85	Haplotype+, with event n=15	P-value
LVEDV	85±14	87±13	82±14	0.04	86±13	92±15	0.19
LVESV	38±8	39±7	37±8	0.14	38±8	42±6	0.09
LVSV	47±8	48±7	45±8	0.04	48±7	50±10	0.28
LVEF(%)	55±4	56±4	55±4	0.70	56±4	54±3	0.31
RVEDV	85±16	87±15	79±16	<.01	87±15	90±17	0.46
RVESV	38±10	40±9	35±10	0.01	40±9	40±9	0.76
RVSV	47±8	48±8	44±8	0.02	47±7	50±10	0.28
RVEF(%)	55±5	55±5	56±5	0.16	55±5	55±5	0.71

Volumes indexed to BSA(ml/m<sup>2</sup>). BSA=body surface area, EDV=end diastolic volume, EF=ejection fraction, ESV=end systolic volume, LV=left ventricle, RV=right ventricle, SV=stroke volume



**Figure 2.** Graphs showing right ventricular end-diastolic volume (RVEDV) and left ventricular end-diastolic volume (LVEDV) of controls and DPP6 risk-haplotype-positive individuals. The X-axis shows individuals (haplotype-positives and controls in separate scatter plots) and the Y-axis the volume corrected for body surface area (ml/m<sup>2</sup>). Haplotype-positives with an event are marked (black dots).

### Ajmaline provocation testing

In 14 patients (10 haplotype-positive), Brugada syndrome provocation testing with ajmaline was performed for diagnostic evaluation of aSCA or family screening. All but 1 patient had a negative test. This particular patient inherited the *DPP6* risk haplotype from his mother but also inherited an *SCN5A* variant from his father, the latter being the likely cause of the positive test. Two patients, both haplotype-positive with a history of aSCA, showed nonsustained VT (LBBB configuration) after administration of ajmaline, and the test was prematurely terminated without development of a type 1BrS ECG. In another patient, ajmaline was successfully attempted to provoke ventricular ectopy during an ablation procedure. Hence, in 3 symptomatic haplotype-positive patients, ajmaline elicited arrhythmias.

### Events and mortality

Twenty-four individuals (all haplotype-positive) experienced aSCA (median age 33 years). Fifty-two haplotype-positive (including 18 obligate haplotype-positive and 25 first-degree family members of a haplotype-positive with SCD <50 years of age) died of SCD (median age 40 years). Thirty-three haplotype-positive individuals died from all causes (median age 69 years), which resulted in a total of 109 events (38%) in the haplotype-positive group. In the haplotype-negative group, 17 patients died from all causes (median age 67 years), and 1 SCD was reported at age 45 years (18 total events [6%]). Median survival of haplotype-positives was significantly decreased compared to haplotype-negatives: 70 years (95%

confidence interval [CI] 64–77 years) vs 93 years (95% CI 81–106 years,  $P < .01$ ; Figure 3). In the haplotype-positives, males had significantly more events than females ( $P < .01$ ; Figure 4). Median survival was 63 years for males vs 83 years for females ( $P < .01$ ). No specific trigger was associated with arrhythmias, but most occurred in resting situations or during sleep. In 286 confirmed or obligate haplotype-positives, 95 deaths were observed in 12,938 person-years between 1879 and 2010. Mean SMR for all haplotype-positives of all ages was significantly increased 1.8 (95% CI 1.4–2.1). In particular, SMR was significantly increased between the ages of 20 and 29 years (SMR 8.5, 95% CI 5.0–13.4), 30 and 39 years (SMR 12.3, 95% CI 8.0–18.2), and 40 and 49 years (SMR 5.3, 95% CI 3.0–8.5; Figure 5).

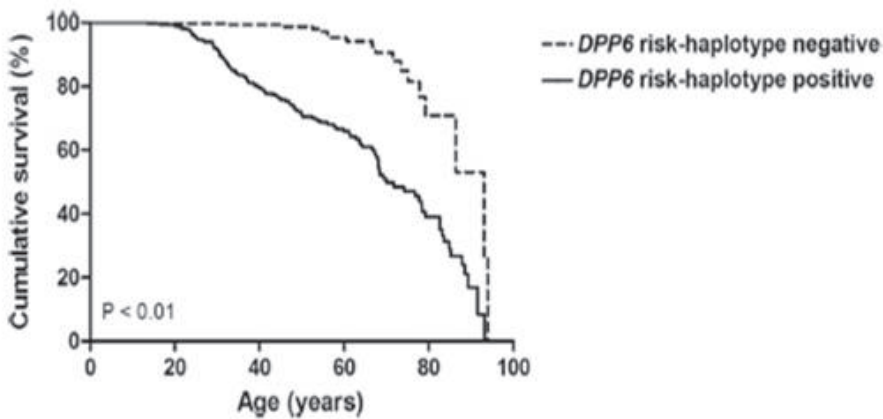


Figure 3. Survival curve showing mortality or cardiac arrest of DPP6 haplotype+ and haplotype-.

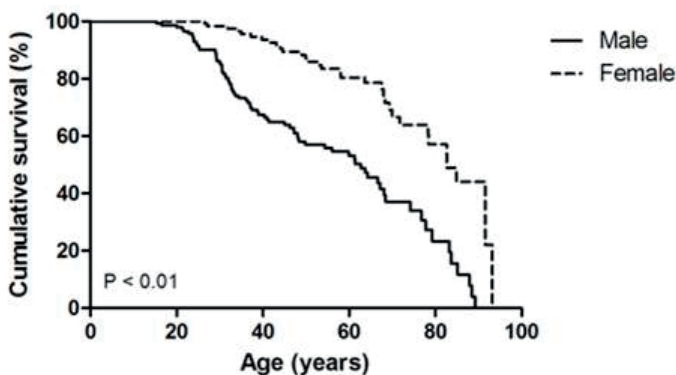
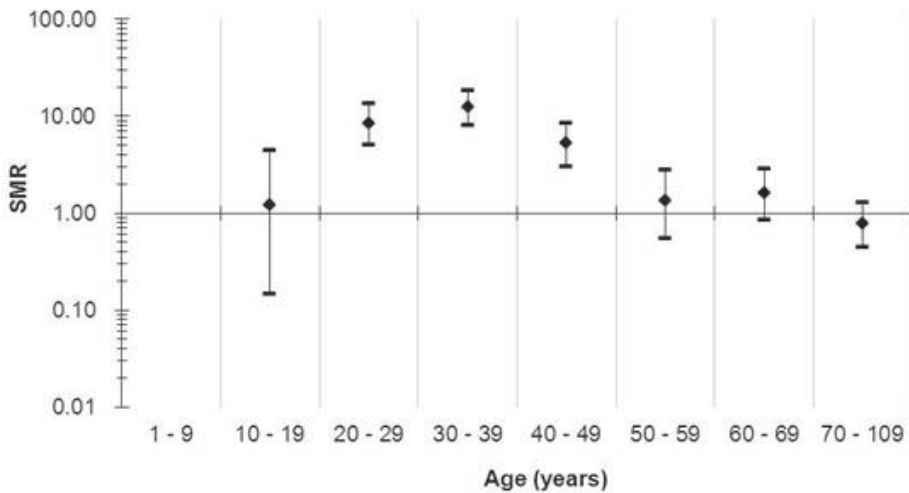


Figure 4. Survival curve showing mortality or cardiac arrest of males and females carrying the DPP6 risk-haplotype.



**Figure 5.** Mortality in 286 DPP6 risk-haplotype+. The mortality to age categories are expressed as standardized mortality ratio (SMR) and depicted as a point estimate. The 95%CI are depicted around the point estimates.

### ICD implantation and arrhythmias

Ninety-five patients received an ICD (mean age at implantation  $36 \pm 11$  years; 51 males [54%]; 72 for primary prevention [76%]). During follow-up of  $5 \pm 3$  years, 19 patients (18%), all except 2 implanted for secondary prevention, had 1 or more appropriate shocks. Thirteen patients received multiple shocks (8 during electrical storm). Five patients (5%) received inappropriate shocks and 3 (3%) appropriate as well as inappropriate shocks. Most inappropriate shocks occurred on T-wave oversensing. Other device-related problems occurred in 7 patients (7%), including infection (1), left cephalic vein thrombosis (3), pneumothorax (1), lead fracture (1), and perforation (1). In 13 patients with aSCA, ECGs of recurrent spontaneous IVF and/or ICD electrograms preceding IVF were available. All VF episodes were initiated by a monomorphic short-coupled ventricular extrasystole (mean coupling interval 247 ms) encroaching around the peak of the T wave, the origin of which could be determined in a subset of patients with available 12-lead ECG ( $n=5$ ). The ectopy appeared to derive solely from the RV apex/lower free wall with LBBB morphology and left axis (Table 3). In only 1 patient (patient I) was the coupling interval longer, but this patient used quinidine. Mean heart rate before IVF onset was  $100 \pm 14$  bpm. Most patients with electrical storms responded well to quinidine ( $n=6$ ), which resulted in less frequent VF episodes and diminishing of ventricular extrasystoles. In a few cases intravenous amiodarone also had favorable effects, although this drug could not prevent the death of 1 haplotype-positive individual during VF storm. Four patients underwent ablation to eliminate ventricular extrasystoles. In 2 of these patients there was 2-year event-free follow-up.

In 2 patients ablation was not successful. However, after quinidine and beta-blockers, IVF occurred significantly less often than before.

**Table 3.** Recorded arrhythmias of 13 individuals with the DPP6 risk-haplotype.

ID	Age	Gender	ECG/ICD	Heart rate	VES morphology	VES axis	VES coupling-interval initiating VT/VF
A	24	Male	ECG/ICD	97	LBBB	Left	220
B	17	Male	ECG	103	LBBB	Left	270
C	50	Male	ECG	100	LBBB	Left/normal	280
D	35	Male	ECG	95	LBBB	Left	180
E	34	Male	ICD	122	monomorphic	NA	190
F	31	Male	ICD	98	monomorphic	NA	270
G	29	Male	ICD	89	monomorphic	NA	230
H	36	Female	ICD	99	monomorphic	NA	220
I	33	Male	ECG	113	LBBB	Left	350*
J	25	Male	ICD	96	monomorphic	NA	235
K	33	Male	ICD	68	monomorphic	NA	295
L#	46	Male	ICD	120	monomorphic	NA	190
M#	39	Male	ICD	110	Monomorphic	NA	290

ECG=electrocardiogram, ICD=implantable cardioverter defibrillator, LBBB=left bundle branch block, NA=not applicable, VES=ventricular extra systole. \*Patient using quinidine. # ICD for primary prevention.

### (Aborted) SCA population analysis

We sought to assess possible differences between haplotype-positives who experienced an aSCA or died of a cardiac arrest (n=286; cardiac events n=76) compared to currently still asymptomatic haplotype-positives. As seen earlier in the survival analysis (Figure 4), gender was an independent predictor for events. Analysis of haplotype-positives with available ECGs (n=167; cardiac events n=27) revealed no distinctive ECG abnormalities. Presence of early repolarization was also not indicative of occurrence of a cardiac event (also not just before the arrhythmia). CMR measured in the subset of haplotype-positives with CMR (n=100; cardiac events n=15) also did not reveal clinically useful distinction features to support risk stratification (Table 2).

## DISCUSSION

Familial IVF represents a severe subset of inheritable arrhythmia syndromes that is difficult to manage in clinical practice<sup>12</sup>. Until recently, no intermediate risk markers were available for risk stratification in asymptomatic family members of patients who experienced (aborted) SCD. However, in 2009 we described an association with a risk haplotype on

chromosome 7 including the *DPP6* gene<sup>3</sup> and demonstrated higher *DPP6* expression in *DPP6* risk haplotype-positive individuals. Determining this *DPP6* risk haplotype has subsequently been used as the only available intermediate marker for increased risk of malignant arrhythmias and sudden death in these families. Through extensive cascade screening and genotyping of many (familial) IVF cases in The Netherlands, we have now extended our knowledge of the families carrying this founder mutation to 4600 family members in the last 6 generations<sup>13, 14</sup>. To pursue better risk stratification of asymptomatic family members, we examined all available clinical data (including ECG, ajmaline provocation, exercise testing, and CMR). However, despite our extensive analysis, the complexity in identifying asymptomatic IVF family members at risk for future arrhythmias based on clinical parameters is once more demonstrated. After intensive analysis of all clinical parameters obtained, no relevant differences between haplotype-positive and haplotype-negative individuals were observed. ECG analysis revealed no distinctive markers. CMR did show slightly larger RV/LV volumes in haplotype-positives, with the largest differences in the RV, so there appears to be a tendency toward mild structural abnormalities. However, these differences were still within the normal range<sup>15</sup>, and haplotype-positive individuals who had experienced an aSCA showed volumes that overlapped the entire spectrum of haplotype-positives and controls (Figure 5), making these differences clinically less relevant and prohibiting discriminative cutoff values useful in primary prevention ICD decision-making. Also, during subanalysis of only the more severely affected male patients or patients  $\leq 40$  years, no cutoff values could be determined. Notwithstanding, these analyses were performed in a subset of haplotype-positives with low event numbers. We cannot rule out that, during longer follow-up, more events will occur and that  $\geq 1$  risk factors, alone or in combination, will surface to support useful cutoff values because only 2 asymptomatic individuals (both males) with a primary ICD implant developed VF 2.5-7 years later (typical onset with short-coupled extrasystole). Hence, at this time we still can only rely on genetic analysis for risk stratification, which is an unique situation. Nonetheless, we also explanted ICDs in 4 patients when they were found not to carry the risk haplotype. This clearly demonstrates the importance of identification of the causal genetic substrate in IVF. Currently, the only treatment option available for asymptomatic haplotype-positive individuals is ICD implantation. ICD implantation is advised for these patients between approximately 20 and 50 years, based on our previous and current survival analysis<sup>5</sup>. During  $5 \pm 3$  years follow-up, one family member experienced an aborted cardiac arrest just before he had undergone presymptomatic genetic testing, and to date only two appropriate interventions have been recorded in all other presymptomatically tested (and treated) family members. The lack of frequent appropriate shocks in this population calls for a continued debate regarding the need for prophylactic ICD implantation and demands better risk markers because implantation is not without risk<sup>6</sup>. Some haplotype-positives did experience inappropriate shocks and/or implantation-related complications indicating possible harm, as we described previously<sup>8</sup>. To our knowledge, no

patients with this *DPP6* haplotype have been identified outside The Netherlands. However, Sturm et al.<sup>16</sup> recently identified a coding variant of *DPP6* in a proband with recurrent IVF, which increases the relevance of the *DPP6* gene worldwide. Yet, this variant was also rather frequently (0.5%) occurring in a control population without that specific phenotype, resulting in a challenging identification of supposedly pathogenic variants. Moreover, as described earlier<sup>17</sup>, 25% of IVF patients have similar short-coupled extrasystoles (encroaching around the peak of the T wave) from the RV with preceding Purkinje potentials and resulting in IVF, suggesting a similar arrhythmia mechanism. It could indeed be that the mechanism of these VT/VF-initiating short-coupled ventricular extrasystoles is similar but is associated with other *DPP6* variants or even other genetic defects impacting on the Purkinje fiber Ito. In search for other therapeutic possibilities in patients with IVF, Knecht et al.<sup>18</sup> described the effect of ablation in a subset of patients with frequent episodes of ventricular arrhythmias, with an almost 100% event-free 52-month follow-up after ablation therapy. In our population, 4 *DPP6* patients with arrhythmic storm(s) underwent ablation therapy to decrease extrasystoles, recurrent VT/VF storm, and ICD shocks, with varying success.

During recurrent IVF, the therapeutic options are limited to suppression of subsequent arrhythmias. Administration of quinidine and/or isoprenaline does have a positive therapeutic effect in most cases. Patients on longterm quinidine treatment also have shown suppression of subsequent arrhythmias. In this respect, the worldwide difficulties regarding access to quinidine are extremely troublesome<sup>19</sup>. The exact arrhythmogenic mechanism under conditions when *DPP6* overexpression causes IVF is still not completely elucidated, but there is sound evidence that this overexpression preferably increases transient outward potassium current ( $I_{to}$ ) in the Purkinje network more so than in ventricular cardiomyocytes<sup>20</sup>. Increased Ito alters Purkinje action potentials by causing a more negative phase 1 and an abnormal plateau phase<sup>21</sup>. *DPP6* overexpression does not result in discernible ECG changes, as Purkinje activity is not recorded on the surface ECG. From our ECG and ICD registrations we can conclude that IVF associated with the *DPP6* risk haplotype is always elicited by monomorphic short-coupled extrasystoles from the RV apex/lower free wall. The few ablation examples of these patients show that these extrasystoles are preceded by Purkinje potentials and that ablation at these sites results in suppression of subsequent IVF episodes. Nonetheless, the question of how these short-coupled afterdepolarizations can excite the surrounding cardiac tissue remains. It could be that reopening of calcium channels in the Purkinje network finds the surrounding tissue excitable and results in initiation of VF.

### Study limitations

Importantly, a limitation of this study could be that the CMR control group was largely based on patients unrelated to the *DPP6* family. It might be that the observed differences, although largely within reference values and without clinical phenotypes, were obtained



because the haplotype-positives were not solely compared to their haplotype-negative family members. Another limitation is that we did not routinely perform Holter monitoring and exercise tests in all family members, which limited our ability to analyze the prognostic relevance of ventricular extrasystoles in the absence of VF. The lack of a significant number of extrasystoles, especially short-coupled extrasystoles, during our rigorous screening protocol in cardiac arrest survivors inhibited us from pursuing Holter monitoring and exercise tests in the remaining family members. Based on the ICD and ECG recordings of spontaneous VF, the episodes of VF could be triggered by single short-coupled extrasystoles, but occasionally we also observed more short-coupled single extrasystoles only in the minutes before the onset of VF. Also, in those patients who presented with repeated arrhythmic episodes, extrasystoles were rarely abundantly present (an important complicating factor in ablation attempts).

## CONCLUSION

Familial IVF remains a disease entity that is difficult to manage in clinical practice. Even after extensive analysis of a relatively large number of symptomatic patients and a large numbers of family members of IVF patients linked to the *DPP6* locus, we were unable to identify clinical parameters linked to SCD/SCA-risk other than their genetic predisposition. Therefore, the importance of better mechanistic understanding of this lethal disease caused by the *DPP6* risk haplotype on chromosome 7 remains mandatory to better guide prophylactic treatment.

## CLINICAL PERSPECTIVES

This study represents a detailed analysis of one of the largest unique founder mutations described in the medical literature, investigating >600 patients from six generations in 26 distantly related families. These patients are subjected to an extremely difficult disease entity: familial idiopathic ventricular fibrillation. Difficulties arise in our inability to recognize any clinical markers that presymptomatically identify those at risk for malignant arrhythmias and sudden cardiac death at a young age, thereby hampering targeted prophylactic treatment. In a subset of these families, we previously identified a risk haplotype linked to the *DPP6*-gene that, uniquely, appeared to be the only risk marker for cardiac events. In an effort to improve patient care, we extended our analysis in these families, including a nearly 4-fold increase in investigated family members and follow-up of  $5\pm 3$  years. Nonetheless, our extensive analysis of the data, including ECG-analysis, provocation testing, and cardiac magnetic resonance imaging, did not reveal any useful clinical

discriminative tool to assess risk in family members who have not yet been resuscitated, apart from their genetic predisposition and their age between 20 and 50 years. Thus, this finding still leaves us advising prophylactic cardioverter-defibrillator implantation in these young patients, with its associated morbidity and without more precise assessment of risk. Therefore, the importance of better mechanistic understanding of this lethal disease caused by the *DPP6* risk haplotype on chromosome 7 remains mandatory to better guide prophylactic treatment.

## REFERENCES

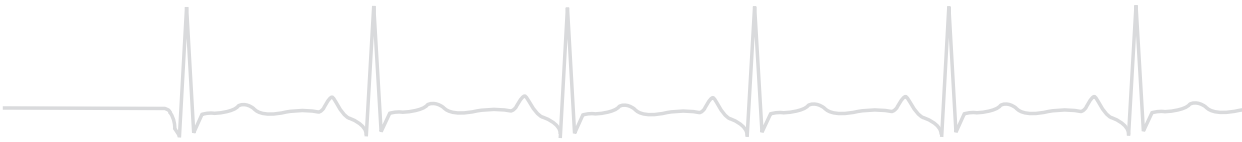
1. Wellens HJ, Schwartz PJ, Lindemans FW, Buxton AE, Goldberger JJ, Hohnloser SH, Huikuri HV, Kaab S, La Rovere MT, Malik M, Myerburg RJ, Simoons ML, Swedberg K, Tijssen J, Voors AA and Wilde AA. Risk stratification for sudden cardiac death: current status and challenges for the future. *Eur Heart J* 2014;35:1642-51.
2. Priori SG, Wilde AA, Horie M, Cho Y, Behr ER, Berul C, Blom N, Brugada J, Chiang CE, Huikuri H, Kannankeril P, Krahn A, Leenhardt A, Moss A, Schwartz PJ, Shimizu W, Tomaselli G and Tracy C. Executive Summary: HRS/EHRA/APHRS Expert Consensus Statement on the Diagnosis and Management of Patients with Inherited Primary Arrhythmia Syndromes. *Heart Rhythm* 2013.
3. Alders M, Koopmann TT, Christiaans I, Postema PG, Beekman L, Tanck MW, Zeppenfeld K, Loh P, Koch KT, Demolombe S, Mannens MM, Bezzina CR and Wilde AA. Haplotype-sharing analysis implicates chromosome 7q36 harboring DPP6 in familial idiopathic ventricular fibrillation. *Am J Hum Genet* 2009;84:468-476.
4. van der Werf C, Hofman N, Tan HL, van Dessel PF, Alders M, van der Wal AC, van Langen IM and Wilde AA. Diagnostic yield in sudden unexplained death and aborted cardiac arrest in the young: the experience of a tertiary referral center in The Netherlands. *Heart Rhythm* 2010;7:1383-1389.
5. Postema PG, Christiaans I, Hofman N, Alders M, Koopmann TT, Bezzina CR, Loh P, Zeppenfeld K, Volders PG and Wilde AA. Founder mutations in the Netherlands: familial idiopathic ventricular fibrillation and DPP6. *Neth Heart J* 2011;19:290-296.
6. van Rees JB, de Bie MK, Thijssen J, Borleffs CJ, Schalij MJ and van EL. Implantation-related complications of implantable cardioverter-defibrillators and cardiac resynchronization therapy devices: a systematic review of randomized clinical trials. *J Am Coll Cardiol* 2011;58:995-1000.
7. Tung R, Zimetbaum P and Josephson ME. A critical appraisal of implantable cardioverter-defibrillator therapy for the prevention of sudden cardiac death. *J Am Coll Cardiol* 2008;52:1111-1121.
8. Olde Nordkamp LR, Wilde AA, Tijssen JG, Knops RE, van Dessel PF and de Groot JR. The ICD for primary prevention in patients with inherited cardiac diseases: indications, use, and outcome: a comparison with secondary prevention. *Circ Arrhythm Electrophysiol* 2013;6:91-100.
9. Sacher F, Probst V, Maury P, Babuty D, Mansourati J, Komatsu Y, Marquie C, Rosa A, Diallo A, Cassagneau R, Loizeau C, Martins R, Field ME, Derval N, Miyazaki S, Denis A, Nogami A, Ritter P, Gourraud JB, Ploux S, Rollin A, Zemmoura A, Lamaison D, Bordachar P, Pierre B, Jais P, Pasquie JL, Hocini M, Legal F, Defaye P, Boveda S, Iesaka Y, Mabo P and Haissaguerre M. Outcome after implantation of a cardioverter-defibrillator in patients with brugada syndrome: a multicenter study-part 2. *Circulation*. 2013;128:1739-1747.
10. Postema PG, De Jong JS, Van der Bilt IA and Wilde AA. Accurate electrocardiographic assessment of the QT interval: teach the tangent. *Heart Rhythm* 2008;5:1015-1018.
11. Nannenberg EA, Sijbrands EJ, Dijkman LM, Alders M, van Tintelen JP, Birnie M, van Langen IM and Wilde AA. Mortality of inherited arrhythmia syndromes: insight into their natural history. *Circ Cardiovasc Genet* 2012;5:183-189.
12. Viskin S and Belhassen B. Idiopathic ventricular fibrillation. *Am Heart J* 1990;120:661-671.
13. Postema PG, Van den Berg M, van Tintelen JP, Van den Heuvel F, Grundeken M, Hofman N, Van der Roest WP, Nannenberg EA, Krapels IP, Bezzina CR and Wilde A. Founder mutations in the Netherlands: SCN5a 1795insD, the first described arrhythmia overlap syndrome and one of the largest and best characterised families worldwide. *Neth Heart J* 2009;17:422-428.

14. Crotti L, Monti MC, Insolia R, Peljto A, Goosen A, Brink PA, Greenberg DA, Schwartz PJ and George AL, Jr. NOS1AP is a genetic modifier of the long-QT syndrome. *Circulation*. 2009;120:1657-1663.
15. Hudsmith LE, Petersen SE, Francis JM, Robson MD and Neubauer S. Normal human left and right ventricular and left atrial dimensions using steady state free precession magnetic resonance imaging. *J Cardiovasc Magn Reson* 2005;7:775-782.
16. Sturm AC, Kline CF, Glynn P, Johnson BL, Curran J, Kilic A, Higgins RS, Binkley PF, Janssen PM, Weiss R, Raman SV, Fowler SJ, Priori SG, Hund TJ, Carnes CA and Mohler PJ. Use of whole exome sequencing for the identification of Ito-based arrhythmia mechanism and therapy. *Journal of the American Heart Association*. 2015;4.
17. Haissaguerre M, Shoda M, Jais P, Nogami A, Shah DC, Kautzner J, Arentz T, Kalushe D, Lamaison D, Griffith M, Cruz F, de PA, Gaita F, Hocini M, Garrigue S, Macle L, Weerasooriya R and Clementy J. Mapping and ablation of idiopathic ventricular fibrillation. *Circulation*. 2002;106:962-967.
18. Knecht S, Sacher F, Wright M, Hocini M, Nogami A, Arentz T, Petit B, Franck R, De CC, Lamaison D, Farre J, Lavergne T, Verbeet T, Nault I, Matsuo S, Leroux L, Weerasooriya R, Cauchemez B, Lellouche N, Derval N, Narayan SM, Jais P, Clementy J and Haissaguerre M. Long-term follow-up of idiopathic ventricular fibrillation ablation: a multicenter study. *J Am Coll Cardiol* 2009;54:522-528.
19. Viskin S, Wilde AA, Guevara-Valdivia ME, Daoulah A, Krahn AD, Zipes DP, Halkin A, Shivkumar K, Boyle NG, Adler A, Belhassen B, Schapachnik E, Asrar F, Rosso R, Fadreguilan EC, Veltman C, Veerakul G, Marquez M, Juneja R, Daoulah AN, Caorsi WR, Cuesta A, Jensen HK, Hamad AK, Spears D, Lozano IF, Urda VC, Peinado R, Panduranga P, Emkanjoo Z, Bergfeldt L and Janousek J. Quinidine, a life-saving medication for Brugada syndrome, is inaccessible in many countries. *J Am Coll Cardiol* 2013;61:2383-2387.
20. Radicke S, Cotella D, Graf EM, Ravens U and Wettwer E. Expression and function of dipeptidyl-aminopeptidase-like protein 6 as a putative beta-subunit of human cardiac transient outward current encoded by Kv4.3. *J Physiol*. 2005;565:751-756.
21. Xiao L, Koopmann TT, Ordog B, Postema PG, Verkerk AO, Iyer V, Sampson KJ, Boink GJ, Mamarbachi MA, Varro A, Jordaens L, Res J, Kass RS, Wilde AA, Bezzina CR and Nattel S. Unique Cardiac Purkinje Fiber Transient Outward Current beta-Subunit Composition: A Potential Molecular Link to Idiopathic Ventricular Fibrillation. *Circ Res* 2013;112:1310-1322.



# **PART II**

## **Characteristics of Arrhythmogenic Substrates of Ventricular Arrhythmias**



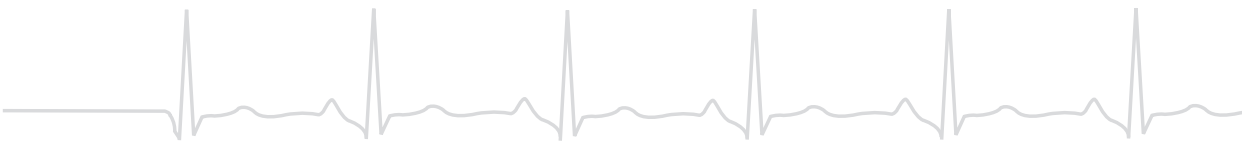


# CHAPTER 5

## Differences in left ventricular remodeling between patients with ischemic and dilated cardiomyopathy

Judith N. ten Sande, Faiz Z. Ramjankhan, Shirley C.M. van Amersfoort, Jaap R. Lahpor,  
Ingeborg van der Made, Esther E. Creemers, Pascal F.H.M. van Dessel, Nicolaas de Jonge,  
Jacques M.T. de Bakker

*In preparation*





## ABSTRACT

### Introduction

In patients with congestive heart failure (CHF) a major cause of death is sudden cardiac death (SCD). The mechanism of related ventricular arrhythmias is different for the etiology of CHF and the relation with the diseased-induced remodeling is unclear. This study will focus on the differences in substrate in end stage heart failure in patients with ischemic (ICM) and dilated cardiomyopathy (DCM).

### Methods

Tissue samples of 15 patients who were eligible for a left ventricular assist device (LVAD) because of end stage heart failure, were collected during LVAD implantation. Collagen, Connexin43, KCNH2, KCNQ1 and miRNA133 expression were determined.

### Results

No differences in clinical parameters were found between patients with ICM or DCM. For ICM and DCM the mean values of collagen were  $47\pm 8\%$  and  $33\pm 12\%$  respectively ( $p=0.07$ ). The ICM samples showed patchy fibrosis, whereas DCM patients showed more diversity of architecture (patchy fibrosis, fibrotic strands as well as compact fibrosis). Cx43 expression did not differ between ICM ( $3.6\pm 0.6\%$ ) compared to DCM ( $4.5\pm 1.2\%$ ,  $p=0.22$ ). However, macro-heterogeneity showed a trend with more heterogeneity in Cx43 expression in patients with DCM (ICM  $0.08\pm 0.00$  and DCM  $0.11\pm 0.02$ ,  $p=0.06$ ). For KCNH2, KCNQ1 and miRNA133 expression, no differences were found.

### Conclusion

Tissue from patients with ICM is characterized by patchy fibrosis and fibrosis tends to be more present in these samples compared to tissue obtained from patients with DCM. Also, Cx43 expression shows more macro-heterogeneity in patients with DCM. These results suggest differences in remodeling between etiology of end stage heart failure.

## INTRODUCTION

Patients with heart failure (HF) are susceptible for ventricular arrhythmias (VA)<sup>1</sup> as a result of structural and electrical remodeling of the ventricular myocardium. Even in the healthy human heart there is electrical heterogeneity in the left ventricular myocardium<sup>2</sup>. This heterogeneity may increase during heart disease. Studies have shown that in diseased hearts reduction in expression of sodium channels<sup>3</sup> and gap junction channels<sup>4</sup> occur, while hypertrophy<sup>5</sup> and interstitial fibrosis<sup>6</sup> are increased. The ionic changes depend on the etiology of the disease<sup>7</sup>. Impaired conduction induced by these changes is a major component for reentry-based VA, but abnormal impulse formation as triggered activity and increased normal or abnormal automaticity may cause rhythm disturbances or act as a trigger in the remodeled hearts as well. Next to the sodium current other depolarizing and repolarizing currents may be remodeled and play a role in arrhythmogenesis. In addition, heart failure is often associated with impaired calcium handling, which prolongs action potential duration and may induce triggered activity<sup>8</sup>. The onset, progress and arrhythmogenic causes and consequences of electrical and structural remodeling are, however, diverse and differ among the etiology of heart failure. Data from patients suggest that the mechanism of VA related with ICM and DCM is different. Pogwizd et al.<sup>9, 10</sup> showed that spontaneous and induced ventricular arrhythmias in patients with idiopathic end-stage HF arise in the subendocardium or subepicardium by a focal mechanism. These investigators showed that both intramural reentry and a focal mechanism underlie sustained VT in patients with healed myocardial infarction. Other mapping studies in patients show that infarct related tachycardia's are mainly based on reentry<sup>11-13</sup>.

Patients with ischemic cardiomyopathy (ICM) often develop VA based on reentry based on anatomic reentry around or through the scar<sup>11</sup>. Triggered activity is more often the underlying mechanism in patients with dilated cardiomyopathy (DCM) where downregulation of repolarizing ion currents is associated with the occurrence of early or delayed after depolarization (EAD, DAD) followed by triggered activity. In late myocardial infarction (6-8 weeks after infarction), connexin43 (Cx43) expression is reduced in areas remote from the infarcted zone and disrupted in the infarct border zone<sup>14</sup>. Sodium current is reduced by approximately 50% depending on the model studied (some report no change), whereas the late sodium current is increased<sup>3</sup>. These altered parameters will impair conduction and may give rise to VA. Also inhomogeneous scarring can occur, resulting in areas of slow conduction, non-uniform anisotropy and channels of conduction, leading to the development of re-entrant ventricular tachycardia<sup>15</sup>. Boulaksil *et al.* concluded from their study in congestive HF-patients that heterogeneous expression of connexin 43 (Cx43) is associated with dispersion in impulse conduction and may underlie enhanced susceptibility to VA<sup>16</sup>.

Non-ischemic DCM is the most common form of cardiomyopathy, but comprises a heterogeneous group of disorders. Histology in DCM is not specific, but shows substantial

myocyte hypertrophy. Focal and interstitial fibrosis as well as “ghost cells”, myocytes without myofibrillary elements, and apoptosis are present. A heterogeneous reduction of Cx43 expression has been reported in patients with DCM<sup>17</sup>. Tissue extracts from patients revealed that the voltage-gated sodium channel was reduced to 30-50% in comparison to controls. These changes may result in conduction abnormalities, ventricular ectopy and non-sustained and/or sustained ventricular tachycardia.

In both cardiomyopathies there is an increase of collagen deposition, although tissue architecture might be different. Accumulation of collagen will result in cardiomyocyte separation, reduction in coupling between the cells and impaired conduction. In this respect, the interaction of the collagen/myocyte substrate is important as well<sup>6</sup>. However, reduced cell-to-cell coupling also plays an important role for arrhythmias based on abnormal impulse formation<sup>18</sup>.

Multiple studies have been conducted on tissue architecture and remodeling in end stage heart failure patients. The purpose of this study was to determine possible differences in substrate based on the etiology of heart failure. By biopsies obtained during thoracic surgery we determined differences in (immuno)histological parameters in DCM and ICM.

## METHODS

In 15 patients with end stage HF a tissue sample was collected during left ventricular assist device (LVAD) implantation (HeartMate-II® (Thoratec Corp., Pleasanton, CA, USA) and the HeartWare® HVAD (HeartWare Inc., Framingham, MA, USA)). The study was performed in accordance with the Declaration of Helsinki, and written informed consent was obtained from all patients.

Patient characteristics (e.g. left ventricular ejection fraction (LVEF), occurrence of VA) were collected using medical records.

### Histology and Immunostaining

Myocardial specimen of the left ventricular apex were obtained using a special coring knife, necessary to create an opening for the inflow cannula of the LVAD. Part of this tissue sample was snap-frozen in liquid nitrogen for transportation and was stored at -80° Celsius. Frozen tissue was cut with a cryotome into tissue sections.

Tissue sections of 7 µm thickness were incubated with Sirius red, Cx43 antibodies or α-actinin. Sirius red staining was performed for visualization and quantification of collagen. Rabbit polyclonal anti-Cx43 (Zymed Invitrogen, Breda, The Netherlands) was used for estimation of Cx43 expression and heterogeneity, whereas a mouse monoclonal α-actinin antibody (Sigma-Aldrich) was applied to determine presence of cardiomyocytes. (Immuno) histologic parameters were determined in at least 3 randomly chosen pictures of 5 ran-

domly selected areas at  $\times 20$  magnification of non-overlapping fields. using ImageJ Analysis was carried out by an operator blinded to the origin of the samples (<http://rsb.info.nih.gov/ij/>) and MatLab (The MathWorks Inc., Natick, MA).

### Measurement of collagen content

Photomicrographs of Sirius red stained sections were transformed into RGB and pixels were used in the 256-leveled green channel using a cut-off level between 90 and 190. The percentage of collagen of the total tissue (collagen and cardiomyocytes) was determined. For myocardial architecture, we used the following classification for collagen:

- 1) patchy fibrosis, alteration of wide and long collagen and myocardial fibers, called parallel and long collagen bundles intermingled with islands of cardiomyocytes.
- 2) compact fibrosis; extensive areas of fibrosis virtually deprived of myocardial tissue,
- 3) strands of fibrosis; isolated thick strands of collagen running parallel to myocardial fibers.

### Connexin43

To quantify Cx43 density, photomicrographs of Cx43 sections were transformed into RGB stack and true Cx43 pixels were used in the 256-leveled green channel using a cut-off level of 50. The same procedure was applied for  $\alpha$ -actinin sections to determine Cx43 expression in myocardial tissue only. The expression of Cx43 was determined as the percentage of Cx43 area (pixels) of the  $\alpha$ -actinin area.

Heterogeneity of Cx43 expression was determined using MatLab, as previously described<sup>16</sup>. In short, we followed the following procedure. The Cx43 photomicrographs were converted into 8-bit black and white pictures and background subtraction performed (rolling ball radius in ImageJ was set to 250). Pictures were divided in 1089 squares of equal size. For each square the total intensity of the white signal (number of white pixels) was determined. Mean intensity of all 1089 squares and the standard deviation of the intensity were determined. Micro heterogeneity was defined as the standard deviation divided by the mean value. For global heterogeneity of Cx43 expression the total intensity (number of white pixels) of each of the 15 pictures of a heart was determined. Then, the average/mean intensity and the standard deviation of these intensities of a heart was calculated. Macro-heterogeneity of a heart was defined as this standard deviation divided by the mean intensity.

### mRNA and microRNA

Part of the tissue samples were used to determine mRNA expression of KCNH2 and KCNQ1. The genes encoding the alpha-subunits of potassium channels that carry *IKr* and *IKs*, respectively. GAPDH was used as a housekeeping gene. In addition the following microRNA's were determined: miR133a, miR133b, miR328 and U6. The latter was used as

the housekeeping gene. Tissue samples of healthy controls were analyzed for comparison with tissue of diseased hearts.

RNA was isolated using Trizol (Invitrogen) following the manufacturer's protocol. cDNA was generated of 400 ng input RNA using miScript reverse transcription kit (Qiagen) for miRNAs and Superscript I (Invitrogen) for mRNA, according to the manufacturer's protocol. Real-time PCR was performed using Lightcycler 480 High Resolution Melting Master (HRM-dye, Roche) for mRNA detection and Sybr green master I (Roche) for miRNAs and run on a Lightcycler system II (Roche). The shape of the amplification curve and the melting curves was analyzed using the Lightcycler 480 software (Roche) and quantification of the results was performed using the LinRegPCR quantitative PCR data analysis program<sup>19</sup>.

**Table 1.** Patient characteristics

Patient	Etiology	Sex	EF(%)	Age (years)	VT yes/no	Fibrosis/collagen %	Cx43 expression %	Cx43 Macro	Cx43 Micro
01	ICMP	Male	12	63	no	43	2.97	0.08	0.20
02	ICMP	Male	17	59	yes	42	3.76	0.08	0.27
03	ICMP	Female	15	61	no	56	4.05	0.08	0.27
04	DCM, TTN	Female	13	43	no (nsVT)	51	3.38	0.12	0.26
05	DCM	Male	15	42	no	16	2.83	0.09	0.21
06	DCM	Female	20	64	yes	38	4.21	0.12	0.29
07	DCM, PLN	Female	8	46	yes	46	6.09	0.10	0.32
08	DCM, LMNA/C	Male	24	35	yes	19	3.61	0.11	0.27
09	DCM, TTN	Male	12	50	no (nsVT)	31	4.01	0.08	0.22
10	DCM, TTN	Male	18	69	no (nsVT)	18	5.79	0.10	0.32
11	DCM	Male	15	51	no	28	3.06	0.08	0.29
12	DCM, TTN	Male	12	53	Yes	26	5.15	0.12	0.28
13	DCM	Male	8	60	No	50	5.36	0.10	0.33
14	DCM after chemo/radiation therapy	Female	10	56	No	33	6.31	0.15	0.24
15	DCM	Female	25	47	No	35	4.48	0.09	0.22

Cx: connexin, DCM: dilated cardiomyopathy, EF: ejection fraction, ICMP: ischemic cardiomyopathy, LMNA/C: lamin A/C mutation, TTN: titin mutation, VT: ventricular tachycardia.

## RESULTS

### Patient characteristics

Mean age was  $53 \pm 10$  years and mean LVEF was  $15 \pm 5\%$ . There were no differences between etiology for age and LVEF. In the ICM group one patient had a VT before LVAD implantation. In the DCM group, 3 patients had non-sustained VT and 4 patients had sustained VT. Tissue samples were obtained from all 15 patients; 12 patients with dilated cardiomyopathy and 3 patients with ischemic cardiomyopathy (Table 1).

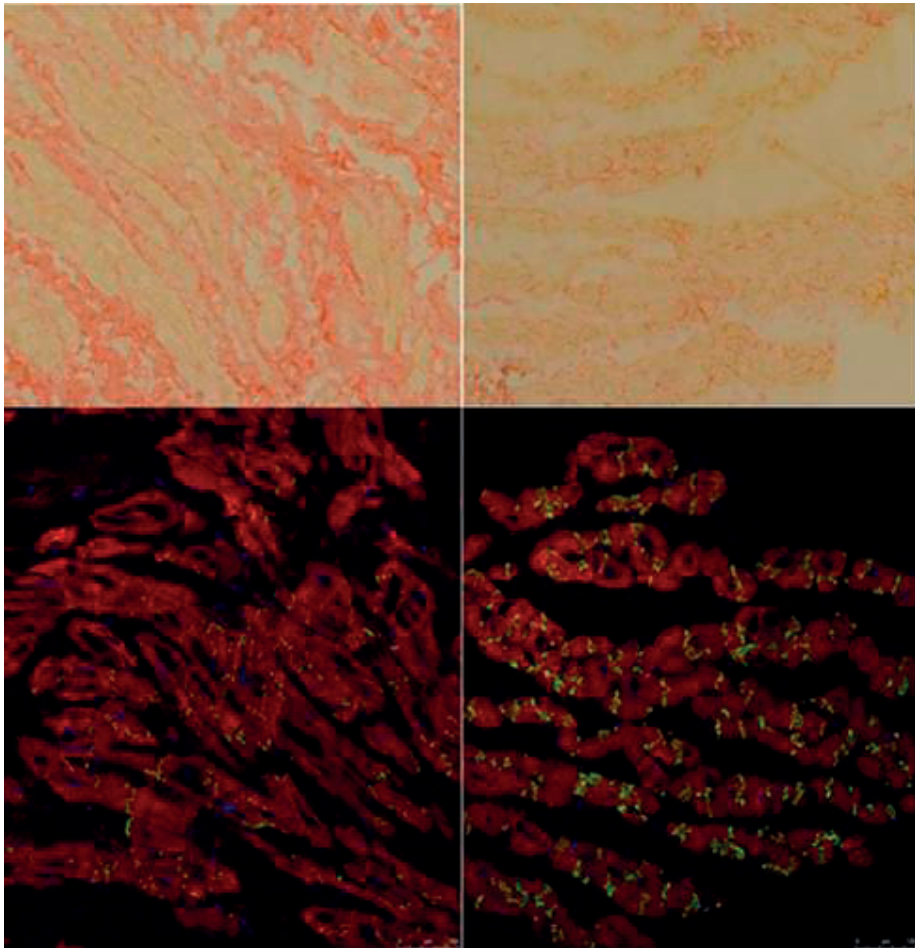


**Figure 1.** Sirius Red staining and Cx43 immunolabeling of left ventricular tissue.

**Upper panel:** Left ventricular Sirius Red staining of ICM (left) and DCM patient demonstrating more patchy fibrosis in patients with ICM.

**Lower panel:** Left ventricular Connexin43 immunolabeling of an ICM (left) and DCM patient. Cx43 showed no differences in Cx43 expression between ICM and DCM. However macro-heterogeneity in Cx43 showed a trend with more heterogeneity in patients with DCM.

## Collagen

The amount of collagen ranged from 16% to 56% with a mean of  $35\pm 13\%$ . For ICM and DCM the mean values were  $47\pm 8\%$  and  $33\pm 12\%$  respectively. Sirius Red staining for the amount of collagen showed no statistical difference between ICM and DCM ( $p=0.07$ , Table 1). In table 2 the tissue architecture of the different cardiomyopathies is shown. Numbers are the number of analyzed sections that revealed the architecture indicated (maximal 15 for each tissue sample). Tissue from patients with ICM is characterized by patchy fibrosis; all tissue samples revealed this type of fibrosis. In two hearts compact fibrosis was present as well. Tissue derived from patients with DCM shows more diversity of tissue architecture; patchy fibrosis, strands as well as compact fibrosis occur (Table 2). Figure 1 shows a typical example of the different amount of collagen in the samples and shows that the architecture of the tissue is different between the etiologies.

## Connexin43 expression and heterogeneity

Analysis of immunolabeling of Cx43 expression did not differ between ICM ( $3.6\pm 0.6\%$ ) compared to DCM ( $4.5\pm 1.2\%$ ) ( $p=ns$ , Table 1). Also, the micro-heterogeneity of Cx43 expression did not differ between the two groups (ICM  $0.25\pm 0.04$  and DCM  $0.27\pm 0.04$ ,  $p=ns$ , Table 1). However, macro-heterogeneity showed a trend with more heterogeneity in Cx43 expression in patients with DCM (ICM  $0.08\pm 0.00$  and DCM  $0.11\pm 0.02$ ,  $p=0.06$ , Table 1).

**Table 2.** Architecture of fibrosis

Patient	Etiology	Patchy fibrosis	Fibrotic strands	Compact fibrosis
1	ICM	15	0	0
2	ICM	15	0	9
3	ICM	15	0	12
4	DCM	14	0	15
5	DCM	0	1	7
6	DCM	2	15	7
7	DCM	1	0	11
8	DCM	0	15	2
9	DCM	0	14	2
10	DCM	0	9	0
11	DCM	0	14	1
12	DCM	0	12	0
13	DCM	15	0	13
14	DCM	0	15	0
15	DCM	0	12	3

DCM: dilated cardiomyopathy, ICM: ischemic cardiomyopathy.

There were no differences between DCM patients with or without VT in relation with fibrosis (32 vs. 33%  $p=ns$ ) and connexin43 (4.8 vs. 4.4%  $p=ns$ ).

### mRNA and microRNA

No differences were seen between mRNA expression for KCNH2 and KCNQ1 between the samples of ICM or DCM patients (Table 3). Also no difference in expression was seen between patients with end stage heart failure and healthy samples. For the selected miRNAs, only the melting curve for miR133a had a good quality. No differences were seen between patients with ICM or DCM (cardiomyopathy) and healthy samples.

**Table 3.** mRNA and miRNA

	ICM	DCM	p-value	Cardiomyopathy	Healthy controls	p-value
KCNH2	1.31±0.62 ×10 <sup>-3</sup> (n=2)	3.41±2.56 ×10 <sup>-3</sup> (n=6)	0.32	2.88±2.38 ×10 <sup>-3</sup> (n=8)	2.84±0.78 ×10 <sup>-3</sup> (n=10)	0.96
KCNQ1	0.94±0.03 ×10 <sup>-3</sup> (n=2)	2.48±0.31 ×10 <sup>-3</sup> (n=7)	0.53	2.14±2.97 ×10 <sup>-3</sup> (n=9)	0.63±0.27 ×10 <sup>-3</sup> (n=10)	0.11
miRNA133a	N=1	N=5		5482±2140 (n=6)	5225±2740 (n=6)	0.86

DCM: dilated cardiomyopathy, ICM: ischemic cardiomyopathy.

## DISCUSSION

In this study we analyzed left ventricular tissue samples of end-stage heart failure patients with ICM or DCM to determine possible differences in structural remodeling.

### Collagen and tissue architecture

Our data show that several remodeled parameters that may enhance arrhythmogenicity in the cardiomyopathic heart do not differ between ICM and DCM. We showed, however, that there was a trend towards more fibrosis in the tissue samples obtained from ICM patients compared to those obtained from patients with DCM. The ICM samples showed more patchy fibrosis. In contrast, tissue samples from DCM patients showed thick fibrotic strands and areas of compact fibrosis, a different type of patchy fibrosis. This finding of differences in architecture between the etiology of heart failure is relevant since the collagen depositions are a substrate for subsequent VA. However, in this study no association was found with VA. Earlier studies have only described fibrosis in cardiomyopathic hearts without making differences between the type of cardiomyopathy<sup>6</sup>. In the current study we were able to differentiate the fibrosis in relation with etiology.



### Connexin43

There were no differences in Cx43 expression between ICM and DCM patients. However the macro-heterogeneity showed a trend with more heterogeneity in Cx43 expression in patients with DCM in comparison to ICM patients. Kitamura et al<sup>17</sup> demonstrated that in DCM the expression of Cx43 is reduced in a heterogeneous way. These observations suggest that differences in the arrhythmogenic substrate are present in ICM and DCM. Cardiomyopathy is accompanied by structural and electrical remodeling. Conduction velocity, reduced cell-to-cell coupling and repolarization are important parameters for arrhythmogenicity. Although reduced conduction velocity will facilitate reentry, increase in the heterogeneity of action potential duration (APD) may promote reentry as well as abnormal impulse formation. The APD prolongation in HF may be antiarrhythmic in terms of reentrant arrhythmias.

In heart failure, Cx43 expression decreases, but we did not observe a difference in Cx43 expression between ICM and DCM. However, we demonstrated that tissue samples from DCM patients showed a trend with more heterogeneity in Cx43 expression compared to ICM patients. This corroborates with earlier studies where increased Cx43 heterogeneity was found to increase the susceptibility for VA<sup>16</sup>.

In the ICM group one patient had a VT before LVAD implantation. In the DCM group, 3 patients had non-sustained VT and 4 patients had sustained VT. Unfortunately, there were no recordings available to analyze these VA. However, these numbers indicate that VA are highly prevalent in end stage HF. No differences in the selected parameters were seen between etiology, suggesting that a trigger should be present for the occurrence of VA.

### RNA and miRNA

No statistically significant differences were seen in the expression of KCNH2, KCNQ1 and miRNA133a. KCNQ1 shows a trend towards higher expression in cardiomyopathy compared to controls, which is in line with observations made by Lundquist<sup>20</sup>. Lack of a significant difference could be a result of the amount of samples analyzed and/or the quality and location (apex) of the biopsies. Other studies show that differences in miRNA133 are related to fibrosis in heart failure<sup>21, 22</sup> and that potassium channels are affected in heart failure<sup>8</sup>. miR-133 controls collagen by affecting CTGF expression<sup>23, 24</sup> but also regulates pacemaker channels HCN2 and HCN4 and controls cardiac repolarization through targeting KCNH2 and KCNQ1<sup>25</sup>. The 2 components of the delayed rectifier potassium current,  $I_{Kr}$  and  $I_{Ks}$  play a dominant role in AP repolarization. There are regional differences in the density of  $I_{Kr}$  and  $I_{Ks}$  transmurally (endocardial-epicardial) and along the apico-basal axis, contributing to spatial heterogeneity of ventricular repolarization. A decrease of  $I_{Kr}$  or  $I_{Ks}$  may result in increased APD that may lead to arrhythmogenic early afterdepolarizations (EADs). On the other hand, regional differences in expression of the repolarizing currents may promote the occurrence of reentry based arrhythmias. In the intact myocardium, gap-

junction coupling may temper APD heterogeneity and dispersion of repolarization. Cardiac disease may reduce coupling between cardiomyocytes due to reduced connexin expression and/or increased collagen deposition.

### *Considerations*

The amount of samples in the ICM group was less than the DCM group, which may have influenced the results. In the DCM group the cause of DCM was diverse, which could have led to the variation in collagen and Cx43 expression in this group. A genetic etiology could influence the architecture of heart failure<sup>26</sup>. However, in most cases of DCM the cause of the cardiomyopathy is not known, making this group heterogenic from the start.

Since the tissue samples were obtained from the left ventricular apex it could be that the samples are not representative for the alterations in the whole heart.

## **CONCLUSION**

Tissue from patients with ICM is characterized by a tendency of more patchy fibrosis than tissue from patients with DCM. Also, the macro heterogeneity of the expression in Cx43 is larger in patients with DCM than in patients with ICM. These results suggest differences in remodeling between etiologies of end stage heart failure.

## REFERENCES

1. Go AS, Mozaffarian D, Roger VL, Benjamin EJ, Berry JD, Blaha MJ, Dai S, Ford ES, Fox CS, Franco S, Fullerton HJ, Gillespie C, Hailpern SM, Heit JA, Howard VJ, Huffman MD, Judd SE, Kissela BM, Kittner SJ, Lackland DT, Lichtman JH, Lisabeth LD, Mackey RH, Magid DJ, Marcus GM, Marelli A, Matchar DB, McGuire DK, Mohler ER, III, Moy CS, Mussolino ME, Neumar RW, Nichol G, Pandey DK, Paynter NP, Reeves MJ, Sorlie PD, Stein J, Towfighi A, Turan TN, Virani SS, Wong ND, Woo D and Turner MB. Executive summary: heart disease and stroke statistics--2014 update: a report from the American Heart Association. *Circulation*. 2014;129:399-410.
2. Wolk R, Cobbe SM, Hicks MN and Kane KA. Functional, structural, and dynamic basis of electrical heterogeneity in healthy and diseased cardiac muscle: implications for arrhythmogenesis and anti-arrhythmic drug therapy. *Pharmacology & therapeutics*. 1999;84:207-31.
3. Valdivia CR, Chu WW, Pu J, Foell JD, Haworth RA, Wolff MR, Kamp TJ and Makielski JC. Increased late sodium current in myocytes from a canine heart failure model and from failing human heart. *J Mol Cell Cardiol* 2005;38:475-483.
4. Peters NS. New insights into myocardial arrhythmogenesis: distribution of gap-junctional coupling in normal, ischaemic and hypertrophied human hearts. *Clin Sci (Lond)*. 1996;90:447-452.
5. Hannan RD, Jenkins A, Jenkins AK and Brandenburger Y. Cardiac hypertrophy: a matter of translation. *Clin Exp Pharmacol Physiol*. 2003;30:517-527.
6. Kawara T, Derksen R, de Groot JR, Coronel R, Tasseron S, Linnenbank AC, Hauer RN, Kirkels H, Janse MJ and de Bakker JM. Activation delay after premature stimulation in chronically diseased human myocardium relates to the architecture of interstitial fibrosis. *Circulation*. 2001;104:3069-3075.
7. Verkerk AO, Baartscheer A, de Groot JR, Wilders R and Coronel R. Etiology-dependency of ionic remodeling in cardiomyopathic rabbits. *International journal of cardiology*. 2011;148:154-60.
8. Nattel S, Maguy A, Le Bouter S and Yeh YH. Arrhythmogenic ion-channel remodeling in the heart: heart failure, myocardial infarction, and atrial fibrillation. *Physiol Rev*. 2007;87:425-56.
9. Pogwizd SM, Hoyt RH, Saffitz JE, Corr PB, Cox JL and Cain ME. Reentrant and focal mechanisms underlying ventricular tachycardia in the human heart. *Circulation*. 1992;86:1872-87.
10. Pogwizd SM, McKenzie JP and Cain ME. Mechanisms underlying spontaneous and induced ventricular arrhythmias in patients with idiopathic dilated cardiomyopathy. *Circulation*. 1998;98:2404-14.
11. de Bakker JM, van Capelle FJ, Janse MJ, Wilde AA, Coronel R, Becker AE, Dingemans KP, van Hemel NM and Hauer RN. Reentry as a cause of ventricular tachycardia in patients with chronic ischemic heart disease: electrophysiologic and anatomic correlation. *Circulation*. 1988;77:589-606.
12. Downar E, Saito J, Doig JC, Chen TC, Sevapsidis E, Masse S, Kimber S, Mickleborough L and Harris L. Endocardial mapping of ventricular tachycardia in the intact human ventricle. III. Evidence of multiuse reentry with spontaneous and induced block in portions of reentrant path complex. *J Am Coll Cardiol*. 1995;25:1591-600.
13. Hsia HH and Marchlinski FE. Characterization of the electroanatomic substrate for monomorphic ventricular tachycardia in patients with nonischemic cardiomyopathy. *Pacing Clin Electrophysiol*. 2002;25:1114-27.

14. Kostin S, Rieger M, Dammer S, Hein S, Richter M, Klovekorn WP, Bauer EP and Schaper J. Gap junction remodeling and altered connexin43 expression in the failing human heart. *Molecular and cellular biochemistry*. 2003;242:135-44.
15. de Bakker JM, van Capelle FJ, Janse MJ, Tasseron S, Vermeulen JT, de Jonge N and Lahpor JR. Slow conduction in the infarcted human heart. 'Zigzag' course of activation. *Circulation*. 1993; 88:915-926.
16. Boulaksil M, Winckels SK, Engelen MA, Stein M, van Veen TA, Jansen JA, Linnenbank AC, Bierhuizen MF, Groenewegen WA, van Oosterhout MF, Kirkels JH, de Jonge N, Varro A, Vos MA, de Bakker JM and van Rijen HV. Heterogeneous Connexin43 distribution in heart failure is associated with dispersed conduction and enhanced susceptibility to ventricular arrhythmias. *European journal of heart failure*. 2010;12:913-21.
17. Kitamura H, Ohnishi Y, Yoshida A, Okajima K, Azumi H, Ishida A, Galeano EJ, Kubo S, Hayashi Y, Itoh H and Yokoyama M. Heterogeneous loss of connexin43 protein in nonischemic dilated cardiomyopathy with ventricular tachycardia. *J Cardiovasc Electrophysiol*. 2002;13:865-70.
18. Jongsma HJ and Wilders R. Gap junctions in cardiovascular disease. *Circ Res* 2000;86:1193-1197.
19. Ruijter JM, Ramackers C, Hoogaars WM, Karlen Y, Bakker O, van den Hoff MJ and Moorman AF. Amplification efficiency: linking baseline and bias in the analysis of quantitative PCR data. *Nucleic acids research*. 2009;37:e45.
20. Lundquist AL, Manderfield LJ, Vanoye CG, Rogers CS, Donahue BS, Chang PA, Drinkwater DC, Murray KT and George AL, Jr. Expression of multiple KCNE genes in human heart may enable variable modulation of I(Ks). *J Mol Cell Cardiol*. 2005;38:277-87.
21. Creemers EE and van Rooij E. Function and Therapeutic Potential of Noncoding RNAs in Cardiac Fibrosis. *Circ Res*. 2016;118:108-18.
22. Lok SI, de Jonge N, van Kuik J, van Geffen AJ, Huibers MM, van der Weide P, Siera E, Winkens B, Doevendans PA, de Weger RA and da Costa Martins PA. MicroRNA Expression in Myocardial Tissue and Plasma of Patients with End-Stage Heart Failure during LVAD Support: Comparison of Continuous and Pulsatile Devices. *PLoS One*. 2015;10:e0136404.
23. Liu N, Bezprozvannaya S, Williams AH, Qi X, Richardson JA, Bassel-Duby R and Olson EN. microRNA-133a regulates cardiomyocyte proliferation and suppresses smooth muscle gene expression in the heart. *Genes & development*. 2008;22:3242-54.
24. Duisters RF, Tijssen AJ, Schroen B, Leenders JJ, Lentink V, van der Made I, Herias V, van Leeuwen RE, Schellings MW, Barenbrug P, Maessen JG, Heymans S, Pinto YM and Creemers EE. miR-133 and miR-30 regulate connective tissue growth factor: implications for a role of microRNAs in myocardial matrix remodeling. *Circ Res*. 2009;104:170-8, 6p following 178.
25. Luo X, Zhang H, Xiao J and Wang Z. Regulation of human cardiac ion channel genes by microRNAs: theoretical perspective and pathophysiological implications. *Cellular physiology and biochemistry : international journal of experimental cellular physiology, biochemistry, and pharmacology*. 2010;25:571-86.
26. Gho JM, van Es R, Stathonikos N, Harakalova M, te Rijdt WP, Suurmeijer AJ, van der Heijden JF, de Jonge N, Chamuleau SA, de Weger RA, Asselbergs FW and Vink A. High resolution systematic digital histological quantification of cardiac fibrosis and adipose tissue in phospholamban p.Arg14del mutation associated cardiomyopathy. *PLoS One*. 2014;9:e94820.



# CHAPTER 6

## **ST-segment elevation and fractionated electrograms in Brugada syndrome patients arise from the same structurally abnormal subepicardial RVOT area but have a different mechanism**

Judith N. ten Sande, Ruben Coronel, Chantal E. Conrath, Antoine H.G. Driessen, Joris R. de Groot, Hanno L. Tan, Koonlawee Nademanee, Arthur A.M. Wilde, Jacques M.T. de Bakker, Pascal F.H.M. van Dessel

*Circulation: Arrhythmia and Electrophysiology* 2015 Dec;8(6):1382-92



## ABSTRACT

### Background

Brugada syndrome (BrS) is characterized by a typical ECG pattern. We aimed to determine the pathophysiologic basis of the ST-segment in the BrS-ECG with data from various epicardial and endocardial right ventricular activation mapping procedures in 6 BrS patients and 5 non-BrS controls.

### Methods and results

In 7 patients (2 BrS, 5 controls) with atrial fibrillation an epicardial 8x6 electrode grid electrode (inter-electrode distance 1mm) was placed epicardially on the RV outflow tract (RVOT) prior to Video Assisted Thoracoscopic Surgical Pulmonary Vein Isolation (VATS-PVI). In two other BrS patients endocardial, epicardial RV (CARTO) and body surface mapping (BSM) was performed. In two additional BrS patients we performed decremental pre-excitation of the RVOT prior to endocardial RV mapping.

During VATS-PVI and CARTO mapping, BrS patients (n=4) showed greater activation delay and more fractionated electrograms in the RVOT region than controls. Ajmaline administration increased the region with fractionated electrograms as well as ST-segment elevation. Pre-excitation of the RVOT (n=2) resulted in ECGs that supported the current to load mismatch hypothesis for ST-segment elevation. BSM mapping showed that the area with ST-segment elevation, anatomically correlated with the area of fractionated electrograms and activation delay at the RVOT epicardium.

### Conclusion

ST-segment elevation and epicardial fractionation/conduction delay in BrS patients are most likely related to the same structural subepicardial abnormalities, but the mechanism is different. ST-segment elevation may be caused by current-to-load mismatch, whereas fractionated electrograms and conduction delay are expected to be caused by discontinuous conduction in the same area with abnormal myocardium.

## INTRODUCTION

Brugada syndrome (BrS) is associated with a familial occurrence of sudden cardiac death (SCD) by ventricular tachycardia and/or ventricular fibrillation (VT/VF)<sup>1</sup>. BrS is diagnosed when the typical ECG pattern (BrS-ECG i.e., coved ST-segment elevation followed by a negative T wave<sup>2</sup>) occurs in at least one right precordial lead positioned at the 2<sup>nd</sup>, 3<sup>rd</sup> or 4<sup>th</sup> intercostal space either spontaneously or after provocation by intravenous administration of class I antiarrhythmic drugs<sup>3</sup>. Occurrence of this BrS-ECG can wax and wane, and often precedes onset of VT/VF<sup>4,5</sup>. In about 20-30% of patients, a mutation in the gene encoding the sodium channel, the L-type Ca<sup>2+</sup>-channel or the channel carrying the transient outward current (*I<sub>to</sub>*) is found<sup>6-8</sup>. Despite earlier studies in which BrS has been described in patients with structurally normal hearts, there is now increasing evidence that subtle structural abnormalities exist in the right ventricle outflow tract (RVOT) of BrS patients and that these may impair impulse propagation and could act as an arrhythmogenic substrate<sup>9-12</sup>. The pathophysiologic basis of BrS remains incompletely understood. Three hypotheses, each with a specific mechanistic basis, have been proposed to explain the BrS-ECG:<sup>13-15</sup> (1) repolarization disorder hypothesis, based on transmural dispersion in repolarization of the right ventricle/right ventricular outflow tract (RV/RVOT); (2) depolarization disorder hypothesis, based on activation delay in the RV/RVOT subepicardium; (3) electrotonic current hypothesis, based on activation block at sites of current-to-load mismatch in the RV/RVOT subepicardium<sup>16</sup> or combinations of the above. Some animal models which include monophasic action potential recordings at the epicardium and endocardium, and clinical studies in Brugada syndrome patients give some support for the repolarization disorder hypothesis<sup>17-21</sup>, other clinical studies provide evidence in favor of the depolarization disorder hypothesis<sup>22-24</sup>, in particular, the recording of fractionated and late potentials. These recordings imply structurally abnormal myocardium in the RV/RVOT region and, as such, also support the electrotonic current hypothesis. Current-to-load mismatch may occur in areas with isthmus sites and at sites of abrupt expansion of myocardial bundles, e.g., where myocardial tissue is intermingled with collagen fibers or adipose tissue. Such structural abnormalities have been found in the RV/RVOT region of the hearts of Brugada syndrome patients<sup>10, 11, 25</sup>. We have demonstrated that the BrS-ECG could only be reproduced when both the structural abnormalities in the RV/RVOT and either a reduced sodium or calcium current or an increased transient outward current were present<sup>16, 26</sup>. These findings support the concept that structural abnormalities together with modulated ion currents play an important role in the pathomechanism of BrS. Because both the depolarization disorder hypothesis and the electrotonic current hypothesis require an abnormal myocardial substrate, we proposed that 1) the myocardial areas which exhibit local ST-elevation coincide with areas of structural changes and fractionated electrograms, 2) the size of the myocardial area with fractionated electrograms is augmented by sodium channel blockade, 3) myocar-



dial areas of BrS patients may contain fractionated electrograms even at times they have no BrS-ECG, 4) ST-elevation extends beyond the duration of fractionated electrograms and 5) ablation of the tissue with fractionated electrograms also attenuates ST-segment elevation because both phenomena occur in the same structurally abnormal area.

We therefore, 1) recorded conduction delay and fractionated electrograms at the epicardial RV/RVOT of patients undergoing a VATS procedure for AF, 2) performed epicardial and endocardial mapping of the RV/RVOT and epicardial ablation of regions with marked fractionated electrograms, 3) administered the sodium channel blocker ajmaline to modulate ST-segment elevation, 4) performed premature stimulation of the RV/RVOT at different intervals after onset QRS during sinus rhythm to shift ST-segment elevation. Because fractionation/conduction delay and ST-segment elevation presumably are caused by the same substrate, we further hypothesize that there is an anatomic correlation between the epicardial areas of delayed RV/RVOT activation and/or fractionated electrograms and ST-segment elevation on the body surface map (BSM).

## METHODS

This study was performed in accordance with the Declaration of Helsinki and written informed consent was obtained from all patients.

Three studies were performed.

Study 1) Multiple epicardial RVOT unipolar electrograms were simultaneously acquired to assess the presence of fractionated electrograms, their related pathways and activation delay in BrS patients and control patients who underwent VATS-PVI (proposal 1,3,4).

Study 2) Endocardial and epicardial mapping and RVOT ablation was performed in two BrS patients to evaluate the effect of ablation of epicardial areas with fractionated electrograms on ST-segment elevation and to correlate epicardial fractionation with ST-segment elevation, before and after infusion of ajmaline (proposal 2-5).

Study 3) Premature stimulation of the RVOT at different times after onset of QRS during sinus rhythm was performed in two other BrS patients in the course of diagnostic electrophysiological evaluation. With this method we advanced the ST-segment elevation, allowing us to distinguish between the electrotonic current hypothesis and repolarization disorder hypothesis for ST-segment elevation (proposal 3-5).

### Procedures

BrS was diagnosed using the consensus criteria<sup>3</sup>. Controls were non-BrS who underwent VATS-PVI for AF<sup>27</sup>. Signals were analyzed using a custom made program<sup>28</sup> based on MATLAB (The MathWorks, Inc., Natick, MA, USA) or CARTO 3 Navigation System (Biosense Webster Inc., Diamond Bar, CA, USA). Unipolar electrograms of poor quality (noise, move-

ment artifacts) were excluded. Cardiac magnetic resonance (CMR) was performed in all BrS patients without implantable cardioverter defibrillator (ICD) or computerized tomography (CT) scan in those with ICD.

### Study 1. Epicardial RVOT mapping during VATS-PVI.

VATS-PVI was performed under general anesthesia. Prior to PVI, and after introduction of the various trocars, a custom made 8x6 electrode grid (interelectrode distance 1mm) was placed under visual guidance on the RVOT to obtain epicardial unipolar electrograms. A 256-channel mapping system (BioSemi, ActiveTwo, Amsterdam, The Netherlands, 24 bit dynamic range, 122.07 nV LSB, total noise 0.5  $\mu$ V) was used with a sampling frequency of 2048 Hz (bandwidth DC - 400 Hz (-3dB)). An indifferent reference electrode was inserted in the skin at one of the incision sites. Activation time (AT) was defined as the point of maximal negative  $dV/dt$  ( $\leq -0.1$  V/sec) of the initial deflection of the unipolar electrogram. Total activation duration (TAD) of the myocardium underlying the grid was defined as the interval between the earliest and latest activation in milliseconds (ms). To distinguish local from remote deflections, the timing of the maximal negative  $dV/dt$  of each deflection was compared with the Laplacian transformation at that same time<sup>29</sup>. An electrogram was considered to be fractionated if multiple deflections with  $dV/dt \leq -0.01$  V/s corresponded to Laplacian deflections. Every local electrogram was manually investigated for fractionation. Fractionation was quantified as the mean number of deflections per electrode per grid. Fractionation duration was measured as the interval between the first and last deflection in ms of a fractionated complex.

### Study 2. CARTO mapping of endocardial and epicardial right ventricle for epicardial ablation.

Antiarrhythmic drugs were withheld for at least five half-lives before the electrophysiology study. Prior to the invasive procedure BSM using a 64-electrode system was obtained and a CT scan was made to obtain a 3D heart-thorax reconstruction. Electro-anatomical endocardial and epicardial mapping of the RV was obtained during sinus rhythm with CARTO 3 and a 3.5 mm tip quadripolar ThermoCool SmartTouch mapping catheter (Biosense Webster Inc.) as described earlier<sup>12</sup>. The same activation and fractionation criteria were applied as in study 1. Repolarization time (RT) was defined as the point of maximal positive  $dV/dt$  in the T wave of the unipolar electrogram<sup>30, 31</sup>. The activation recovery interval (ARI), a surrogate for action potential duration, was the interval between AT and RT. To avoid interference by remote signals, bipolar signals obtained from the mapping catheter (signal at the tip – signal from the first ring electrode) were also analyzed. First, endocardial mapping was performed. Thereafter, pericardial puncture was performed according to Sosa et al.<sup>32</sup> and baseline epicardial mapping was performed. Sites displaying fractionated electrograms were marked on the CARTO map. Subsequently, ajmaline was administered i.v. and epicardial mapping was repeated. Guided by the location of fractionated electro-

grams, radiofrequency ablation of these sites was performed. Radiofrequency ablations were performed at a power from 30 to 40 W, with the maximum temperature set at 43°C. After ablation of abnormal (fractionated) sites, the epicardial RV was remapped and the absence of abnormal electrograms was used as endpoint for the ablation.

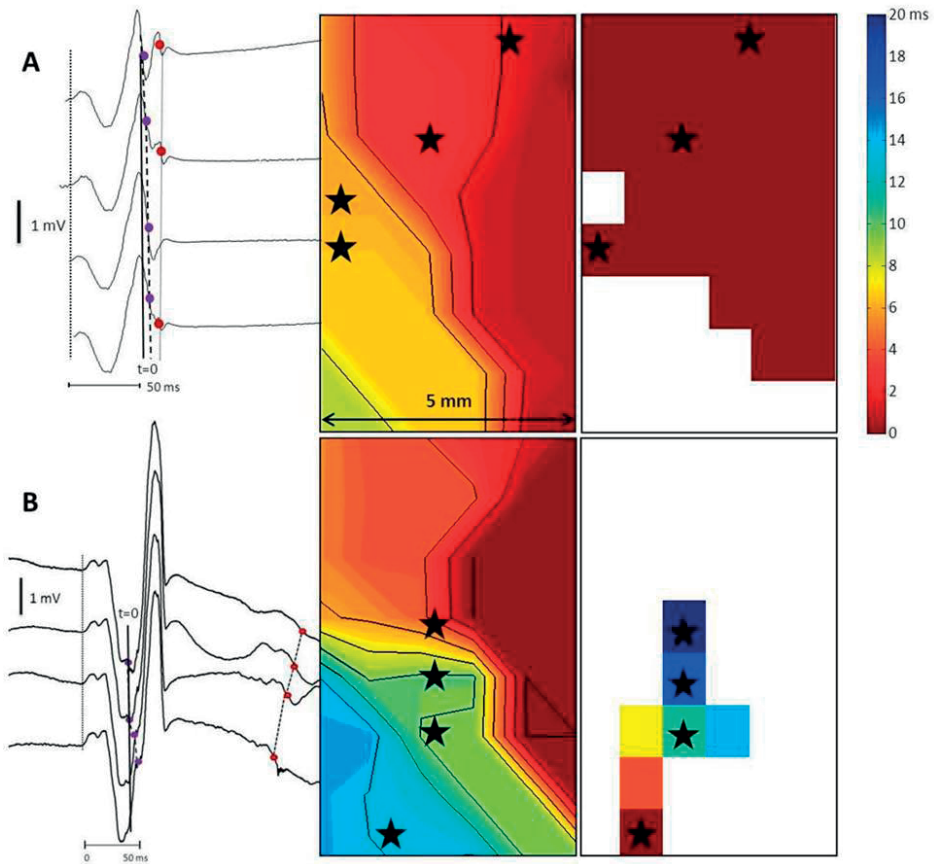


**Figure 1.** Activation maps with corresponding electrograms obtained by the 8×6 grid during Video Assisted Thoracoscopic Surgical Pulmonary Vein Isolation (VATS-PVI). Two examples of activation maps (control and Brugada syndrome [BrS] patient). Colors correspond with activation time in milliseconds with regard to earliest activation within the grid. Red is earliest and blue latest activation. Asterisks are locations of the 8×6 electrode grid where unipolar electrograms at the left were recorded before PVI. **A**, Activation map of a control patient (**middle**) Purple dots in tracings correspond with the steepest negative  $dV/dt$ . Deflections prior and post the initial activation are remote as shown by the second activation map where no propagation is seen (and therefore representing remote activity)- **B**. Color map of the propagation of the main activation (**middle**) and of the late potentials (**right**) seen in a BrS patient. Purple dots in tracings correspond with the steepest negative  $dV/dt$ . whereas red dots are the late potentials after initial activation. The secondary deflections propagate and therefore represent local activity. mV indicates millivolts.

### Study 3. Endocardial CARTO 3 mapping of RV and stimulation of RV/RVOT.

In 2 patients undergoing diagnostic electrophysiological assessment for risk stratification for SCD in BrS, a programmed electrical stimulation protocol was performed including premature stimulation of the endocardial RV/RVOT region. A decapolar catheter was placed in the coronary sinus for atrial stimulation. The mapping catheter was placed in the RVOT for ventricular stimulation and was performed at different intervals after the onset of the QRS complex during SR. Following a drive train of 8 atrial stimuli at a cycle length (CL) of 800 ms, a single ventricular extrastimulus – initially timed at the end of the last atrially stimulated and atrioventricular conducted QRS complex - was delivered. The ventricular coupling interval was decreased in subsequent sequences with 10 ms intervals, allowing progressive pre-excitation of the RVOT. This was repeated until fusion between AV conducted ventricular activation and RVOT paced ventricular activation was no longer present and the last QRS complex was fully paced from the ventricular myocardium.

## RESULTS

Eleven individuals were studied (Table 1); six BrS patients and five controls. Age at time of studies was  $45\pm 16$  years in BrS patients and  $57\pm 9$  years in control patients. Five of six BrS patients were symptomatic, including two with an ICD for secondary prevention (documented VT/VF). Non-invasive cardiac imaging of the BrS patients (CMR n=4, CT scan n=2) revealed no overt structural abnormalities, in particular, no signs of myocardial fibrosis on CMR. In two patients a mutation in SCN5A was identified (c.2635T>C and c.3228+2delT).

### Study 1: Epicardial right ventricle mapping prior to VATS-PVI.

In seven patients (BrS n=2, controls n=5) unipolar ventricular electrograms were recorded during SR (n=3) or AF (n=4). In all patients, no ST-segment elevation on the ECG was seen on the day of the procedure. Patient 1 was admitted after a VF episode accompanied by a spontaneous BrS-ECG during fever. Patient 2 had a drug induced BrS-ECG. BrS patients had longer TAD than controls (21 vs. 9 ms, Table 2), more extensive fractionation (number of deflections 4.5 vs. 2), and longer fractionation duration (48 vs. 8 ms). Heart rate during the procedure (cycle length 560 to 1200 ms) was unrelated to TAD or fractionation. One control (no. 3 in Table 2) showed long fractionation duration compared to the other controls, although it was shorter than in the BrS patients and not associated with a longer TAD. Both BrS patients revealed clear late potentials; these were not seen in controls (Fig.1).

Table 1. Patient characteristics

Patient	Age (years)	Sex	Procedure	Diagnosis BrS	Mutation
1.	56	M	Epicardial RV mapping during VATS-PVI	OHCA, Spontaneous type I ECG	no
2.	56	M	Epicardial RV mapping during VATS-PVI	Asymptomatic, Drug induced BrS	no
3.	18	M	Endocardial and epicardial RV mapping	IHCA, Spontaneous type I ECG	yes
4.	57	M	Endocardial and epicardial RV mapping	Syncope, polymorphic VT, Drug induced BrS	no
5.	36	M	Endocardial mapping and RV stimulation	Syncope, Spontaneous type I ECG	yes
6.	49	M	Endocardial mapping and RV stimulation	Syncope, Drug induced BrS	no
7.	58	M	Epicardial RV mapping during VATS-PVI	Control	NP
8.	68	M	Epicardial RV mapping during VATS-PVI	Control	NP
9.	58	M	Epicardial RV mapping during VATS-PVI	Control	NP
10.	43	M	Epicardial RV mapping during VATS-PVI	Control	NP
11.	57	F	Epicardial RV mapping during VATS-PVI	Control	NP

BrS: Brugada syndrome, ECG: electrocardiogram, F: Female, IHCA: in hospital cardiac arrest, M: Male, NP: no mutation analysis performed, OHCA: out of hospital cardiac arrest, RV: right ventricle, VATS-PVI: Video assisted thoracic surgical pulmonary vein isolation.

Table 2. Electrophysiological parameters

	Rhythm and CL in ms	AT in ms	No. of deflections	Fractionation duration in ms
1. BrS	SR, 660	27	5	31
2. BrS	AF, 560	15	4	64
3. Control	SR, 850	9	3	25
4. Control	AF, 600	5	1	0
5. Control	AF, 600	12	3	10
6. Control	AF, 900	9	2	3
7. Control	SR, 1200	9	2	1

AF: atrial fibrillation, AT: activation time, BrS: Brugada syndrome, CL: average cycle length, ms: milliseconds, SR: sinus rhythm.

### Study 2: CARTO mapping of endocardial and epicardial right ventricle for epicardial ablation.

In two patients (no. 3 and 4, Table 1), endocardial and epicardial RV mapping was performed (Fig. 2; epicardial activation (panel A) and fractionation (panel B) map at baseline and during ajmaline administration) prior to the mapping and ablation procedures. Patient 3 was diagnosed with BrS after an in hospital cardiac arrest based on VF and a type I BrS-ECG. In this patient a mutation in the *SCN5A* gene was found. A type 1 BrS-ECG was present at the beginning of the procedure. This patient had experienced several VT/VF episodes with multiple ICD shocks per year. Body surface voltage map showed the tallest ST-segment elevation at electrode E3, which was located immediately over the RVOT (Fig.

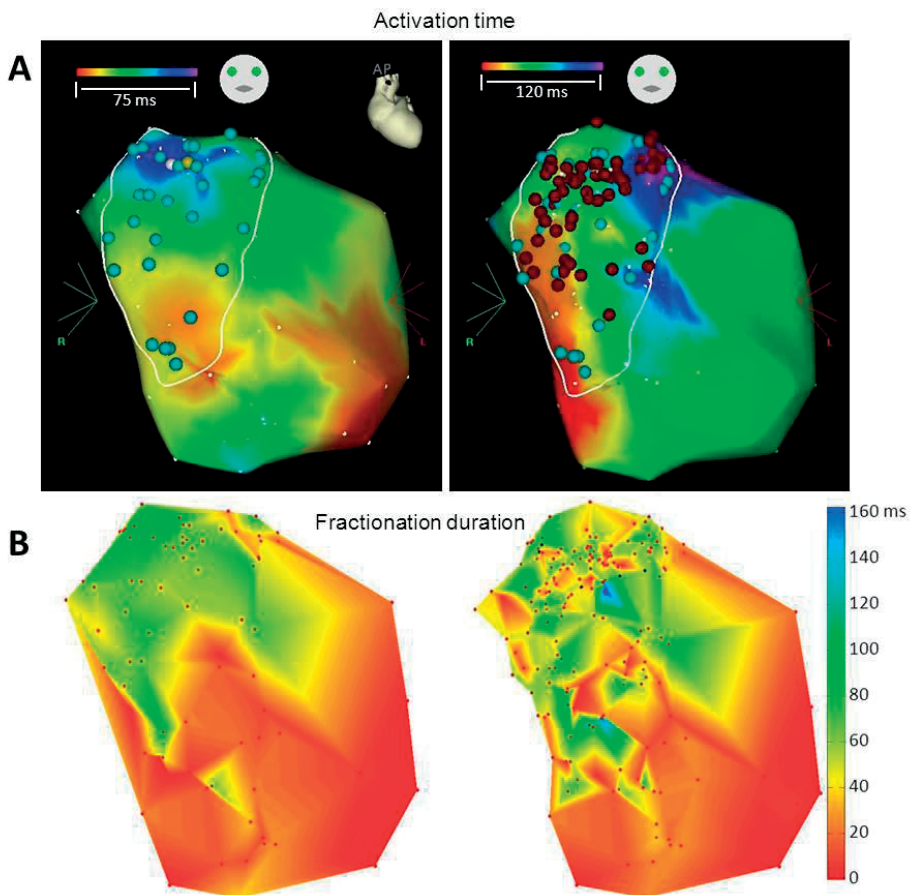


**Figure 2.** Epicardial right ventricular (RV) CARTO map of patient no. 3 displaying activation (**top**) and fractionation duration (**bottom**) before (**left**) and after ajmaline (**right**) administration. Color bars show activation and fractionation duration (ms). Red areas indicate short activation time or electrograms of short duration, and blue areas indicate longer activation time or fractionation duration. Note that during administration of ajmaline, the area of longer fractionation duration is expanding and becomes more heterogeneous.

3, circled electrogram in panel C). The electrophysiology study was performed under general anesthesia with rocuronium, propofol and sufentanil. Figure 4B shows the patients' ECGs with type 1 BrS-ECG during baseline, at maximal ajmaline level and after epicardial ablation. Ajmaline increased ST-segment elevation markedly. After epicardial ablation of the area with fractionated electrograms, typical ST-segment elevation almost disappeared as compared to the ST-segment elevation prior to ajmaline administration. One month after epicardial ablation, ST-segment elevation was still absent. During CARTO mapping, the RV endocardial unipolar voltage map showed no abnormalities (data not shown) and endocardial RV electrograms showed only a small area of fractionated signals. Endocardial ARIs were  $395 \pm 13$  ms on average at the RV free wall and  $370 \pm 6$  ms at the RVOT. In

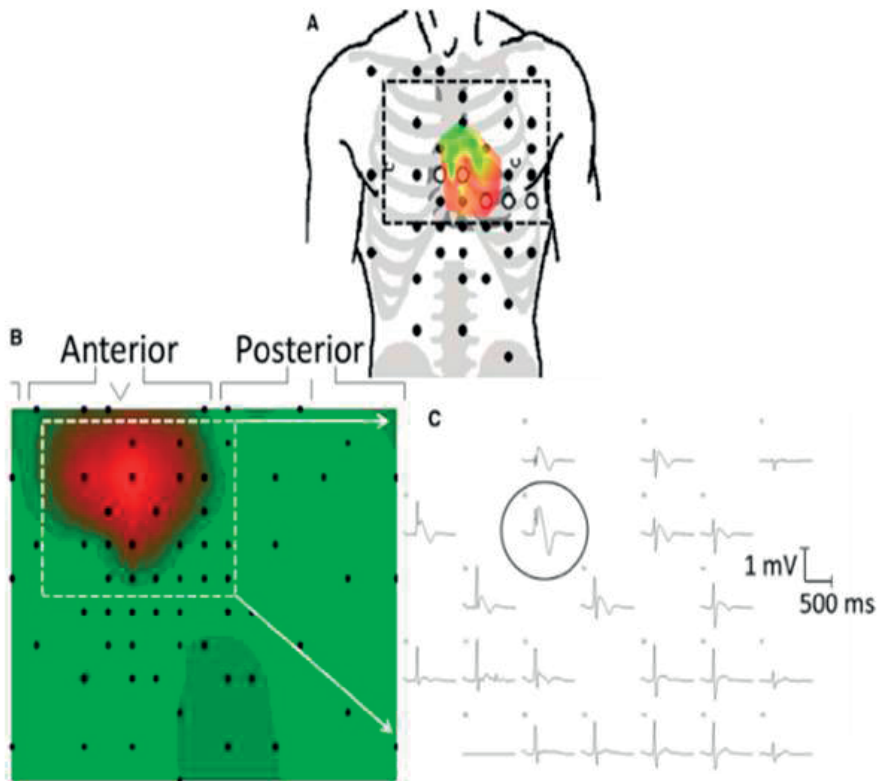


**Figure 3.** Body surface ST-segment potential map of patient no. 3. **A.** A torso with epicardial right ventricular (RV) CARTO map of fractionated electrograms (green areas are highly fractionated) as in Figure 2 with the positions of the body surface mapping (BSM) electrodes. **B.** ST-segment potentials measured at the indicated BSM electrodes. Red represent a higher potential (1 mV); and green, zero potential. Black dots represent the electrode positions. **C.** The electrocardiograms corresponding with the black dots within the white rectangle on the body surface potential map in **B** and the torso in **A**. The area with the highest ST-segment potential (red), including ECG (circle) is immediately overlying the area of RV outflow tract (RVOT) fractionation (**A**).

contrast, epicardial RV mapping showed an area of low voltage and fractionated signals extending from the subpulmonary area to mid wall RV (Fig. 2B, left panel). Epicardial ARIs were  $360 \pm 12$  ms at the RV free wall and  $310 \pm 11$  ms at the RVOT. Administration of ajmaline increased the area with fractionated electrograms (Fig. 2B, right panel). After epicardial ablation, ventricular arrhythmias occurred less frequently, although, the patient

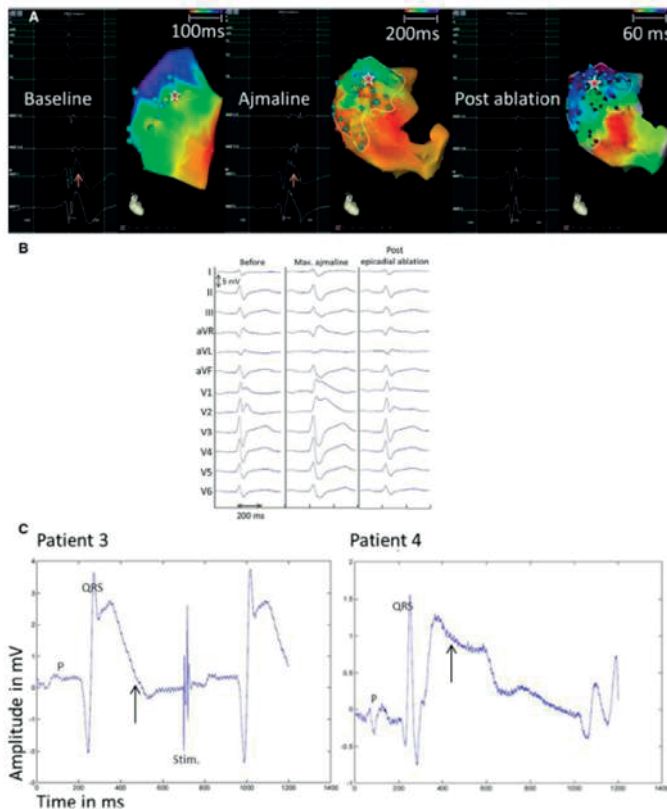


**Figure 4.** A. Epicardial right ventricular (RV) CARTO map of patient no. 4 displaying activation at baseline (left), during ajmaline (middle) administration, and after epicardial ablation of the fractionated signals (right). Left to the CARTO images are the corresponding electrograms. Blue dots are recording points, and red points indicate ablation sites. Please note that color bars have different ranges. B. Twelve lead ECG of one of the Brugada syndrome (BrS) patients who underwent epicardial ablation. The ECG shows a type 1 Brugada syndrome during baseline, maximal ajmaline level, and after epicardial ablation of areas with outspoken fractionated electrograms. Note that ST-segment elevation increases with ajmaline and virtually disappears after ablation. C. Tracings are the difference between V1 during baseline and V1 at maximal ajmaline level of 2 Brugada syndrome patients (no. 3 and 4). Patient 3 has a type 1 and patient 4 a type 2 Brugada syndrome. In both signals, the deflection marking the difference in QRS (V) is followed by a pulse-shaped deflection with a duration of 220 and 300 ms, respectively. Arrows mark the time of latest epicardial late potentials in the patients. P indicates atrial complex; and Stim., stimulation artifact.



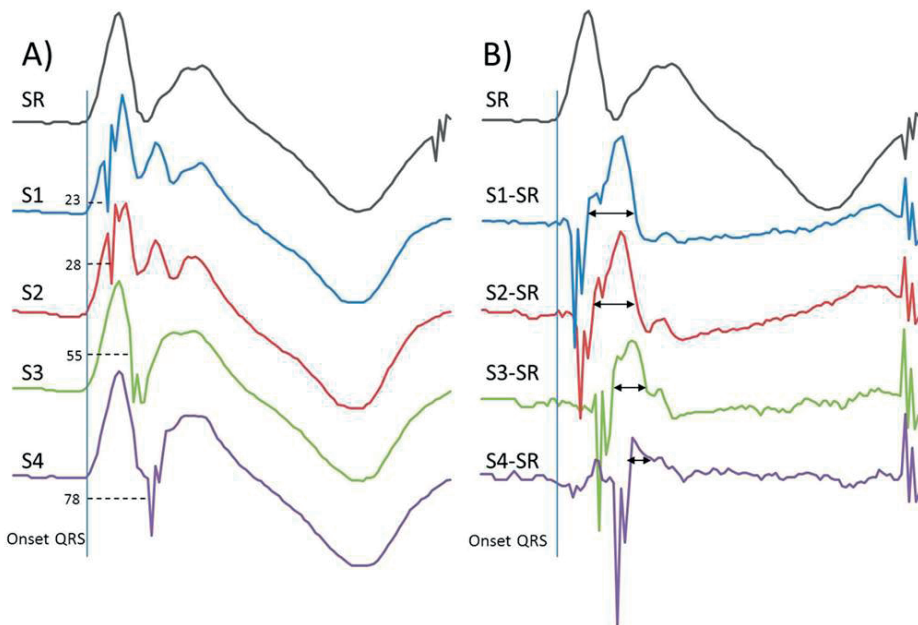


**Figure 5.** A. Tracings are V1 of a type 1 Brugada syndrome patient during sinus rhythm (SR) and during SR with RV outflow tract (RVOT) stimulation at different times after onset of the QRS complex (S1-S4). Delay between onset ORS and the stimulus is indicated by a number left from the dashed line. Sharp deflections right from the dashed lines are the stimulus artifacts. B. Tracings are the difference between the stimulated complexes in S1 till S4 in A and the SR complex. Sharp deflections are stimulus artifacts, which are followed by a pulse-shaped signal. The width of the pulses is indicated by an arrow and increases with prematurity of the stimulus. See text for discussion-

experienced appropriate ICD shocks six weeks after ablation, after which quinidine therapy was reinstated.

Patient 4 had 1 mV ST-segment elevation in the right precordial leads at baseline and BrS was diagnosed after episodes of polymorphic VT and a type 1 BrS-ECG after ajmaline administration (he had type 2 BrS-ECG at baseline). The patient also had coronary artery disease. The electrophysiology study was performed under general anesthesia with sufentanil and thiopental. The effect of ajmaline administration and epicardial ablation on ST-segment elevation was less prominent than in patient 3. There was a moderate increase in ST-segment elevation with ajmaline and ST-elevation was slightly lower after ablation. The endocardial unipolar electrograms of the RVOT showed no fractionated signals (data not shown). Epicardial mapping showed fractionated electrograms at the superior, mid, and posterior site of the RVOT. ARIs were  $310 \pm 18$  ms on average at the epicardial RVOT and  $405 \pm 9$  ms at the epicardial RV free wall. After ajmaline administration, the area with abnormal electrograms expanded towards the anterior and inferior RVOT. This area was

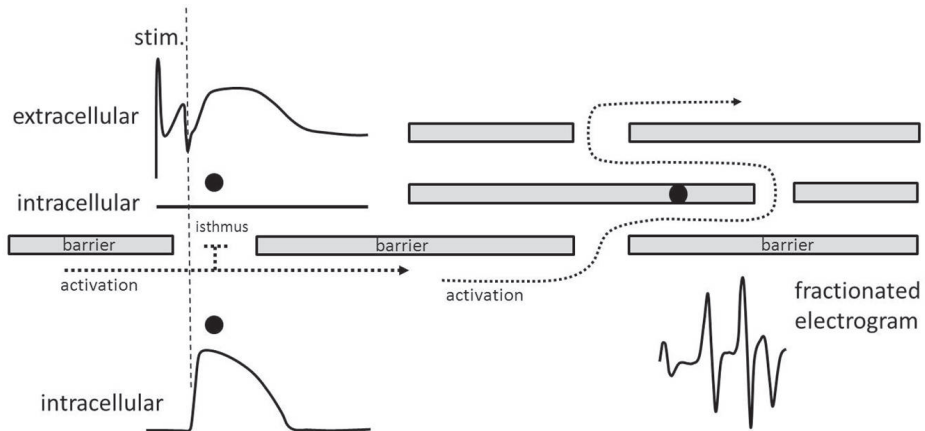


**Figure 6.** Schematic drawing of intra and extracellular signals recorded near an isthmus site where activation in myocardial tissue proximal from the isthmus is blocked toward myocardium distal from the isthmus. Activation in the proximal area generates an action potential (intracellular) at the recording site. Because of activation block, the distal area is not activated, and the intracellular signal is a flat line (intracellular). True upper tracing shows the extracellular signal, which consists of a stimulus artifact, a remote deflection of the activation front in the proximal area, and an action potential-shaped deflection caused by electrotonic current flowing through the isthmus. At the right site, schematics of myocardial tissue subdivided in multiple myocardial bundles by electrically inexcitable barriers. Bundles are interconnected at different sites by an isthmus. Activation has to follow a tortuous route between the barriers, which results in activation delay because of the increased path length. Fractionated electrograms occur because of the asynchronous activation between the barriers. Black dots are recording sites.

additionally marked and successfully ablated. After epicardial ablation of the fractionated signals, late potentials and fractionation diminished (Fig.4A). Following the procedure the patient remained free of ventricular arrhythmias during 12 months of follow-up. Ultimate fractionated electrograms were 270 ms and 220 ms (patient 3 and 4 respectively) after onset QRS, and occurred far before ST-segment elevation ended.

To reveal changes in V1 caused by ajmaline, we subtracted the ECG during baseline from the ECG during peak ajmaline (Fig.4C) in both patients. This procedure revealed that, after the deflection that exposes the QRS difference, a pulse shaped deflection arises with a width of 220 to 310 ms. This indicates that the effect of ajmaline on the ST-segment operates over this time interval. The pulse shaped pattern mimics the configuration of an action potential as expected for an electrotonic component. The arrow in the signal marks the time of the latest epicardial late potential.

### Study 3: Pre-excitation of the RVOT.

In two BrS patients (no. 5 and 6) pre-excitation of the RVOT was performed during a diagnostic electrophysiologic study. Panel A of Figure 5 shows leads V1 during SR alone and during SR and RVOT pre-stimulation at different delays after onset QRS (numbers indicate

the delay in ms). Note that there is ST-segment elevation and a negative T-wave in both the basic and premature activations. Sharp deflections in the signals are the stimulus artefacts (indicated by numbers of measured coupling intervals). Panel B shows the subtraction of the electrograms in V1 during SR with stimulation and the SR electrogram in V1 alone (matched at onset QRS). Striking in all these differential signals is the pattern-wave that follows directly after the stimulus artefact. The width of the wave (arrows) becomes wider with increasing prematurity of the stimulus after onset QRS. By premature stimulation of the RVOT, ST-segment elevation (irrespective of its mechanism) occurs earlier in time and partly within the QRS complex, but is not removed as is evident from Figure 5. Premature stimulation of the RVOT region therefore only slightly altered the QRS configuration. As a result, the difference of a stimulated and a SR complex is mainly the difference of the ST-segment elevated signal during SR and virtually the same signal during stimulation but now shifted in time. The resulting pulse shaped signal increases in width with prematurity of stimulation and is compatible with our hypothesis that ST-segment elevation is caused by an electrotonic signal due to current to load mismatch (further explanation in supplement, Fig.1). In both patients the ST-segment morphology of the RVOT pre-excited complex changed in a similar fashion.

## DISCUSSION

This study shows that ST-segment elevation and fractionated electrograms/activation delay in BrS patients arise both from the same (structurally abnormal) subepicardium of the RV/RVOT region (Fig 6). Study 1 shows that local electrograms in the RVOT are more fractionated in BrS patients than in controls. However, they may also be present in control patients, but are not related to ST-segment elevation (neither in control, nor in BrS patients). Study 2 demonstrates that ST-elevation in one patient disappeared when areas with fractionated local electrograms were ablated. The area of fractionation increased after sodium channel blockade. In the other patient, the typical BrS-ECG was absent despite extensive fractionation. Study 3 shows that the difference of a pre-stimulated and a SR complex is mainly the difference of the ST-segment elevated signal during SR and virtually the same signal during stimulation, but now shifted in time. The resulting difference wave (fig.5B) increases in width with prematurity of stimulation. This is consistent with our hypothesis that ST-segment elevation is caused by an electrotonic signal due to current to load mismatch. This study with various mapping and stimulation protocols shows that BrS patients have longer activation delay, more and longer fractionated epicardial electrograms and late potentials in the RV/RVOT compared to controls and that local fractionation is not solely responsible for the ST-elevation in the BrS-ECG. We additionally show that the area with

ST-segment elevation on the BSM-ECG corresponds with the area of fractionated epicardial electrograms in the RV/RVOT.

The mechanism causing the typical ST-segment elevation in the right precordial leads in BrS patients has still not completely been elucidated. Three hypotheses have been proposed. The repolarization disorder hypothesis is based on transmural voltage gradients caused by heterogeneity in action potential duration between the RV epicardium and endocardium, resulting in dispersion of repolarization measured in canine wedge preparations<sup>18</sup>. According to the depolarization disorder hypothesis late activation of the RVOT is the underlying mechanism<sup>22</sup>. The electrotonic current hypothesis explains ST elevation by electrotonic currents caused by current to load mismatch in a structurally abnormal subepicardium of the RV/RVOT area<sup>26</sup>. There is growing evidence that mild structural abnormalities in BrS patients, that are not detectable on conventional imaging modalities, result in discontinuous conduction<sup>10-12</sup>. In our study population, BrS patients showed clear fractionated electrograms at the RVOT epicardium compared to controls, which indicate discontinuous electrical impulse conduction that occurs if patchy fibrosis is present in the myocardium<sup>33</sup>.

Supplemental Figure 1 demonstrates the different hypotheses on cellular level. The first column (action potentials) shows 3 combinations of schematic epicardial and endocardial action potentials that could cause an electrotonic component for ST-segment elevation. The upper left panel shows an endocardial action potential only. Activation toward the epicardium is blocked due to current to-load-mismatch in the structurally abnormal subepicardium (electrotonic current hypothesis). The left middle and lower panels show a gradient in APD from endocardium to epicardium and a strong spike and dome configuration for the epicardial action potential respectively (repolarization disorder hypothesis). The middle column displays the configuration of the electrotonic signals that are generated due to the difference in epi- and endocardial action potentials as illustrated at the left. The signals are low pass filtered (3dB at 60Hz), to cope with their electrotonic feature. The third column shows the difference between the electrotonic component and its time shifted equivalent for the 3 electrotonic components. The electrotonic components are shifted over 15, 30 and 45 units (ms), simulating premature stimulation at different coupling intervals. The pulse shaped signals in the upper right panel best correspond with the recorded signals from Figure 5. Signals in the middle right panel start later and are more sinusoidal, whereas signals in the lower right panel have a biphasic pulse shaped form. The figure illustrates that results obtained during premature stimulation at different coupling intervals (Fig.5, top row of Supplemental Fig.1) fit best with the electrotonic current hypothesis.

Figure 4 shows that if the ajmaline level increases, the ST-segment elevation increases. We expect that this occurs because ajmaline increases the number of sites with conduction block<sup>26</sup>. Subtracting electrograms recorded during different ajmaline levels gives the change in the signal caused by the increase in the ajmaline concentration. Figure 4C shows

that subtraction reveals a wide signal compatible with an electrotonic component generated by the duration of the action potential in the activated area. If the electrotonic current was based on a shorter APD at the epicardium compared to the endocardium, electrotonic current would only flow during the time the difference in APD is present and thus during a shorter period. In addition this would occur later after depolarization. A role for activation delay as a single mechanism for ST segment elevation is also unlikely, because late potentials are not present at the end of the pulse signal as Figure 4C illustrates. In addition, late potentials with a delay > 160 ms were present in only 0.04% of the electrograms with fractionation. When the substrate was modulated by catheter ablation the ST-segment elevation diminished corroborating the study performed by Nademanee et al<sup>12</sup>. Nademanee et al. previously identified low voltage areas with fractionated electrograms and severe activation delay at the anterior epicardial aspect of the RVOT, and diminishing of preexistent ST-segment elevation after ablation of this area. Recently, Szél et al.<sup>34</sup> also observed fractionated electrograms in the RV epicardium, but they suggested that this is due to a heterogeneous epicardial loss of dome and local re-excitation via a concealed phase 2 re-entry, challenging abnormal depolarization or structural abnormalities as a mechanism. However, the data in our patients suggest differently. Fractionated signals were clearly associated with diastolic potentials in the BrS patients undergoing VATS-PVI (see Fig.1), whereas diastolic potentials were not observed in control patients except 1 (control 3). This is not surprising because structural subepicardial abnormalities have been observed in the RVOT of healthy pig hearts. To lead to ST-elevation, however, additional electrophysiological changes, e.g. reduced sodium current, are necessary.

Normally, the RV/RVOT area is activated relatively late during sinus rhythm. The effect of alteration of activation of the endocardial RVOT on ST-segment elevation was investigated by premature RVOT stimulation in two BrS patients. Pre-excitation of the right ventricular apex was described earlier by Chiale et al.<sup>35</sup> Their study describes a maneuver to unmask the BrS-ECG by pre-excitation of the RV apex when a right bundle branch block (RBBB) pattern is present on the surface ECG. Our study followed a different line of reasoning: instead of unmasking ST-segment elevation, we sought to study whether ST-segment elevation in patients without intraventricular conduction block could be caused by current to load mismatch of the RVOT. To test this, we advanced activation of the RVOT by pacing the RVOT instead of the RV apex. An electrotonic component that would cause ST-segment elevation must also start late after onset QRS. If, however, the RV/RVOT area during sinus rhythm is activated prematurely by stimulation, the electrotonic current will start earlier as well. Indeed the electrotonic current (elevation of the signal) started directly after the stimulus at every coupling interval (Fig.5). To reveal the electrotonic component (and discard the activation component), the electrogram during sinus rhythm was subtracted from the stimulated one. By doing so, mainly the difference between the electrotonic components during SR alone and of SR with stimulation remains (small additional changes

may be present due to altered activation in RV). The earlier the RV/RVOT is stimulated after onset of QRS of the sinus beat, the earlier the electrotonic component arises and the wider the component will be (Fig.5). Although subtle structural abnormalities have been described in hearts of BrS patients, during postmortem analyses<sup>9, 11</sup> or in explanted hearts<sup>10, 16</sup>, we could not document these in our patients. The standard imaging techniques may not have been sensitive enough to detect these subtle changes in RVOT architecture. However, based on the available data the presence of subclinical structural changes in these patients is likely<sup>11</sup>. In addition, ablation aimed at anatomically abnormal tissue was effective as a therapy.

### Methodological considerations and limitations

The number of patients is small. However, we used three different types of experiments in 2 of which the patients served as their own control (study 2 and 3) and these studies point to a same mechanism for the electrophysiological characteristics of Brugada syndrome. Analysis of the electrograms of the epicardial grid was performed during spontaneous SR or conducted AF and heart rate may have influenced the TAD. However, we did not observe differences in AT between patient with AF or SR and with different cycle lengths.

## CONCLUSION

ST-segment elevation and fractionated electrograms/activation delay in BrS patients are most likely related to the (structurally abnormal) subepicardium of the RV/RVOT region. Such abnormalities may cause conduction block due to current-to-load mismatch at tissue discontinuities resulting in ST-segment elevation. Our currently presented data support this hypothesis. The same structural abnormalities may cause fractionated electrograms and conduction delay if excitability is appropriate. These electrophysiological parameters can be modulated by sodium channel blockers like ajmaline.

## ACKNOWLEDGEMENTS

We would like to thank V.M.F. Meijborg and dr. A.C. Linnenbank for the technical support.

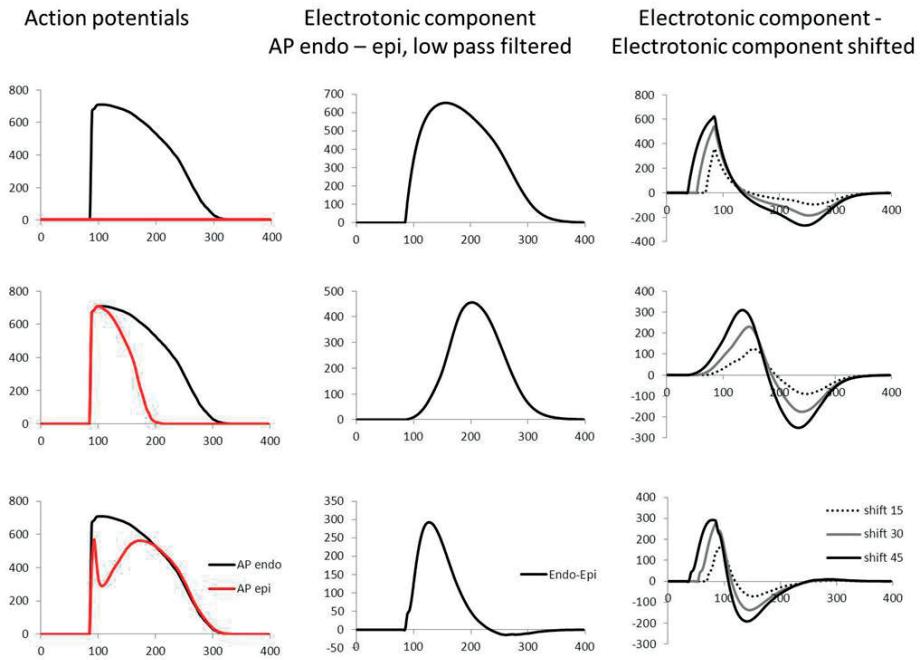
## REFERENCES

1. Antzelevitch C, Brugada P, Borggrefe M, Brugada J, Brugada R, Corrado D, Gussak I, LeMarec H, Nademanee K, Perez Riera AR, Shimizu W, Schulze-Bahr E, Tan H, Wilde A. Brugada syndrome: report of the second consensus conference: endorsed by the Heart Rhythm Society and the European Heart Rhythm Association. *Circulation*. 2005;111:659-670.
2. Brugada P, Brugada J. Right bundle branch block, persistent ST segment elevation and sudden cardiac death: a distinct clinical and electrocardiographic syndrome. A multicenter report. *J Am Coll Cardiol* 1992;20:1391-1396.
3. Priori SG, Wilde AA, Horie M, Cho Y, Behr ER, Berul C, Blom N, Brugada J, Chiang CE, Huikuri H, Kannankeril P, Krahn A, Leenhardt A, Moss A, Schwartz PJ, Shimizu W, Tomaselli G, Tracy C. Executive summary: HRS/EHRA/APHRS expert consensus statement on the diagnosis and management of patients with inherited primary arrhythmia syndromes. *Heart Rhythm* 2013; 10:e85-108.
4. Kasanuki H, Ohnishi S, Ohtuka M, Matsuda N, Nirei T, Isogai R, Shoda M, Toyoshima Y, Hosoda S. Idiopathic ventricular fibrillation induced with vagal activity in patients without obvious heart disease. *Circulation*. 1997;95:2277-2285.
5. Matsuo K, Shimizu W, Kurita T, Inagaki M, Aihara N, Kamakura S. Dynamic changes of 12-lead electrocardiograms in a patient with Brugada syndrome. *J Cardiovasc Electrophysiol*. 1998;9: 508-512.
6. Priori SG, Napolitano C, Gasparini M, Pappone C, Della BP, Brignole M, Giordano U, Giovannini T, Menozzi C, Bloise R, Crotti L, Terreni L, Schwartz PJ. Clinical and genetic heterogeneity of right bundle branch block and ST-segment elevation syndrome: A prospective evaluation of 52 families. *Circulation*. 2000;102:2509-2515.
7. Smits JP, Eckardt L, Probst V, Bezzina CR, Schott JJ, Remme CA, Haverkamp W, Breithardt G, Escande D, Schulze-Bahr E, LeMarec H, Wilde AA. Genotype-phenotype relationship in Brugada syndrome: electrocardiographic features differentiate SCN5A-related patients from non-SCN5A-related patients. *J Am Coll Cardiol* 2002;40:350-356.
8. Mizusawa Y, Wilde AA. Brugada syndrome. *Circ Arrhythm Electrophysiol* 2012;5:606-616.
9. Corrado D, Basso C, Buja G, Nava A, Rossi L, Thiene G. Right bundle branch block, right precordial st-segment elevation, and sudden death in young people. *Circulation*. 2001;103: 710-717.
10. Coronel R, Casini S, Koopmann TT, Wilms-Schopman FJ, Verkerk AO, de Groot JR, Bhuiyan Z, Bezzina CR, Veldkamp MW, Linnenbank AC, van der Wal AC, Tan HL, Brugada P, Wilde AA, de Bakker JM. Right ventricular fibrosis and conduction delay in a patient with clinical signs of Brugada syndrome: a combined electrophysiological, genetic, histopathologic, and computational study. *Circulation*. 2005;112:2769-2777.
11. Frustaci A, Priori SG, Pieroni M, Chimenti C, Napolitano C, Rivolta I, Sanna T, Bellocci F, Russo MA. Cardiac histological substrate in patients with clinical phenotype of Brugada syndrome. *Circulation*. 2005;112:3680-3687.
12. Nademanee K, Veerakul G, Chandanamattha P, Chaothawee L, Ariyachaipanich A, Jirasirornjanakorn K, Likittanasombat K, Bhuripanyo K, Ngarmukos T. Prevention of ventricular fibrillation episodes in Brugada syndrome by catheter ablation over the anterior right ventricular outflow tract epicardium. *Circulation*. 2011;123:1270-1279.
13. Meregalli PG, Wilde AA, Tan HL. Pathophysiological mechanisms of Brugada syndrome: depolarization disorder, repolarization disorder, or more? *Cardiovasc Res* 2005;67:367-378.

14. Hoogendijk MG, Opthof T, Postema PG, Wilde AA, de Bakker JM, Coronel R. The Brugada ECG pattern: a marker of channelopathy, structural heart disease, or neither? Toward a unifying mechanism of the Brugada syndrome. *Circ Arrhythm Electrophysiol* 2010;3:283-290.
15. Wilde AA, Postema PG, Di Diego JM, Viskin S, Morita H, Fish JM, Antzelevitch C. The pathophysiological mechanism underlying Brugada syndrome: depolarization versus repolarization. *J Mol Cell Cardiol* 2010;49:543-553.
16. Hoogendijk MG, Potse M, Linnenbank AC, Verkerk AO, den Ruijter HM, van Amersfoort SC, Klaver EC, Beekman L, Bezzina CR, Postema PG, Tan HL, Reimer AG, van der Wal AC, Ten Harkel AD, Dalinghaus M, Vinet A, Wilde AA, de Bakker JM, Coronel R. Mechanism of right precordial ST-segment elevation in structural heart disease: excitation failure by current-to-load mismatch. *Heart Rhythm* 2010;7:238-248.
17. Di Diego JM, Sun ZQ, Antzelevitch C. I(to) and action potential notch are smaller in left vs. right canine ventricular epicardium. *The American journal of physiology*. 1996;271:H548-561.
18. Yan GX, Antzelevitch C. Cellular basis for the Brugada syndrome and other mechanisms of arrhythmogenesis associated with ST-segment elevation. *Circulation*. 1999;100:1660-1666.
19. Shimizu W, Aiba T, Kurita T, Kamakura S. Paradoxical abbreviation of repolarization in epicardium of the right ventricular outflow tract during augmentation of Brugada-type ST segment elevation. *J Cardiovasc Electrophysiol*. 2001;12:1418-1421.
20. Kurita T, Shimizu W, Inagaki M, Suyama K, Taguchi A, Satomi K, Aihara N, Kamakura S, Kobayashi J, Kosakai Y. The electrophysiologic mechanism of ST-segment elevation in Brugada syndrome. *J Am Coll Cardiol*. 2002;40:330-334.
21. Noda T, Shimizu W, Taguchi A, Satomi K, Suyama K, Kurita T, Aihara N, Kamakura S. ST-segment elevation and ventricular fibrillation without coronary spasm by intracoronary injection of acetylcholine and/or ergonovine maleate in patients with Brugada syndrome. *J Am Coll Cardiol*. 2002;40:1841-1847.
22. Tukkijärvi R, Sogaard P, Vleugels J, de Groot IK, Wilde AA, Tan HL. Delay in right ventricular activation contributes to Brugada syndrome. *Circulation*. 2004;109:1272-1277.
23. Nagase S, Kusano KF, Morita H, Fujimoto Y, Kakishita M, Nakamura K, Emori T, Matsubara H, Ohe T. Epicardial electrogram of the right ventricular outflow tract in patients with the Brugada syndrome: using the epicardial lead. *J Am Coll Cardiol*. 2002;39:1992-1995.
24. Takami M, Ikeda T, Enjōji Y, Sugi K. Relationship between ST-segment morphology and conduction disturbances detected by signal-averaged electrocardiography in Brugada syndrome. *Ann Noninvasive Electrocardiol*. 2003;8:30-36.
25. Catalano O, Antonaci S, Moro G, Mussida M, Frascaroli M, Baldi M, Cobelli F, Baiardi P, Nastoli J, Bloise R, Monteforte N, Napolitano C, Priori SG. Magnetic resonance investigations in Brugada syndrome reveal unexpectedly high rate of structural abnormalities. *Eur Heart J*. 2009;30:2241-2248.
26. Hoogendijk MG, Potse M, Vinet A, de Bakker JM, Coronel R. ST segment elevation by current-to-load mismatch: an experimental and computational study. *Heart Rhythm* 2011;8:111-118.
27. Krul SP, Driessen AH, van Boven WJ, Linnenbank AC, Geuzebroek GS, Jackman WM, Wilde AA, de Bakker JM, de Groot JR. Thoracoscopic video-assisted pulmonary vein antrum isolation, ganglionated plexus ablation, and periprocedural confirmation of ablation lesions: first results of a hybrid surgical-electrophysiological approach for atrial fibrillation. *Circ Arrhythm Electrophysiol*. 2011;4:262-270.



28. Potse M, Linnenbank AC, Grimbergen CA. Software design for analysis of multichannel intracardial and body surface electrocardiograms. *Computer methods and programs in biomedicine*. 2002;69:225-236.
29. Coronel R, Wilms-Schopman FJ, de Groot JR, Janse MJ, van Capelle FJ, de Bakker JM. Laplacian electrograms and the interpretation of complex ventricular activation patterns during ventricular fibrillation. *J Cardiovasc Electrophysiol*. 2000;11:1119-1128.
30. Haws CW, Lux RL. Correlation between in vivo transmembrane action potential durations and activation-recovery intervals from electrograms. Effects of interventions that alter repolarization time. *Circulation*. 1990;81:281-288.
31. Coronel R, de Bakker JM, Wilms-Schopman FJ, Opthof T, Linnenbank AC, Belterman CN, Janse MJ. Monophasic action potentials and activation recovery intervals as measures of ventricular action potential duration: experimental evidence to resolve some controversies. *Heart Rhythm*. 2006;3:1043-1050.
32. Sosa E, Scanavacca M, d'Avila A, Pilleggi F. A new technique to perform epicardial mapping in the electrophysiology laboratory. *J Cardiovasc Electrophysiol* 1996;7:531-536.
33. de Bakker JM, van Capelle FJ, Janse MJ, Tasseron S, Vermeulen JT, de Jonge N, Lahpor JR. Slow conduction in the infarcted human heart. 'Zigzag' course of activation. *Circulation*. 1993;88:915-926.
34. Szel T, Antzelevitch C. Abnormal repolarization as the basis for late potentials and fractionated electrograms recorded from epicardium in experimental models of brugada syndrome. *J Am Coll Cardiol* 2014;63:2037-2045.
35. Chiale PA, Garro HA, Fernandez PA, Elizari MV. High-degree right bundle branch block obscuring the diagnosis of Brugada electrocardiographic pattern. *Heart Rhythm*. 2012;9:974-976.



**Supplemental Figure 1.** Simulation of epicardial and endocardial action potentials to differentiate between the repolarization and current to load mismatch hypothesis for ST-segment elevation on the base of the signals obtained by premature stimulation of the RVOT. Signals in the upper right panel correspond best with the recorded signals in figure 6B as for morphology and timing. Stimulus artefacts are not indicated in the simulated signals.



# CHAPTER 7

## Differential mechanisms of myocardial conduction slowing by adipose tissue-derived stromal cells derived from different species

Judith N. ten Sande<sup>#</sup>, Nicoline W. Smit<sup>#</sup>, Mojtaba Parvizi<sup>#</sup>, Shirley C.M. van Amersfoort, Josée A. Plantinga, Pascal F.H.M. van Dessel, Jacques M.T. de Bakker, Marco C. Harmsen, Ruben Coronel

*# contributed equally.*

*STEM CELLS Translational Medicine, 2016;5:1-9*



## ABSTRACT

Stem cell therapy is a promising therapeutic option to treat patients after myocardial infarction. However, the intramyocardial administration of large amounts of stem cells might generate a proarrhythmic substrate. Proarrhythmic effects can be explained by electrotonic and/or paracrine mechanisms. The narrow therapeutic time window for cell therapy and the presence of comorbidities limit the application of autologous cell therapy. The use of allogeneic or xenogeneic stem cells is a potential alternative to autologous cells, but differences in the proarrhythmic effects of adipose derived stromal cells (ADSCs) across species are unknown.

Using microelectrode arrays and microelectrode recordings, we obtained local unipolar electrograms and action potentials from monolayers of neonatal rat ventricular myocytes (NRVMs) that were cocultured with rat, human or pig ADSCs (rADSCs, hADSCs, pADSCs). Monolayers of NRVMs were cultured in the respective conditioned medium to investigate paracrine effects.

We observed significant conduction slowing in all cardiomyocyte cultures containing ADSCs, independent of species used ( $p < 0.01$ ). All cocultures were depolarized compared to controls ( $p < 0.01$ ). Only conditioned medium taken from cocultures with pADSCs and applied to NRVM monolayers demonstrated similar electrophysiological changes as the corresponding cocultures.

We have shown that independent of species used, ADSCs cause conduction slowing in monolayers of NRVMs. In addition, pADSCs exert conduction slowing mainly by a paracrine effect, whereas the influence on conduction by hADSCs and rADSCs is preferentially by electrotonic interaction.

## INTRODUCTION

Up to one third of the patients with myocardial infarction develop heart failure despite improvements in reperfusion therapy<sup>1</sup>. Stem cell-based therapy has been suggested as a promising therapeutic modality to improve cardiac function in these patients<sup>2-4</sup>. However, there are concerns for the potential proarrhythmic effects of stem cell therapy<sup>5-7</sup>. One proposed mechanism for the proarrhythmic potential is the formation of electrotonic interaction between cardiomyocytes and stem cells, allowing interaction between the interiors of the two cells<sup>8</sup>. The membrane potential of mesenchymal stem cells is approximately  $-35$  mV<sup>9, 10</sup>. As a consequence, electrotonic coupling between a stem cell and a ventricular myocyte is expected to cause depolarization and a change in the action potential morphology of the myocytes. This may result in conduction slowing, conduction heterogeneity and unidirectional conduction block, together facilitating re-entrant arrhythmias<sup>11, 12</sup>. A second suggested pathway is the involvement of paracrine factors that can either directly or indirectly (paracrine cross talk) influence cardiomyocyte and/or stem cell function<sup>7</sup>.

Another drawback of cell-based therapies concerns the availability of stem cells. Autologous stem cells, such as mesenchymal stem cells from bone marrow, are not only rare but also difficult to obtain and expand to the large number required for treatment. Multipotent cells, such as adipose tissue-derived stromal cells (ADSCs) are, however, highly abundant in lipo-aspirates, which are easy to obtain from healthy individuals. ADSCs are not only abundantly present, but also a source of multipotent cells capable of differentiating along multiple lineage pathways with little immunological effects<sup>13, 14</sup>. In addition, ADSCs secrete a wide variety of factors known to stimulate angiogenesis<sup>15</sup> and neovascularization<sup>16</sup>, making them clinically relevant for possible cell based therapies; their use is favored to date. However, the function of autologous stem cells can deteriorate because of age and risk factors such as hyperglycemia and hyperlipidemia, which are present in the elderly population, in whom myocardial infarctions are most prevalent<sup>17, 18</sup>. Current studies that describe the safety and efficacy of allogeneic stem cells indicate these can be used as a "off -the-shelf" alternative for autologous stem cells<sup>19, 20</sup>. In addition, xenogeneic stem cells, are considered an alternative to autologous stem cell administration and have been described frequently<sup>21-24</sup>. The potential difference in the proarrhythmic effects of adipose derived stromal cells across species is unknown.

In this *in vitro* study we specifically address the potential adverse electrophysiological effects that different adipose tissue-derived stromal cells have on a confluent layer of neonatal rat ventricular (cardio)myocytes (NRVMs). We specifically studied the different (allogeneic and xenogeneic) species sources of ADSCs namely rat, human and pig.

## Significance

Cell-based therapy is a promising option to treat patients after myocardial infarction. Although cell-based therapy may help replace infarcted heart tissue by functional tissue, it has some limitations. First, it may cause life-threatening arrhythmias. Slow conduction facilitates arrhythmias induction. Second, cells derived from and administered to the same patients may be affected by age and disease. Therefore, cells from other patients or other species may be used. This study shows that application of stromal cells caused conduction slowing in cardiomyocyte monolayers, irrespective of the specific origin of the cells, but that the conduction slowing is conferred through soluble factors or through coupling between fat-derived cells and cardiac myocytes in a species-dependent manner.

## MATERIAL AND METHODS

A detailed description of the methods can be found in the supplemental online data. *Isolation and Culturing of Neonatal Rat Ventricular Myocytes*

All animal experiments were approved by the local Animal Experiments Committee (Academic Medical Center, University of Amsterdam and University Medical Center Groningen, University of Groningen and carried out in accordance with national and institutional guidelines.

Briefly, hearts were explanted from 1- to 2-day-old Wistar rats. Ventricles were dissected into pieces and dissociated with trypsin (Becton Dickinson BV, Breda, The Netherlands, <https://www.bd.com>) and collagenase (230 unites/mg; Worthington Biochemical Corp., Vollenhove, The Netherlands, <http://www.worthington-biochem.com>). Cells were preplated to minimize fibroblasts contamination. The remaining myocardial cells were plated on fibronectin (BD Biosciences) coated multi-electrode-arrays (MEAs; Multi Channel Systems MCS GmbH, Reutlingen, Germany, <http://multichannelsystems.com/>) at a density of  $1.4 \times 10^5$  cells per  $\text{cm}^2$ .

### Isolation and Culture of Adipose Tissue-Derived Stromal Cells

ADSCs were isolated and cultured as described previously<sup>25</sup>. Inguinal rat fat (male, Wistar, 7-8 months), porcine subcutaneous abdominal fat (male, 3-4 months [provided by the Department of Experimental Surgery of the Academic Medical Center]), and human subcutaneous abdominal fat (donated by healthy patients with body mass index  $<30 \text{ kg/m}^2$ ; Bergman Clinics, The Netherlands) were used. Tissue was minced and washed extensively with phosphate-buffered saline, before being subjected to dissociation steps with collagenase (Roche Diagnostics, Mannheim, Germany, <http://www.roche.com>). The obtained stromal vascular fraction was then incubated with erythrocyte lysis buffer; after this, the cells were seeded at a density of  $4 \times 10^4$  cells per  $\text{cm}^2$ , and ADSCs were propagated at a 1:2

ratio and used from passage 3 onwards. Cells were referred to rat ADSCs (rADSCs), human ADSCs (hADSCs) or pig ADSCs (pADSCs).

The use of liposuction material as source of ADSCs was approved by of the local Ethics Committee of University Medical Center Groningen, because it was considered anonymized waste material. Yet, for each of these anonymous donations the clients gave their consent after information.

### Experimental Conditions

To investigate effects of ADSCs, cocultures of NRVM and ADSC were prepared. Four days after seeding NRVMs, ADSCs were added to the monolayers at a ratio of 1:1, and 2 days later electrophysiological measurements were performed.

To assess paracrine effects, conditioned medium (Cme) was collected from monolayers of NRVMs, (Cme NRVM), cocultures (Cme NRVMs:ADSCs), and confluent cultures of ADSCs (Cme ADSC). Medium was also collected from cocultures with transwell inserts: this medium was called Cme transwell ADSC. In transwell experiments, NRVMs and ADSCs are cultured together without making direct contact. Cme was filtered (0.22 $\mu$ m) before being added to monolayers of NRVMs only on day 4 of culture and 2 days before measurements.

### Electrical Mapping and Microelectrode Measurements

Electrophysiological parameters were determined by mapping the electrical activity of the monolayers. MEAs harbored 60 electrodes terminals, aligned in an 8 by 8 matrix with terminals in the core portion of the MEA (supplemental online Fig.1). Cultures were stimulated using a bipolar extracellular stimulus electrode (twice diastolic stimulation threshold, 1-or-2 millisecond pulse width). Conduction velocity (CV), and conduction heterogeneity were determined from the unipolar electrograms recorded. For each experiment two monolayers of NRVMs served as control. Values obtained under different conditions were compared with the values of control monolayers of the same isolation. Resting membrane potential (RMP) and upstroke velocity of an action potential were determined from action potentials recorded during microelectrode measurements.

### Immunostainings

Cells plated in 12-wells plates used for immunofluorescence were cultured under the same conditions as cells on MEAs. Briefly, after fixation in 4% paraformaldehyde cells were permeabilized and blocked before staining with primary and secondary antibodies. Examination was performed by Leica SPE confocal laser scanning and Leica Application Suite Advanced Fluorescence software (Leica Microsystems, Buffalo Grove IL, <https://www.leica-microsystems.com>). Immunofluorescence images were analyzed using ImageJ software, version 1.50i (National Institutes of Health, Bethesda, MD, <https://imagej.nih.gov/ij>).



## Statistical Analysis

Continuous and normally distributed variables are presented as mean  $\pm$  SD (unless otherwise mentioned) and were compared by using an independent t-test. For more than two groups, a one-way analysis of variance was performed with the Bonferroni correction as post-hoc analysis. In case of a skewed distribution, data are presented as median with the interquartile range and tested with the Mann Whitney test; in case of more than two groups a Kruskal-Wallis analysis was performed with post-hoc analysis using the Dunn test. A p-value of  $<.05$  was considered to indicate statistically significant differences. All graphs were made by using GraphPad Prism software, version 5 (Graphpad Software, La Jolla, CA, <http://graphpad.com/>).

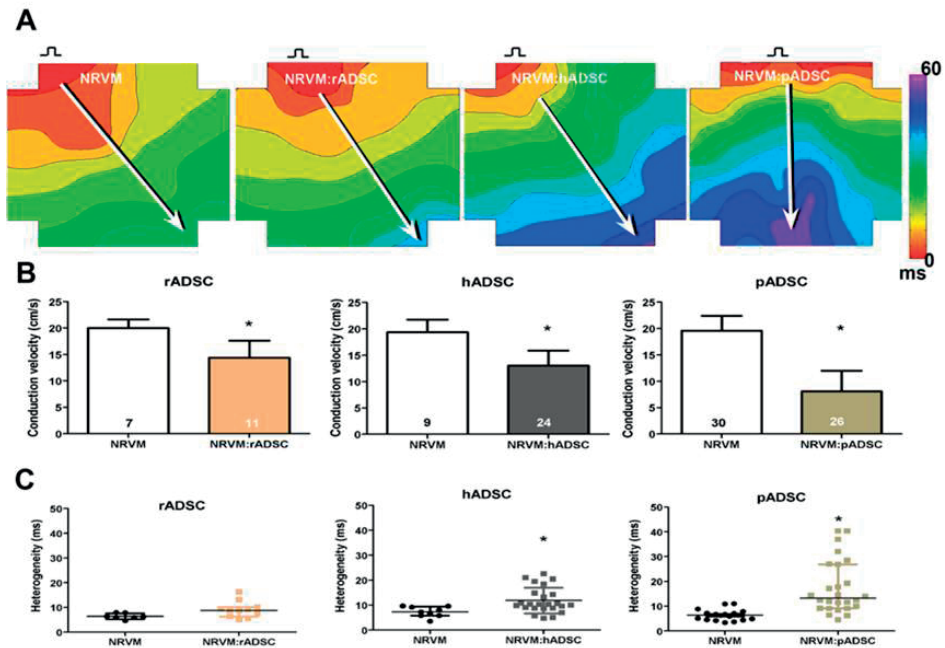


Figure 1. Effect of ADSCs on conduction velocity and heterogeneity in monolayers of NRVMs. (A): Activation map of a monolayer of NRVMs, a monolayer cultured with rADSCs, a monolayer with hADSCs, and a monolayer with pADSCs. Conduction velocity is determined along white arrows perpendicular to isochronal lines. (B): conduction velocity of controls and different cocultures (mean  $\pm$  SD). (C): conduction heterogeneity (median with IQR). \* indicates  $p < .001$  compared with the monolayers of NRVM. Abbreviations: ADSC, adipose tissue-derived stromal cell; hADSC, human adipose tissue-derived stromal cell; NRVM, neonatal rat ventricular myocyte; pADSC, pig adipose tissue-derived stromal cell; rADSC, rat adipose tissue-derived stromal cell.

## RESULTS

### Effects of co-culturing ADSC with NRVM

Monolayers of NRVMs cocultured with rADSCs demonstrated conduction slowing compared with monolayers of NRVMs only (Fig. 1A). On average, conduction velocity was  $14.4 \pm 3.2$  cm/second in monolayers of NRVM, cocultured with rADSCs, compared to  $20.0 \pm 1.6$  cm/second in control monolayers ( $p < .001$ , Fig. 1B). Similar to rADSCs, monolayers that were cocultured with hADSCs ( $13.0 \pm 2.8$  cm/second) or pADSCs ( $8.0 \pm 3.9$  cm/second) also demonstrated significant conduction slowing compared with their respective controls ( $19.3 \pm 2.4$  and  $20.2 \pm 2.8$  cm/second, respectively;  $p < .001$ , Fig. 1. A and B).

Conduction heterogeneity in monolayers of NRVM cocultured with rADSCs demonstrated a trend to be higher compared with control monolayers (8.75 (3.8) vs. 6.2 (1.95) milliseconds,  $p = .056$ , Fig. 1C). Heterogeneity in cocultures with hADSCs was on average higher than in control monolayers (10.3 (5.9) vs 7.2 (5.1) milliseconds;  $p < .01$ , Fig. 1C). Monolayers cocultured with pADSCs (13.3 (17.7) milliseconds) also demonstrated a significant increase in conduction heterogeneity compared with monolayers of NRVMs only (6.4 (2.9) milliseconds;  $p < .001$ , Fig. 1C).

### Effects of conditioned medium of NRVM:ADSC

To determine the mechanisms behind the conduction slowing, we cultured NRVM monolayers in Cme obtained from the various cocultures. Conduction velocity in NRVM monolayers cultured in Cme of the NRVM:rADSC cocultures was not different from conduction velocity ( $19.2 \pm 2.0$  cm/second) or conduction heterogeneity (7.0 (5.4) milliseconds) in control monolayers ( $21.8 \pm 1.8$  cm/seconds and 5.9 (1.9) milliseconds;  $p = \text{n.s.}$ , Fig. 2A and B). Conduction velocity in NRVM monolayers cultured with Cme of NRVM:hADSC cocultures was also not affected compared with controls ( $18.5 \pm 2.2$  vs.  $19.0 \pm 1.2$  cm/seconds;  $p = \text{n.s.}$ , Fig. 2A). Conduction heterogeneity was not affected when NRVM monolayers were cultured in Cme NRVM:hADSC (4.9 (2.0) vs. 5.3 (1.9);  $p = \text{n.s.}$ , Fig. 2B). In contrast, Cme NRVM:pADSC slowed conduction velocity significantly compared with control monolayers ( $7.0 \pm 2.9$  vs.  $19.6 \pm 2.4$  cm/second;  $p < .001$ , Fig. 2A). Conduction heterogeneity was also significantly increased by Cme NRVM:pADSC compared with control monolayers (16.3 (13.2) vs. 5.5 (1.5) milliseconds;  $p < .001$ , Fig. 2B). Cme NRVM served as control for the conditioned medium conditions and did not differ from control monolayers in any of the groups (Fig. 2A, B). The CV or the heterogeneity in monolayers cocultured with pADSCs was not significantly different from the CV or the heterogeneity in monolayers of NRVMs cultured in Cme NRVM:pADSC (compare Fig. 1B, C vs. 2A, B).

Conditioned medium of the cocultures NRVM:pADSC affected conduction properties of NRVM monolayers. To distinguish whether this effect is attributed to soluble factors of pADSCs or whether there is an interaction (cross talk and/or electrotonic connections)

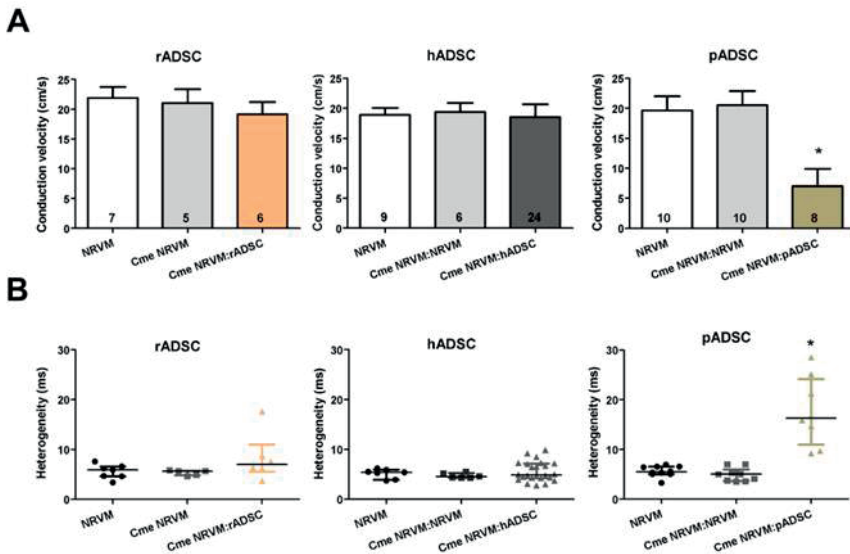


Figure 2. Effect of Cme ADSC:NRVM on conduction velocity and heterogeneity in monolayers of NRVM. Effects on conduction velocity (mean  $\pm$  SD) (A) and conduction heterogeneity (median with IQR) (B) in monolayers of NRVM cultured in the Cme obtained from the different cocultures. \* indicates  $p < .01$  compared with control monolayers and monolayers of NRVM cultured in Cme NRVM. Abbreviations: Cme, conditioned medium; hADSC, human adipose tissue-derived stromal cell; NRVM, neonatal rat ventricular myocyte; pADSC, pig adipose tissue-derived stromal cell; rADSC, rat adipose tissue-derived stromal cell.

between pADSCs and NRVMs, we further explored the effects of Cme pADSC and Cme transwell pADSCs. NRVM monolayers cultured in Cme pADSC and Cme transwell pADSCs both demonstrated significant lower conduction velocities compared to controls ( $16.3 \pm 2.4$ , and  $14.6 \pm 1.6$  vs.  $19.6 \pm 1.8$  cm/second, respectively;  $p < .05$ , Fig. 3A). Conduction heterogeneity was only affected by Cme transwell pADSC ( $11.1$  ( $4.9$ ) vs.  $5.7$  ( $3.8$ ) milliseconds;  $p < .05$ , Fig. 3B).

Conditioned medium obtained from only hADSCs and rADSCs did not affect conduction velocity or the heterogeneity of NRVM monolayers (supplemental online Fig. 2). In contrast to when monolayers of NRVM were incubated for 48 hours with Cme NRVM:pADSC, application immediately before electrical mapping of Cme NRVM:pADSC did not have an effect (results not shown).

### Microelectrode Measurements

Microelectrode measurements were performed to study whether the observed conduction slowing could be explained by depolarization. As expected, monolayers of NRVM cocultured with rADSCs, hADSCs and pADSCs were depolarized compared with control monolayers (RMP,  $-50.95 \pm 9.45$  vs.  $-65.06 \pm 5.98$  mV,  $-52.6 \pm 15.2$  vs.  $-71.2 \pm 13.1$  mV and  $-44.7 \pm$

16.2 vs.  $-66.0 \pm 7.9$  mV respectively;  $p < .01$ , Fig. 4). Although monolayers cultured in Cme NRVM:rADSC and Cme NRVM:hADSC demonstrated no effect on conduction velocity, these monolayers were depolarized compared to controls ( $-55.4 \pm 6.2$  vs.  $-65.1 \pm 6.0$  mV and  $-52.1 \pm 12.8$  vs.  $-71.2 \pm 13.1$  mV, respectively;  $p < .01$ ). Cme NRVM:pADSC elicited heterogeneous conducting slowing, and these cultures were also depolarized compared to controls ( $-44.0 \pm 9.0$  vs.  $-66.0 \pm 7.9$  mV;  $p < .01$ , Fig. 4). Depolarization in monolayers of NRVM induced by Cme NRVM:pADSC was significantly more compared to depolarization induced by Cme NRVM:rADSC ( $p < .01$ ) and Cme NRVM:hADSC ( $p < .01$ ).

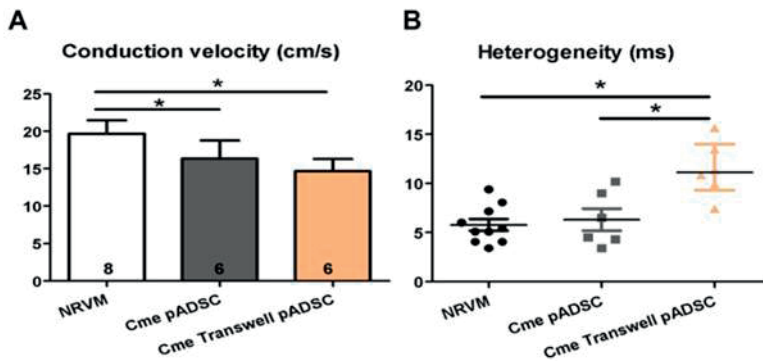
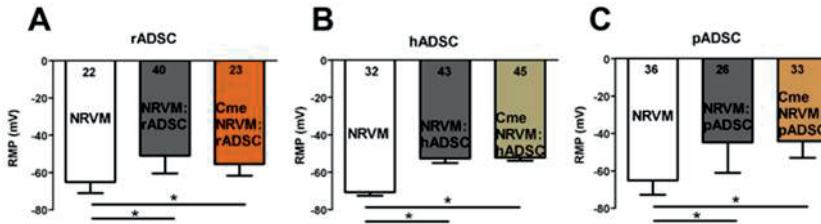


Figure 3. Effect of Cme pADSC transwell and Cme pADSC on conduction velocity and heterogeneity in monolayers of NRVM. Effects on conduction velocity (mean  $\pm$  SD) (A) and conduction heterogeneity (median with IQR) (B) in monolayers of NRVM cultured in condition medium obtained from the transwell cocultures and pADSC culture, \* indicates  $p < .05$ . Abbreviations: Cme, conditioned medium; NRVM, neonatal rat ventricular myocyte; pADSC, pig adipose tissue-derived stromal cell.

### Relationship between RMP and Conduction Velocity

A theoretical sigmoid relation exists between RMP and CV<sup>26, 27</sup>. We studied whether the relation between local RMP and conduction velocity was maintained in cocultures and after culturing in the presence of Cme. Figure 5A shows the relation between RMP and CV in the three different cocultures as well as in the pooled control monolayers (NRVM). In a similar fashion, Figure 5B shows the combined data of monolayers subjected to Cme of the various species and their corresponding pooled controls. In both panels, a sigmoid function is fitted through the combined data points (black lines).

Because the average data do not appear to deviate from the theoretical sigmoid function, the figures show that the degree of depolarization of each monolayers is the main determinant of the conduction velocity and that the degree of depolarization is different in the various conditions (Fig. 4).



**Figure 4.** Effects of adipose tissue-derived stromal cells and Cme on membrane potential. The effects of coculturing rADSC (A), hADSC (B), and pADSC (C) together with NRVM and the effects of conditioned medium on resting membrane potential (mean  $\pm$  SD). \*,  $p < .001$  compared with control monolayers (N = impalements). Abbreviations: Cme, conditioned medium; hADSC, human adipose tissue-derived stromal cell; NRVM, neonatal rat ventricular myocyte; pADSC, pig adipose tissue-derived stromal cell; rADSC, rat adipose tissue-derived stromal cell.

### Cell Characterization and Gap Junctions

Confluent monolayers of NRVM and cocultures were visualized with light microscopy and immunostaining at day 6. Immunofluorescence staining was performed using the cardiomyocyte and ADSC marker,  $\alpha$  actinin and CD44, respectively (supplemental online Fig. 3). Fluorescent microscopy results revealed that ADSCs were scattered heterogeneously throughout the NRVM monolayer (supplemental online Fig. 3). Immunofluorescence was performed to visualize connexin 43 (Cx43) and connexin 45 (Cx45) on cardiomyocytes or ADSCs. Cocultures were stained for CD44 and the connexins Cx43 (supplemental online Fig. 4.1A-D) and Cx45 (supplemental online Fig. 4.2A-D). In monolayers of NRVM Cx43 and Cx45 are abundantly present (supplemental online Fig. 4.1A and 4.2A).

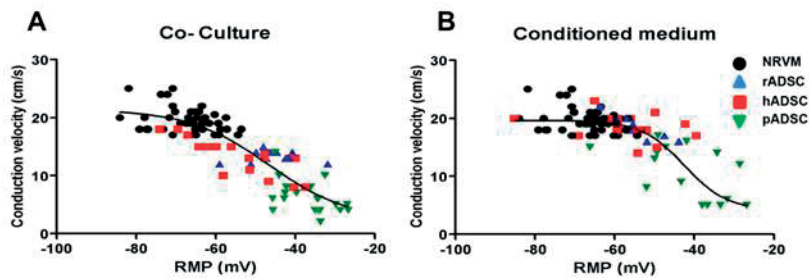


**Figure 5.** Relationship between RMP and conduction velocity. The relationship between RMP and CV in coculture situations (A) and in monolayers cultured in conditioned medium from the respective cocultures (B). Abbreviations: hADSC, human adipose tissue-derived stromal cell; NRVM, neonatal rat ventricular myocyte; pADSC, pig adipose tissue-derived stromal cell; rADSC, rat adipose tissue-derived stromal cell; RMP, resting membrane potential.

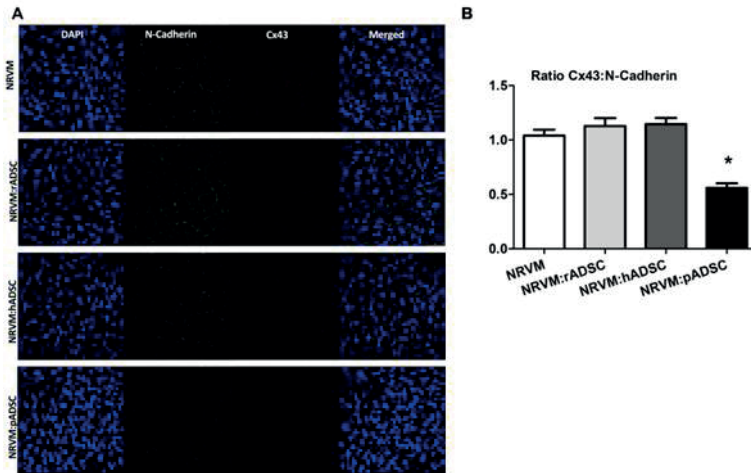


**Figure 6.** Immunofluorescence micrographs of the various cultures stained with N-cadherin and Cx43. (A): Monolayers of NRVM and monolayers of NRVM cocultured with rADSCs, hADSCs or pADSCs are stained for N-Cadherin and Cx43 (original magnification, x40). (B): the Cx43: N-Cadherin ratio in the various cultures determined by the number of pixels. Ratios (mean±SEM) are based on 5-10 images taken in each of three independent experiments \*,  $p < .001$ . Abbreviations: ADSC, adipose tissue-derived stromal cell; DAPI, 49,6-diamidino-2-phenylindole; NRVM, neonatal rat ventricular myocyte; pADSC, pig adipose tissue-derived stromal cell; rADSC, rat adipose tissue-derived stromal cell.

In monolayers of NRVM cocultured together with either rADSC or hADSC Cx43 and Cx45 are also seen (supplemental online Fig. 4, white arrowheads). However, in the monolayers of NRVM co-cultured with pADSC, Cx43 and Cx45 are rarely seen (supplemental online Fig. 4.1D and 4.2D). To quantify these observations, immunofluorescence was performed for N-Cadherin and Cx43 (Fig. 6A) and the ratio of Cx43:N-Cadherin was quantified (Fig. 6B). NRVM monolayers cultured with pADSCs demonstrated significantly lower levels of Cx43:N-Cadherin ratio than control monolayers ( $0.56 \pm 0.04$  [ $\pm$ SEM] vs.  $1.04 \pm 0.05$ ;  $p < .001$ ) and then monolayers of NRVM cultured with either rADSCs or hADSCs, respectively ( $1.12 \pm 0.08$  and  $1.15 \pm 0.06$ ;  $p < .001$ , Fig. 6B).

## DISCUSSION

In this study we have shown that application of ADSCs, regardless of the species origin, causes heterogeneous conduction slowing in NRVM monolayers. The conduction effect could be attributed to electrotonic interaction and/or paracrine mechanisms. To distinguish between these mechanisms, we first investigated the effects of conditioned medium obtained from the various cocultures. Only conditioned medium from cocultures of NRVMs and pADSCs replicated the effects observed in the cocultures. This indicates the involve-

ment of soluble factors and possible paracrine cross talk between the two cell types, in a deleterious way. In humans and rats the paracrine effects could not be replicated, suggesting that electrotonic coupling plays a more prominent role in these species.

The existence of paracrine cross-talk between cardiomyocytes and non-cardiomyocytes has been suggested by Pedrotty et al.<sup>28</sup> and others<sup>7, 29</sup>. Pedrotty et al. demonstrated that conditioned medium from a culture of cardiac fibroblasts altered electrophysiological properties of NRVMs. However, when the same fibroblasts were grown in the presence of NRVMs and the resulting conditioned medium was used, all arrhythmogenic effects disappeared, suggesting that cardiomyocytes were 'activated' to produce protective factors that protect them from damaging soluble factors secreted by the fibroblasts<sup>28</sup>. To determine whether the observed heterogeneous conduction slowing could be attributed to paracrine cross talk between NRVMs and pADSCs or solely to the soluble factors of pADSCs, we used transwell inserts. In these cultures pADSCs and NRVMs are unable to physically connect, eliminating electrotonic interactions, but allowing the exchange of soluble factors. Conditioned media from transwell conditions were used to culture NRVM monolayers and the results were compared with those obtained in conditioned medium from pADSCs only. Our results show that ADSCs produce adverse soluble factors that slow the conduction velocity of NRVM monolayers. However, because the conduction slowing by Cme pADSC ( $16.3 \pm 2.4$  cm/second) and Cme transwell pADSC ( $14.6 \pm 1.6$  cm/second) is less outspoken than in Figure 1 (coculture NRVM:pADSC,  $p < .001$  and  $p < .01$  respectively) and Figure 2 (Cme NRVM:pADSC  $p < .01$ , and  $p < .001$  respectively), we deduce that the physical interaction between pADSCs and NRVMs is a prerequisite for this fully paracrine effect. The fact that heterogeneity is not altered with the Cme pADSC whereas the conduction velocity is significantly changed may be related to a different sensitivity to change in uncoupling, resting membrane potential and/or capacitance. We surmise that Cme transwell pADSC influences the interaction in a more severe manner than Cme pADSC alone. In Cme transwell pADSC and NRVM:pADSC, the cells have had a chance to influence each other and therefore the composition of the conditioned medium is likely to be different from that of the Cme pADSC. Therefore, the communication between pADSCs and NRVMs is necessary for both CV reduction and increased heterogeneity.

In the interaction between NRVMs and ADSCs derived from human and rats, electrotonic coupling likely plays a role. First, condition medium obtained from the coculture of NRVM and rat or human ADSC did not replicate the results from the corresponding coculture and the physical presence of the ADSC is therefore required for the production of conduction slowing. However, conditioned medium of NRVM:rADSC and NRVM:hADSC cocultures did induce depolarization in NRVM monolayers that was not different from the depolarization in the co-cultures. This suggests that soluble factors are responsible for the depolarization but that this is not sufficient for conduction slowing. The relation between RMP and conduction velocity is non-linear<sup>26, 27</sup>, and it is possible that the depolarization

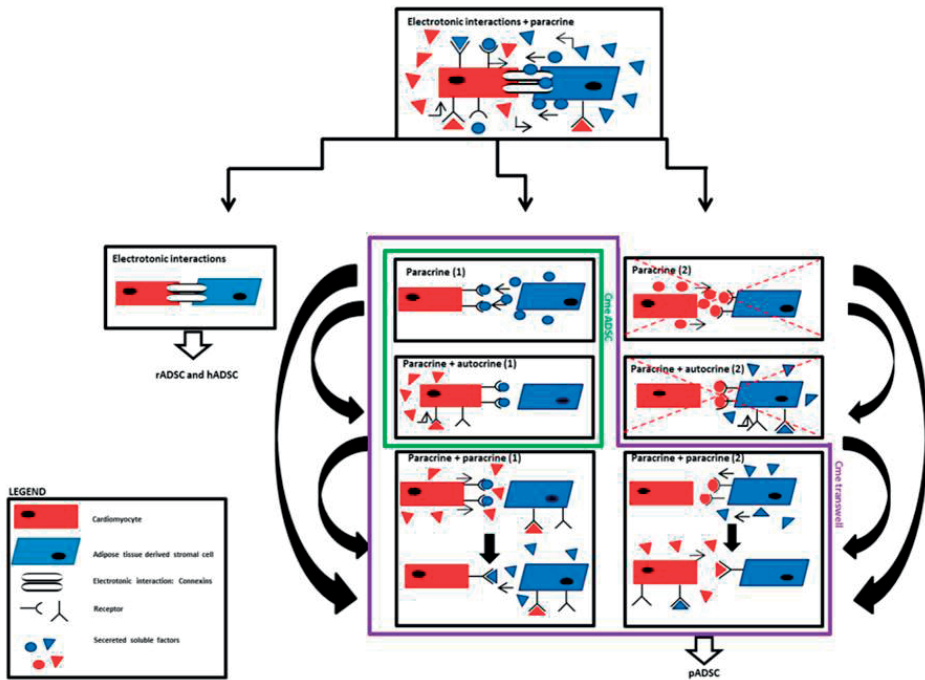


Figure 7. Schematic illustration of the various interactions between neonatal rat ventricular myocytes (NRVM) and ADSC. The figure summarizes the study. First, cocultures of cardiomyocytes and ADSCs are studied. In this scenario, all situations are possible: electrotonic interactions and the various paracrine interactions. We can therefore not exclude or identify which of the situations explains the heterogeneous conduction slowing. The next step is to distinguish between electrotonic interactions and the paracrine interactions. Experiments with conditioned medium (Cme) transwell conditions can allow simple to complicated cross-talk situations; **paracrine** only, **paracrine + autocrine** or, **paracrine + paracrine**, wherein soluble factors of one cells leads to the secretion of soluble factors by the other cells. This, in turn, stimulates the first cell to secrete different soluble factors. Experiments done with Cme ADSC can only be explained by **paracrine (1)** effects of ADSCs on NRVMs, or paracrine factors from ADSCs initiate NRVMs to secrete soluble factors that have an autocrine effect (**paracrine + autocrine(1)**). The situations that are crossed out can also occur, however, the focus of the study is on the effects ADSC have on NRVM conduction properties and not on the effects of NRVM on ADSC. Therefore these situations are omitted. If we follow the logic of the scheme, we can conclude that the primary mechanism for hADSCs and rADSCs is electrotonic as heterogeneous conduction slowing is not observed when Cme ADSC are used. When Cme ADSC and Cme transwell of pADSC are used, we still observe heterogeneous conduction slowing, suggesting the primary effect is paracrine based. Abbreviations: ADSC, adipose tissue-derived stromal cell; hADSC, human adipose tissue-derived stromal cell; pADSC, pig adipose tissue-derived stromal cell; rADSC, rat adipose tissue-derived stromal cell.

induced by conditioned medium of rADSC and hADSC cocultures was slightly less than in the conditioned medium of pADSC cocultures and therefore insufficient to lead to a conduction slowing. Therefore, it is more probable that the depolarization induced by the soluble factors alone is not enough to induce the heterogeneous conduction slowing



in rat and human ADSC cocultures, and additional intercellular coupling is required. The additional intercellular coupling between the rat/human ADSCs and the myocytes would then provide additional depolarization<sup>9</sup>, may lead to additional capacitive loading of the NRVM<sup>30</sup>, or cause interference with sodium channel function. We have also shown that the relationship between the RMP and the conduction velocity does not deviate from the theoretical sigmoid relation and that it is the same in cocultures and in monolayers subjected to Cme alone (Fig. 5). This suggests that the degree of depolarization determines conduction velocity in each condition. Whether the RMP is determined by paracrine factors or by electrotonic coupling depends on species and conditions.

From the immunofluorescence data, we deduce that connexins (Cx43 and Cx45) are present at the interface between NRVMs and ADSCs in the cocultures with rADSCs and hADSCs. The ratio Cx43: N-Cadherin in these cocultures is not different from that in the control. In these cocultures, electrotonic interaction is therefore possible, although we cannot exclude that the connexins are not entirely electrophysiologically functional (this would require double voltage clamp, which is not feasible in a coculture). Taken together, these data support the idea that electrotonic interaction is the main contributor of the significant heterogeneous conduction slowing in cocultures with rADSCs and hADSCs. This is supported by the observation that Cme of rADSCs and hADSCs were not effective. In contrast, connexins are barely present, and the ratio of Cx43:N-Cadherin is significantly lower in cocultures with pADSCs. We demonstrated that the electrophysiological effects of pADSCs are caused through paracrine mechanisms because they are also present in monolayers cultured in Cme NRVM:pADSC. The loss of the connexins can in addition increase the axial resistance, which is important for the propagation of the cardiac impulse.

All cells have a wide secretome of soluble factors that are secreted and that can influence the behavior and the secretome of other cells. However, these soluble factors in turn can be influenced by environmental factors as well as other soluble factors secreted either by other cells or indirectly by the cell itself (autocrine). The exact nature of the soluble factor(s) responsible for inducing the observed heterogeneous conduction slowing is unlikely to be identified and outside the scope of this paper. Figure 7 gives a schematic summary of this study and the possible cross-talk interactions that can take place between cardiomyocytes and the various ADSC used.

Our findings that ADSC influence electrophysiological properties of NRVM corroborates those of previous studies, both *in vitro* and *in vivo*, that demonstrated that stem cells influence electrophysiological properties<sup>5, 6, 31, 32</sup>. However, in this study we specifically studied three different species sources of ADSC: rat, human and swine. Human and porcine ADSCs were chosen to investigate their arrhythmogenic potential and to see whether porcine ADSCs react differently than human ADSCs. rADSC were chosen to model allogeneic stem cell application. We have shown that cells of the same species as the monolayer cause similar conduction slowing as xenogeneic stem cells.

The study has some limitations. Culturing the two cell types may introduce heterogeneous depolarization of the resting membrane by (a) coupling between ADSCs and NRVMs or (b) paracrine depolarization. Regarding coupling, two potential mechanisms are operative: (a) ADSCs have a less negative RMP than NRVMs and, coupling may cause depolarization of the NRVMs and (b) coupling may induce a capacitive coupling between the cells that will impede transmission of a propagated impulse. Although we cannot entirely discriminate between the mechanisms, we have addressed the main determinants of CV in our approach. Although repolarization changes may well affect conduction velocity (if the stimulus coincides with the end of the repolarization, as with short premature stimuli), the influence of repolarization abnormalities can be excluded since we did not apply short coupled stimuli.

Although NRVMs and human cardiomyocytes differ, the use of NRVMs (cultured on MEAs) has been established as a reliable model for electrophysiological studies<sup>33-35</sup>. Compared with adult models, the RMP and CV values obtained in this and other studies are rather low<sup>7, 36, 37</sup>. In NRVM monolayers therefore sodium channels are partially inactivated. In view of these and our own observations, we assume that propagation in the NRVM monolayers subjected to ADSCs is, (also because of depolarization) partially carried by the calcium current resulting in relatively low conduction velocities. The advantage of the *in vitro* model of ADSC transplantation is that it allows a controlled application of stromal cell number and conditioned medium to a 2D model excluding the influence of confounding factors.

## CONCLUSIONS

Our results show that ADSCs cause heterogeneous conduction slowing when cocultured on a monolayer of NRVM. Paracrine modulation and intercellular coupling between these two cell types contribute to the formation of a potentially proarrhythmic substrate. We have generated a paracrine-based proarrhythmic cell model with pADSCs and an electrotonic-based proarrhythmic cell model with hADSCs and rADSCs. The study shows that adipose stromal cells from different species may interfere with host cardiomyocytes via different mechanisms. We have also demonstrated that the arrhythmic potential of stem cells is maintained even when cross-species transplantation is used.

Our study was designed to address potential adverse electrophysiological effects of ADSC-based therapies. Although the question of whether the excreted soluble factors are “beneficial” (e.g., the potential hemodynamic benefit seen in a more clinical setting) is outside the scope of this paper, we have shown that conditioned medium from hADSCs alone does not cause conduction slowing and could thus potentially be used for the

possible beneficial soluble factors it contains without having the adverse effects of the interactions these cells can form with cardiomyocytes.

## ACKNOWLEDGMENTS

We gratefully acknowledge the technical support of A.C. Linnenbank. The financial contributions of ICARUS of the BioMedical Materials program (project-P5.01) and the LeDucq (SHAPEHEART network) are acknowledged.

## REFERENCES

1. Mozaffarian D, Benjamin EJ, Go AS, Arnett DK, Blaha MJ, Cushman M, de Ferranti S, Despres JP, Fullerton HJ, Howard VJ, Huffman MD, Judd SE, Kissela BM, Lackland DT, Lichtman JH, Lisabeth LD, Liu S, Mackey RH, Matchar DB, McGuire DK, Mohler ER, 3rd, Moy CS, Muntner P, Mussolino ME, Nasir K, Neumar RW, Nichol G, Palaniappan L, Pandey DK, Reeves MJ, Rodriguez CJ, Sorlie PD, Stein J, Towfighi A, Turan TN, Virani SS, Willey JZ, Woo D, Yeh RW, Turner MB, American Heart Association Statistics C and Stroke Statistics S. Heart disease and stroke statistics--2015 update: a report from the American Heart Association. *Circulation*. 2015;131:e29-322.
2. Wollert KC, Meyer GP, Lotz J, Ringes-Lichtenberg S, Lippolt P, Breidenbach C, Fichtner S, Korte T, Hornig B, Messinger D, Arseniev L, Hertenstein B, Ganser A and Drexler H. Intracoronary autologous bone-marrow cell transfer after myocardial infarction: the BOOST randomised controlled clinical trial. *Lancet*. 2004;364:141-148.
3. Bolli R, Chugh AR, D'Amario D, Loughran JH, Stoddard MF, Ikram S, Beache GM, Wagner SG, Leri A, Hosoda T, Sanada F, Elmore JB, Goichberg P, Cappetta D, Solankhi NK, Fahsah I, Rokosh DG, Slaughter MS, Kajstura J and Anversa P. Cardiac stem cells in patients with ischaemic cardiomyopathy (SCIPIO): initial results of a randomised phase 1 trial. *Lancet*. 2011;378:1847-1857.
4. Makkar RR, Smith RR, Cheng K, Malliaras K, Thomson LE, Berman D, Czer LS, Marban L, Mendizabal A, Johnston PV, Russell SD, Schuleri KH, Lardo AC, Gerstenblith G and Marban E. Intracoronary cardiosphere-derived cells for heart regeneration after myocardial infarction (CADUCEUS): a prospective, randomised phase 1 trial. *Lancet*. 2012;379:895-904.
5. Price MJ, Chou CC, Frantzen M, Miyamoto T, Kar S, Lee S, Shah PK, Martin BJ, Lill M, Forrester JS, Chen PS and Makkar RR. Intravenous mesenchymal stem cell therapy early after reperfused acute myocardial infarction improves left ventricular function and alters electrophysiologic properties. *IntJCardiol*. 2006;111:231-239.
6. Chang MG, Tung L, Sekar RB, Chang CY, Cysyk J, Dong P, Marban E and Abraham MR. Proarrhythmic potential of mesenchymal stem cell transplantation revealed in an in vitro coculture model. *Circulation*. 2006;113:1832-1841.
7. Askar SF, Ramkisoensing AA, Atsma DE, Schaliij MJ, de Vries AA and Pijnappels DA. Engraftment patterns of human adult mesenchymal stem cells expose electrotonic and paracrine proarrhythmic mechanisms in myocardial cell cultures. *CircArrhythmElectrophysiol*. 2013;6:380-391.
8. Valiunas V, Doronin S, Valiuniene L, Potapova I, Zuckerman J, Walcott B, Robinson RB, Rosen MR, Brink PR and Cohen IS. Human mesenchymal stem cells make cardiac connexins and form functional gap junctions. *J Physiol*. 2004;555:617-26.
9. Heubach JF, Graf EM, Leutheuser J, Bock M, Balana B, Zahanich I, Christ T, Boxberger S, Wettwer E and Ravens U. Electrophysiological properties of human mesenchymal stem cells. *JPhysiol*. 2004;554:659-672.
10. Sundelacruz S, Levin M and Kaplan DL. Membrane potential controls adipogenic and osteogenic differentiation of mesenchymal stem cells. *PLoS One*. 2008;3:e3737.
11. Lammers WJ, Schaliij MJ, Kirchhof CJ and Allesie MA. Quantification of spatial inhomogeneity in conduction and initiation of reentrant atrial arrhythmias. *The American journal of physiology*. 1990;259:H1254-63.

12. de Bakker JM, van Capelle FJ, Janse MJ, Tasseron S, Vermeulen JT, de Jonge N and Lahpor JR. Slow conduction in the infarcted human heart. 'Zigzag' course of activation. *Circulation*. 1993; 88:915-26.
13. Madonna R, Geng YJ and De Caterina R. Adipose tissue-derived stem cells: characterization and potential for cardiovascular repair. *Arterioscler Thromb Vasc Biol*. 2009;29:1723-9.
14. Nakagami H, Morishita R, Maeda K, Kikuchi Y, Ogihara T and Kaneda Y. Adipose tissue-derived stromal cells as a novel option for regenerative cell therapy. *J Atheroscler Thromb*. 2006;13: 77-81.
15. Rehman J, Traktuev D, Li J, Merfeld-Clauss S, Temm-Grove CJ, Bovenkerk JE, Pell CL, Johnstone BH, Conside RV and March KL. Secretion of angiogenic and antiapoptotic factors by human adipose stromal cells. *Circulation*. 2004;109:1292-8.
16. Miranville A, Heeschen C, Sengenès C, Curat CA, Busse R and Bouloumie A. Improvement of postnatal neovascularization by human adipose tissue-derived stem cells. *Circulation*. 2004; 110:349-55.
17. Golpanian S, El-Khorazaty J, Mendizabal A, DiFede DL, Suncion VY, Karantalis V, Fishman JE, Ghersin E, Balkan W and Hare JM. Effect of aging on human mesenchymal stem cell therapy in ischemic cardiomyopathy patients. *J Am Coll Cardiol*. 2015;65:125-32.
18. Efimenko A, Dzhoyashvili N, Kalinina N, Kochegura T, Akchurin R, Tkachuk V and Parfyonova Y. Adipose-derived mesenchymal stromal cells from aged patients with coronary artery disease keep mesenchymal stromal cell properties but exhibit characteristics of aging and have impaired angiogenic potential. *Stem Cells Transl Med*. 2014;3:32-41.
19. Hare JM, Fishman JE, Gerstenblith G, DiFede Velazquez DL, Zambrano JP, Suncion VY, Tracy M, Ghersin E, Johnston PV, Brinker JA, Breton E, Davis-Sproul J, Schulman IH, Byrnes J, Mendizabal AM, Lowery MH, Rouy D, Altman P, Wong Po Foo C, Ruiz P, Amador A, Da Silva J, McNiece IK, Heldman AW, George R and Lardo A. Comparison of allogeneic vs autologous bone marrow-derived mesenchymal stem cells delivered by transendocardial injection in patients with ischemic cardiomyopathy: the POSEIDON randomized trial. *JAMA*. 2012;308:2369-79.
20. Premer C, Blum A, Bellio MA, Schulman IH, Hurwitz BE, Parker M, Dermarkarian CR, DiFede DL, Balkan W, Khan A and Hare JM. Allogeneic Mesenchymal Stem Cells Restore Endothelial Function in Heart Failure by Stimulating Endothelial Progenitor Cells. *EBioMedicine*. 2015;2: 467-75.
21. Li J, Ezzelarab MB and Cooper DK. Do mesenchymal stem cells function across species barriers? Relevance for xenotransplantation. *Xenotransplantation*. 2012;19:273-85.
22. Lin CS, Lin G and Lue TF. Allogeneic and xenogeneic transplantation of adipose-derived stem cells in immunocompetent recipients without immunosuppressants. *Stem Cells Dev*. 2012;21: 2770-8.
23. Paul A, Srivastava S, Chen G, Shum-Tim D and Prakash S. Functional assessment of adipose stem cells for xenotransplantation using myocardial infarction immunocompetent models: comparison with bone marrow stem cells. *Cell Biochem Biophys*. 2013;67:263-73.
24. Lee K, Kwon DN, Ezashi T, Choi YJ, Park C, Ericsson AC, Brown AN, Samuel MS, Park KW, Walters EM, Kim DY, Kim JH, Franklin CL, Murphy CN, Roberts RM, Prather RS and Kim JH. Engraftment of human iPSCs and allogeneic porcine cells into pigs with inactivated RAG2 and accompanying severe combined immunodeficiency. *Proc Natl Acad Sci U S A*. 2014;111: 7260-5.

25. Przybył E, Krenning G, Brinker MG and Harmsen MC. Adipose stromal cells primed with hypoxia and inflammation enhance cardiomyocyte proliferation rate in vitro through STAT3 and Erk1/2. *J Transl Med.* 2013;11:39.
26. Sheets MF, Hanck DA and Fozzard HA. Nonlinear relation between Vmax and INa in canine cardiac Purkinje cells. *Circulation research.* 1988;63:386-98.
27. Maruyama T, Cascio WE, Knisley SB, Buchanan J and Gettes LS. Effects of ryanodine and BAY K 8644 on membrane properties and conduction during simulated ischemia. *Am J Physiol.* 1991; 261:H2008-15.
28. Pedrotty DM, Klinger RY, Kirkton RD and Bursac N. Cardiac fibroblast paracrine factors alter impulse conduction and ion channel expression of neonatal rat cardiomyocytes. *CardiovascRes.* 2009;83:688-697.
29. Cartledge JE, Kane C, Dias P, Tesfom M, Clarke L, McKee B, Al Ayoubi S, Chester A, Yacoub MH, Camelliti P and Terracciano CM. Functional crosstalk between cardiac fibroblasts and adult cardiomyocytes by soluble mediators. *Cardiovasc Res.* 2015;105:260-70.
30. McSpadden LC, Nguyen H and Bursac N. Size and ionic currents of unexcitable cells coupled to cardiomyocytes distinctly modulate cardiac action potential shape and pacemaking activity in micropatterned cell pairs. *Circ Arrhythm Electrophysiol.* 2012;5:821-30.
31. Chong JJ, Yang X, Don CW, Minami E, Liu YW, Weyers JJ, Mahoney WM, Van BB, Cook SM, Palpant NJ, Gantz JA, Fugate JA, Muskheili V, Gough GM, Vogel KW, Astley CA, Hotchkiss CE, Baldessari A, Pabon L, Reinecke H, Gill EA, Nelson V, Kiem HP, Laflamme MA and Murry CE. Human embryonic-stem-cell-derived cardiomyocytes regenerate non-human primate hearts. *Nature.* 2014;510:273-277.
32. Fukushima S, Varela-Carver A, Coppen SR, Yamahara K, Felkin LE, Lee J, Barton PJ, Terracciano CM, Yacoub MH and Suzuki K. Direct intramyocardial but not intracoronary injection of bone marrow cells induces ventricular arrhythmias in a rat chronic ischemic heart failure model. *Circulation.* 2007;115:2254-61.
33. Thomas CA, Jr., Springer PA, Loeb GE, Berwald-Netter Y and Okun LM. A miniature microelectrode array to monitor the bioelectric activity of cultured cells. *Exp Cell Res.* 1972;74:61-6.
34. Zhang Y, Sekar RB, McCulloch AD and Tung L. Cell cultures as models of cardiac mechanoelectric feedback. *Prog Biophys Mol Biol.* 2008;97:367-82.
35. Iravanian S, Nabutovsky Y, Kong CR, Saha S, Bursac N and Tung L. Functional reentry in cultured monolayers of neonatal rat cardiac cells. *Am J Physiol Heart Circ Physiol.* 2003;285:H449-56.
36. Rohr S, Scholly DM and Kleber AG. Patterned growth of neonatal rat heart cells in culture. Morphological and electrophysiological characterization. *Circulation research.* 1991;68: 114-30.
37. Beeres SL, Atsma DE, van der Laarse A, Pijnappels DA, van TJ, Fibbe WE, de Vries AA, Ypey DL, van der Wall EE and Schalij MJ. Human adult bone marrow mesenchymal stem cells repair experimental conduction block in rat cardiomyocyte cultures. *JAmCollCardiol.* 2005;46:1943-1952.

## SUPPLEMENTARY MATERIAL

### Differential mechanisms of myocardial conduction slowing by adipose tissue-derived stromal cells derived from different species

*STEM CELLS Translational Medicine*, 2016;5:1-9

## METHODS

### Isolation and culturing of neonatal rat ventricular myocytes

Neonatal rat ventricular myocytes (NRVM) were isolated as follows. One to two days old Wistar rats were decapitated and the hearts were rapidly explanted. Atrial tissue was removed and ventricles were dissected into pieces and left to rotate overnight at 4 °C in HBSS (Gibco, Den Haag, Netherlands) containing trypsin (1 mg/mL; Becton Dickinson BV, Breda, The Netherlands). The following day the enzymatic effect of trypsin was inactivated with culture medium (M199 medium; Gibco; supplemented with 10% heat inactivated fetal bovine serum (FBS; Gibco), 1% HEPES (Gibco #5630-0-80), 5000 U/L penicillin-G (Sigma, #P7794), 2 mg/L vitamin B12 (Sigma, #V2876), 3,5 g/L glucose, 1% non-essential amino acids (Gibco, #11140-050), and 1% L-glutamine (Gibco, #25030-081)), ventricles were enzymatically dissociated in HBSS containing collagenase type 2 (1 mg/mL, Worthington Vollenhove, The Netherlands, 230 units/mg) at 37 °C, centrifuged at 160 g, 5 minutes and cells were re-suspended in culture medium. To separate fibroblasts from cardiomyocytes, cells were pre-plated in a polystyrene treated T175 cell culture flask at 37°C in 5% CO<sub>2</sub>, 95% humidity and 21% O<sub>2</sub>. After two hours, non-adherent cells, i.e. predominantly NRVM, were collected and were seeded at  $1.4 \times 10^5/\text{cm}^2$  onto microelectrode arrays (MEAs; Multi Channel Systems MCS GmbH, Reutlingen, Germany). This array has 60 integrated extracellular electrodes aligned in an 8 by 8 matrix at interelectrode distances of 0.7 mm. MEAs were coated with fibronectin (125 µg/ml BD Biosciences, Breda, The Netherlands) at least two hours prior to NRVM seeding. NRVM were cultured at 37 °C 5% CO<sub>2</sub>, 95% humidity and 21% O<sub>2</sub> in culture medium, which was switched to 2% FBS two days after cells were seeded on the MEA. The day after seeding, NRVM were washed twice with HBSS (Gibco) and fresh culture medium was added. Light microscopy was used to determine if a confluent monolayer had formed in each of the cultures.

### Isolation and culture of adipose tissue-derived stromal cells

ADSC were isolated and cultured as described previously<sup>1</sup>. Adipose tissue was dissected from rats' inguinal fat (male, Wistar, 7-8 months), porcine (male, 3-4 months old, kindly provided by the department of experimental surgery of the AMC) or human subcutaneous abdominal fat (donated by healthy patients with body mass index below 30 ;Bergman Clin-

ics, The Netherlands) and stored at 4 °C. Within 24 hours, the adipose tissue was minced and washed extensively with PBS. The tissue fragments were incubated in an equal volume of PBS with 0.1% Collagenase A (Roche Diagnostics, Mannheim, Germany), containing 1% bovine serum albumin (BSA; Sigma-Aldrich, Boston, MA) at 37 °C for 1 hour while exposed to continuous shaking. The enzymatic activity of collagenase was stopped by adding PBS, 1% BSA and digested tissue were filtered through 70 mm filters. The collected cell suspension was subjected and centrifuged at 600xg for 10 min. The supernatant was discarded and stromal vascular fraction (SVF) was incubated with an erythrocyte lysis buffer at 4°C for 5 min. Then, SVF pellet was collected by additional centrifugation. Cells were suspended in culture medium that consisted of DMEM (Lonza Biowhittaker, Verviers, Belgium), supplemented with 10% FBS (Thermo Scientific, Hemel Hempstead, UK), 100 U/mL penicillin, 100 mg/mL streptomycin (Gibco, Invitrogen, Carlsbad, CA) and 2 mM L-glutamine (Lonza Biowhittaker, Verviers, Belgium). The ADSC were seeded at a density of  $4 \times 10^4$  cells/cm<sup>2</sup> and cultured at 37 °C, 5% CO<sub>2</sub>, 95% humidity and 21% O<sub>2</sub>. Culture medium was refreshed every two days till 80-90% confluence was reached. ADSC were propagated at a 1:2 ratio and used from passage 3 onwards for the experiments. Cells were referred to either rat ADSC (rADSC) or human ADSC (hADSC) or pig ADSC (pADSC).

For conditioned medium; confluent flasks of ADSC were cultured in NRVM culture medium containing 2%, after twenty-four hours medium was collected, filtered through a 0.22 µm filter (MILLEX®GV SLGV033RS) labelled Cme-ADSC and stored at -20 °C until use.

### Experimental conditions

Monolayers of NRVM containing ADSC were prepared by treating ADSC with mitomycin-C (Sigma M4287-2MG) and were labeled with CDFA-SE (Invitrogen Vybrand® CFDA SE Cell Tracer Kit) according to manufactures protocol. ADSC were collected using accutase (Gibco, A11105-01 StemPro®Accutase®), and centrifuged for 5 minutes at 160g. Supernatant was removed and the pellet was re-suspended in NRVM culture medium containing 2% FBS. ADSC were then added to monolayers of NRVM in cell ratios of NRVM:ADSC 1:1. Monolayers of NRVM serving as controls received fresh NRVM culture medium containing 2% FBS. Two days later electrical mapping was performed.

Medium from NRVM monolayers and the monolayers containing the different species of ADSC was collected after two days, filtered through a 0.22 µm filter (MILLEX®GV SLGV033RS) and stored at -20 °C until use. This medium was referred to as conditioned medium (Cme) and labeled as follows; Cme NRVM, and Cme NRVM:ADSC.

For the transwell setup monolayers were created in fibronectin coated T12 wells, as described above. On day 4, transwell inserts were placed inside the well and ADSC were seeded into these inserts. The ratio of NRVM:ADSC was 1:2 as the surface area of the inserts is smaller than the T12 wells. Two days later medium was collected, filtered, labelled Cme transwell ADSC and stored at -20 °C until used.



In the experiments investigating the paracrine effects, conditioned medium was added to monolayers of NRVM only, two days prior to electrical mapping.

### Electrical mapping and microelectrode measurements

The MEAs containing the different cultures were positioned in a temperature controlled (37 °C MEA holder (TC01/02 Multichannel Systems MSC GmbH). Each MEA harbored 60 electrodes which had terminals in the core portion of the MEA (Supplemental Fig.1). On every day of experimentation two monolayers of NRVM from the same cell isolation served as controls. All cultures were stimulated from at least two stimulation sites using a bipolar extracellular stimulus electrode (twice diastolic stimulation threshold, 1 ms or 2 ms rectangular current pulses). Unipolar electrograms were recorded with a 256-channel amplifier (BioSemi, ActiveTwo, Amsterdam, The Netherlands, 24 bit dynamic range, 122.07 nV LSB, total noise 0.5  $\mu$ V). Signals were recorded with a sampling frequency of 2048 Hz (filter setting of the amplifiers DC – 400 Hz (- 3dB point). The recordings were made with respect to the integrated reference electrode of the MEA. Conduction velocity (CV) was determined from activation maps constructed using the maximum negative dV/dt as activation time (AT; relative to the time of earliest activation) with the use of a custom made program <sup>2</sup> based on MATLAB R2006b (The MathWorks, Inc., Natick, MA, USA). CV was determined along lines perpendicular to isochronal lines by dividing the distance by the difference in local activation time. Lines had a length of at least 4 electrode distances. Local activation times in the figures are color coded in classes of 5 ms. CV was determined at a basic cycle length (BCL) of 600 ms or during spontaneous activity if pacing was not possible. Based on the method described by Lammers et al. <sup>3</sup> we quantified the heterogeneity in conduction as a measure of arrhythmia vulnerability. Maximum AT differences between each adjacent electrode quartet in the grid were obtained and the total range of maximal AT differences was plotted in a histogram.

Microelectrodes were pulled from glass capillaries (Harvard apparatus GC100F-10) and filled with 3 M KCl. An AgCl covered silver wire was used as a reference electrode. Following activation mapping, action potentials were recorded during pacing at BCL 600 ms. Resting membrane potential (RMP) was taken as the highest negative membrane potential recorded, upstroke velocity was taken as dV/dt max.

### Immunostaining and fluorescence imaging

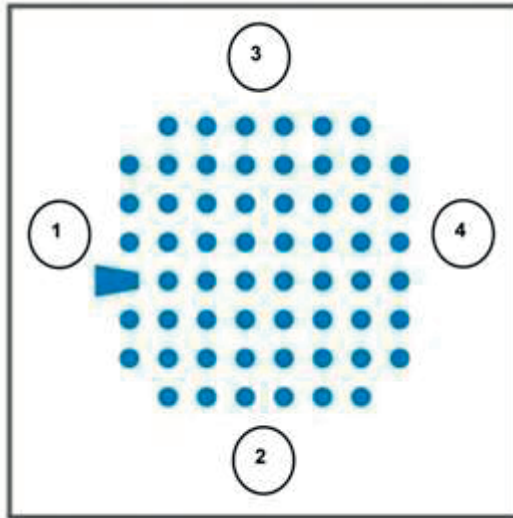
For immunofluorescence, cells ( $1.25 \times 10^5$  cells/cm<sup>2</sup>) were plated in 12-well plates (MP Biomedicals) containing fibronectin-coated (125  $\mu$ g/ml BD Biosciences) coverslips and cultured under the same conditions as cells on MEAs. Separate cultures were made as immunofluorescence could not be performed on MEAs. On the day of the electrophysiological recordings these cultures were fixed with 4% PFA for 10 minutes, permeabilized with 0.1% Triton X-100, and blocked with 1% BSA (Roche BSA fraction V #10735094001). Cells

were stained with primary antibodies (mouse anti-sarcomeric-actinin primary antibody; Sigma 1:1000), mouse anti-human monoclonal CD44 primary antibody (Lifespan Biosciences, LS-B1862; 1:250), rabbit anti Connexin 43 (Invitrogen 574366A; 1:200), rabbit anti Connexin 45 (Santa Cruz Biotechnology, sc-25716, 1:100) and mouse anti N-Cadherin (Sigma C2542, 1:100) in 1% BSA overnight at room temperature, washed three times with PBS, and then incubated with secondary antibodies (Alexa Fluor-647 goat anti-mouse IgG (Life Technology, A21235; 1:250), Alexa Fluor-488 goat anti-mouse/rabbit IgG (Life Technology, A11008/A21222; 1:250), for two hours in 1% BSA. Cover-slips were washed an additional three times in PBS and incubated for an additional 10 minutes with either cyto@orange (Life Technology, S11368, 1:1000) or DAPI (Sigma, D9542, 1:40000), washed again with PBS and embedded in 50% glycerol/50% PBS. Examination was performed by Leica SPE confocal laser scanning and Leica Application Suite Advanced Fluorescence (LAS AF) software.

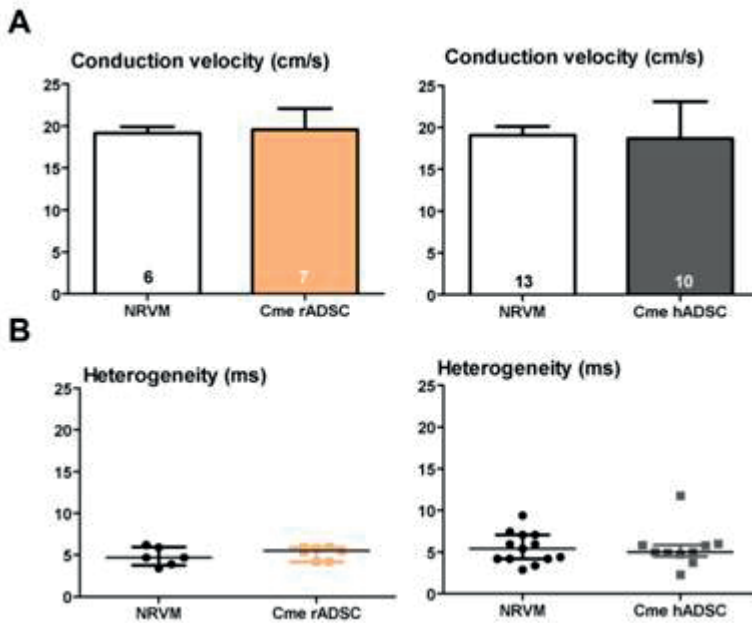
The images obtained from cultures stained for N-Cadherin and Cx43 were analyzed using Image J. Five to ten images were taken in each of three independent experiments, Image J was used to determine the number of pixels for either the Cx43 or N-cadherin channel in each image. Based on the number of pixels we then determined the ratio of Cx43: N-cadherin in each image.

## REFERENCES

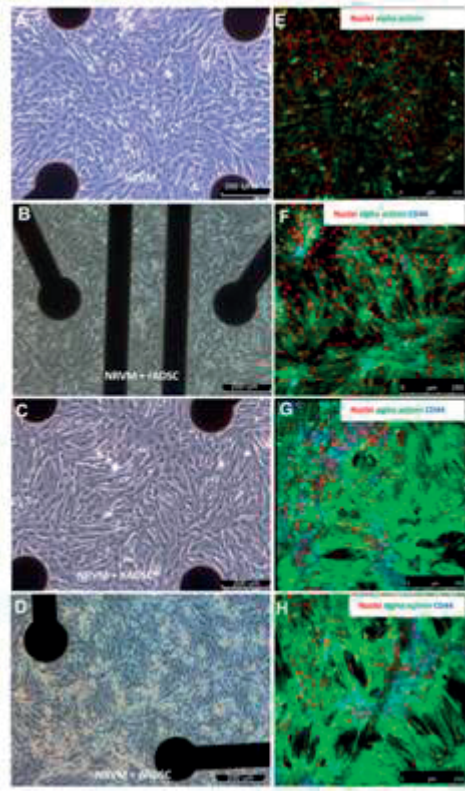
1. Przybyt E, Krenning G, Brinker MG and Harmsen MC. Adipose stromal cells primed with hypoxia and inflammation enhance cardiomyocyte proliferation rate in vitro through STAT3 and Erk1/2. *J Transl Med.* 2013;11:39.
2. Potse M, Linnenbank AC and Grimbergen CA. Software design for analysis of multichannel intracardial and body surface electrocardiograms. *Computer methods and programs in biomedicine.* 2002;69:225-36.
3. Lammers WJ, Schalij MJ, Kirchhof CJ and Allessie MA. Quantification of spatial inhomogeneity in conduction and initiation of reentrant atrial arrhythmias. *The American journal of physiology.* 1990;259:H1254-63.



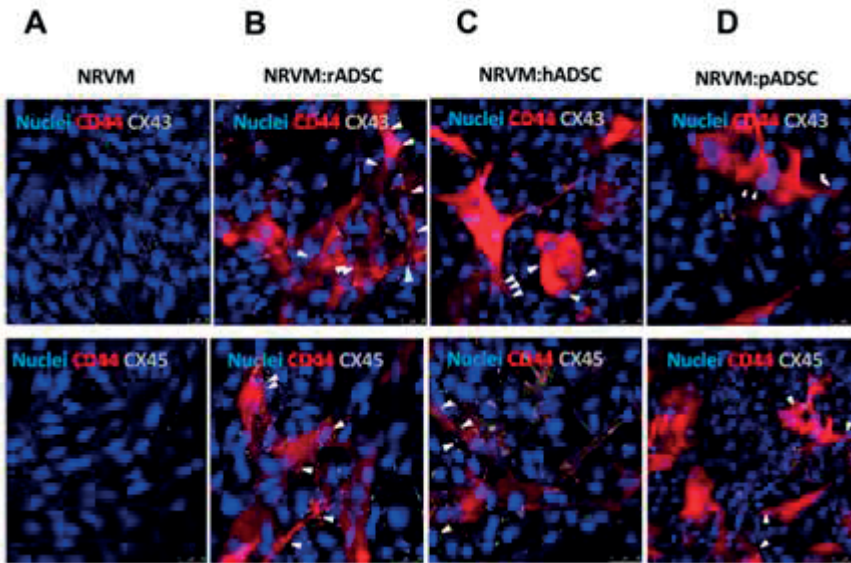
Supplemental Figure 1. Layout of the 60 electrodes in the MEA. Each electrode has a diameter of 100  $\mu\text{m}$  and an interelectrode distance of 700  $\mu\text{m}$ . Numbers 1-4 represent stimulation positions.



Supplemental Figure 2. Effect of Cme rADSC and Cme hADSC on monolayers of NRVM. Bar graphs illustrating the effects on A: conduction velocity and B: conduction heterogeneity in monolayers of NRVM cultured in condition medium obtained from rADSC and hADSC cultures.



**Supplemental Figure 3. Micrographs of the various cultures.** Transmitted light and immune-fluorescent micrographs. A –D: Transmitted light micrographs of NRVM monolayer and NRVM monolayers co-cultured with the different ADSC. Black dots and lines are the electrodes in the MEA. E-H: Immune-fluorescent micrographs of NRVM monolayer and NRVM monolayers co-cultured with the different ADSC. Please note that these are not the same monolayers as panels A-D. Scale bars located at the bottom right of each image indicate size in  $\mu\text{m}$ .



Supplemental Figure 4. Immunofluorescence micrographs of the various cultures stained with CD44 and Cx43 and Cx45. Monolayers of NRVM are stained with CD44 and Cx43 (A1) and with CD44 and Cx45 (A2). Monolayers of NRVM co-cultured with rADSC (B1+B2), NRVM monolayers co-cultured with hADSC (C1+C2) or pADSC (D1+D2) are stained for the same markers. Scale bars located at the bottom right of each image indicate size in  $\mu\text{m}$ .

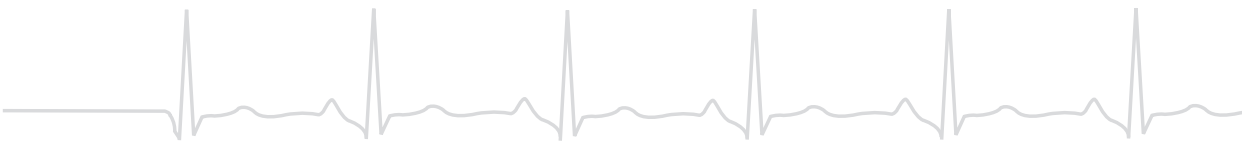


# CHAPTER 8

## Modulators of ventricular arrhythmias in structurally normal and abnormal hearts

### Summary and future directions

Judith N. ten Sande







## SUMMARY AND FUTURE DIRECTIONS

This thesis was designed to investigate the underlying mechanism of and risk factors for ventricular arrhythmias (VA) in structurally normal and abnormal hearts. Based on Coumel's three components of arrhythmogenesis<sup>1</sup> we investigated different mechanisms of VA and their variations in clinical expression with Coumel's triangle as backbone. Until now, many studies have been conducted to determine the substrate, triggers and modulating factors that result in (ventricular) arrhythmias. Before VA actual occur, trigger, substrate and modulators have to be present, creating "the right situation at the right time" for VA to occur. For example, the arrhythmic substrate may be present in a patient for years on end, but will not lead to VA until an adequate trigger occurs.

Despite having the same underlying disease, some patients are more at risk for VA than others with a similar diagnosis and we demonstrated that the development of the underlying substrate, whether or not as a result of genetic predisposition, is of great importance to develop VA. Therefore, triggers and modulation factors play a crucial role in the occurrence of VA. Worldwide, the incidence of SCD is declining due to better insights in its pathophysiological mechanisms and appropriate therapy. Nevertheless, despite progress in knowledge concerning diagnosis and treatment of cardiovascular diseases, many patients remain at risk for lethal arrhythmias. Better understanding of the interplay between different components responsible for VA will result in a more accurate risk stratification and, eventually, in better treatment for patients at risk for VA. The various topics presented in this thesis are incorporated in the following figure.

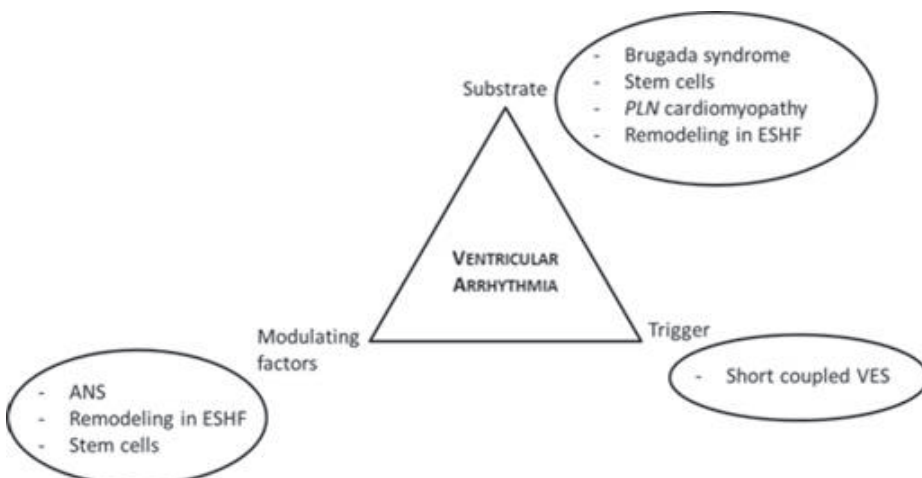


**Figure.** Thesis incorporated in a triangle of arrhythmogenesis. ANS: autonomic nerve system, ESHF: end stage heart failure, PLN: phospholamban, VES: ventricular extrasystole.

## PART I MARKERS OF VULNERABILITY FOR VENTRICULAR ARRHYTHMIAS

In the first part of this thesis several aspects derived from Coumel's triangle (figure) were investigated to identify patients at risk for ventricular arrhythmias.

Earlier studies have demonstrated that the autonomic nervous system plays a pivotal role in the development of VA<sup>2</sup> and can be considered a modulating factor in Coumel's triangle. The altered state of the autonomic nervous system in patients with heart failure enhances susceptibility for VA. In patients with heart failure (HF) there is a disbalance between the parasympathetic and sympathetic nerve system. Heart rate variability (HRV) is a measure for this dysfunction and is often decreased in patients with heart failure<sup>3-5</sup>. In CHAPTER 2 we show that in patients with an implantable cardioverter defibrillator for either primary or secondary prevention, HRV is a predictor for imminent appropriate ICD shocks and thus VA. We demonstrated that - when HRV is decreased - the risk for an appropriate ICD shock is significantly increased. HRV dynamics might be a clinically feasible predictor for identification of patients at risk since HRV is easily and directly available from continuously monitoring implanted ICD devices. Increasing participation in ICD home-monitoring programs makes HRV a potential tool to guide adjustments in HF and/or antiarrhythmic treatment at times of suspected increased risk for appropriate therapy. In this thesis a retrospective design was used resulting in different intervals between HRV measurements and a limited number of patients. We therefore would advise to prospectively analyze the usefulness of HRV dynamics in a larger group on pre-specified time intervals.

In CHAPTER 3 we focused on the substrate according to the triangle of Coumel in a well-known hereditary cardiomyopathy. We investigated index patients and relatives, with or without HF, with a known mutation for arrhythmogenic cardiomyopathy in order to determine the value of non-invasive diagnostics for estimation of the extension of the disease and their value as possible predictors of VA. All patients had a p.ARG14del mutation in the phospholamban (*PLN*) gene. The *PLN* gene is involved in cellular calcium homeostasis<sup>6</sup>. Patients with this mutation often show malignant VA, have low voltage QRS complexes on the surface ECG and develop end-stage HF combined with extensive myocardial fibrosis<sup>7, 8</sup>. In fact, low voltage QRS complexes on the surface ECG is a prominent, often first, manifestation of this disease, even in asymptomatic carriers. We therefore investigated whether low voltage body surface R-wave amplitude represented myocardial fibrosis detected by cardiac magnetic resonance imaging (CMR). We analyzed different non-invasive clinical parameters obtained from the surface ECG (conduction intervals, R-wave amplitude and the presence of inverted T-waves) in relation with myocardial fibrosis (late gadolinium enhancement) detected on CMR. We showed that in patients with *PLN* cardiomyopathy low voltage QRS complexes are associated with fibrosis. However, when corrected for age and the presence of inverted T-waves, this parameter was no longer predictive. Interestingly, inverted T waves did correlate with fibrosis on CMR also after

correction for other predictors. Since inverted T-waves are easily identifiable on the surface ECG, their presence might be a risk marker for fibrosis and possible subsequent VA. To determine if these inverted T-waves and/or R-wave amplitude below the median could be a risk factor for future VA, further prospective research will have to be conducted. According to Coumel's triangle we surmise that the substrate alone is not an adequate predictor for VA without an appropriate trigger. The results of chapter 2 appear to support this idea. Currently, we are investigating patients with PLN cardiomyopathy prospectively to determine the occurrence of VA during follow-up in relation with ECG parameters and fibrosis on CMR. Also, the reason why T-wave inversion has such a strong relation with the presence of myocardial fibrosis is yet unclear. Reduced compliance of the ventricular wall caused by myocardial fibrosis resulting in altered mechano-electrical feedback can be postulated but further investigation is needed to elucidate the relation between surface ECG T-wave inversion and the presence of myocardial fibrosis.

This thesis also focused on a specific form of familial idiopathic ventricular fibrillation (IVF) characterized by the presence of the *DPP6* risk haplotype. Other than in Brugada syndrome or long QT syndrome, in idiopathic VF there usually are no clinical signs indicating risk for cardiac arrest in individual patients, making it exceedingly difficult to identify patients prone for VF. As earlier described, only the presence of the *DPP6* risk haplotype indicated risk for malignant VA in this particular type of idiopathic VF<sup>9</sup>. In CHAPTER 4 we demonstrated that, despite extensive analysis, risk stratification remains difficult since no clinical parameters other than presence of the *DPP6* haplotype and an age between 20 and 50 years could be identified. This, unfortunately, makes advising prophylactic cardioverter defibrillator implantation mandatory in these young *DPP6* patients, exposing them to device implantation related complications without being able to provide a more precise selection by individual assessment of VA risk.

At present, we can only speculate how overexpression of *DPP6* results in IVF. It is still not clear why patients with IVF have these short coupled monomorphic ventricular extrasystoles directly resulting in VF. In myocardial tissue samples obtained from 5 risk-haplotype positive patients a 22-fold increase of *DPP6* mRNA expression<sup>10</sup> has been observed. *DPP6* is involved in the transient outward potassium current (I<sub>to</sub>) in the heart. However, no ECG abnormalities are seen in these patients. A possible mechanism is exclusive shortening of the Purkinje action potential (due to increased amplitude of the transient outward current caused by *DPP6* overexpression), enabling local micro-reentry in the specialized conduction system<sup>11</sup>. Short coupled extrasystoles can be considered the trigger in Coumel's triangle. To understand how overexpression of *DPP6* results in IVF, further research will have to focus on electrophysiological testing, with emphasis on electrophysiological properties of the Purkinje system.

Detailed histological studies may give more insight in potential ultrastructural changes in myocardial architecture. Since there was only a limited number of CMRs available in our

study, we speculate that more extensive cardiac imaging during a longer follow-up may reveal the development of cardiomyopathy-like structural abnormalities over time. However, in the patient population presented in CHAPTER 4, predominantly younger patients experienced VF pleading against age-related changes necessary for the development of a VF substrate.

Lastly, only a limited number of patients who received an ICD for primary prevention did experience appropriate ICD therapy. If during longer follow-up more primary prevention patients will experience appropriate ICD therapy it may become more feasible to identify additional clinical risk factors.

## **PART II CHARACTERISTICS OF ARRHYTHMOGENIC SUBSTRATES OF VENTRICULAR ARRHYTHMIAS**

In the second part of this thesis we focused on the characteristics of the arrhythmic substrate in patients with end stage heart failure (HF) and Brugada syndrome (BrS). Because stem cells have been shown to be a promising therapeutic option for HF treatment but also have drawbacks concerning possible pro-arrhythmic effects, the effect of stem cells as potential arrhythmic substrate was investigated.

In CHAPTER 5 we investigated the differences in substrate on cellular and molecular level of patients end-stage HF, requiring a left ventricular assist device (LVAD). In these patients we were able to analyze the diseased-induced remodeling of left ventricular tissue. Since samples were obtained in patients with different etiologies underlying HF, we also investigated the differences in substrate between patients with ischemic cardiomyopathy (ICM) and dilated cardiomyopathy (DCM) in terms of fibrosis and connexins43 (Cx43). Also ion channels are altered and miRNA expression differ in patients with HF<sup>12, 13</sup>. In this chapter the substrate as well as modulating factors were investigated. Our data show that fibrosis has a different architecture in patients with DCM compared to ICM. In myocardial tissue samples from patients with ICM patchy fibrosis tended to be more present as compared to tissue samples obtained from patients with DCM. Also the expression of Cx43 was different with more macro-heterogeneous Cx43 expression in patients with DCM. These results suggest differences in remodeling specific for heart failure etiology. There was no relation between structural changes and the occurrence of VA. Again, this illustrates the complex interaction between substrate and triggering in the genesis of VA, this time in HF patients. To actually differentiate between the precise mechanism of VA in relation with myocardial architecture and etiology one should therefore perform extensive electrophysiological testing (including the application of an external trigger). The LVAD has become more and more a destination therapy. Therefore less explanted heart are available for research. Still,

there are opportunities for further research in tissue samples since the number of LVAD implantations is increasing and these samples are, after informed consent, easy to obtain.

Patients with BrS have a typical ECG pattern; coved ST-segment elevation followed by a negative T-wave<sup>14</sup> (type 1 BrS-ECG) in at least one right precordial lead positioned at the 2<sup>nd</sup>, 3<sup>rd</sup> or 4<sup>th</sup> intercostal space, either spontaneously or after provocation by intravenous administration of class I antiarrhythmic drugs<sup>15</sup>. This typical ST-segment elevation often precedes onset of VA<sup>16, 17</sup>. These VA can result in cardiac arrest or syncope<sup>18</sup>. As a result, syncope is a sign of increased risk for VA together with a type 1 BrS-ECG<sup>19</sup>. Although much is known about modulators and triggers facilitating or eliciting type I ST elevation in BrS, the underlying substrate causing the ECG abnormalities is still a matter of debate. Several hypotheses have been proposed to explain the ST-segment elevation in BrS. The repolarization disorder hypothesis is based on dispersion in repolarization as a result of transmural voltage gradients caused by heterogeneity in action potential duration between the RV epicardium and endocardium<sup>20</sup>. The depolarization disorder hypothesis is based on late activation of the RVOT<sup>21</sup> and the electrotonic current hypothesis reports current-to-load mismatch and failure to excite of the terminal RVOT in structurally abnormal subepicardium of the RV/RVOT<sup>22</sup> as cause of coved type ST elevation in this area. Therefore, in CHAPTER 6 we studied the pathophysiologic mechanism of the characteristic ST-segment elevation in BrS patients. By using multiple clinical observations on epicardial and endocardial right ventricular activation mapping procedures and additional pacing maneuvers we were able to show that ST-segment elevation and epicardial fractionation/conduction delay in BrS patients are most likely related to the same structural subepicardial abnormalities, but that the mechanism is different. The different mapping and stimulation protocols showed that BrS patients have longer activation delay, show more and longer fractionated epicardial electrograms and late potentials in the RV/RVOT compared with controls. In addition, data revealed that local fractionation is not solely responsible for the ST-segment elevation on the surface ECG. ST-segment elevation is most likely caused by current-to-load mismatch and excitation failure of the RVOT where fractionated electrocardiogram and conduction delay are expected to be caused by discontinuous conduction in the same area with abnormal myocardium. Further research may want to focus on excitation failure in parts of the RVOT. During epicardial mapping one could try to stimulate the terminal part of the RVOT during the QRS complex with just above threshold strength and see if the typical ST-segment elevation diminishes when myocardial tissue that failed to excite is depolarized.

In CHAPTER 7 we investigated the effect of stem cells application on electrophysiological parameters. This has been advocated as a promising therapeutic option in patients with reduced left ventricular ejection fraction due to myocardial infarction and/or HF<sup>23-25</sup>. By using stem cells, the architecture of the myocardium is changed resulting in differences in conduction such as conduction slowing, heterogeneity of conduction and conduction block. Earlier studies suggest that this could be a result of either electrotonic or paracrine

effects<sup>26</sup>. Stem cells can create a substrate and can act as modulating factors according to Coumel's triangle. In CHAPTER 7 we analyzed adipose tissue derived stromal cells (ADSC) from different species and its effect on a monolayer of neonatal rat ventricular myocytes (NRVM). ADSCs were chosen because they are easy to obtain, are abundantly present, and are also a source of multipotent cells capable of differentiating along multiple lineage pathways with little immunological effects<sup>27, 28</sup>. In addition, ADSCs secrete a wide variety of factors known to stimulate angiogenesis<sup>29</sup> and neovascularization<sup>30</sup>.

The results show that ADSC cause conduction slowing and that paracrine modulation and intracellular coupling form a potentially arrhythmogenic substrate. We demonstrated that, despite promising results in earlier trials, one should be cautious to administer stem cells since adverse paracrine and electrotonic effects on cellular electrophysiological physiology may result in a potential higher susceptibility for VA when applied to an *in vivo* setting. Despite the fact that we used a 2D model with different species our results indicated that stem cells have effect on electrophysiological parameters resulting in potential substrate for VA. Even if stem cells do not alter cellular architecture, paracrine factors will affect cellular electrophysiology resulting in a potentially increased susceptibility for VA. The exact nature of the soluble factor(s) responsible for the changes in electrophysiological properties was outside the scope of this chapter and is difficult to determine since all cells have a secretome of soluble factors that can potentially influence behavior including secretome of other cells. Currently we are investigating stem cell application in porcine hearts to evaluate the electrophysiological effects *in vivo*. The study design gives us the opportunity to analyze the effects *in vivo* and *in vitro*.

In the past, much has been learned about lethal VA every day. However, there is still much to learn about the factors responsible for VA. This thesis comprehends a broad variety of topics related to VA in structurally normal and abnormal hearts. During the progress of this work it became once again clear that further research is mandatory. This thesis illustrates that a close collaboration between basic and clinical research is required for better insights in modulators of ventricular arrhythmias, similar to the close interrelation between trigger and substrate in the genesis of ventricular arrhythmias.

## REFERENCES

1. Coumel P. Cardiac arrhythmias and the autonomic nervous system. *J Cardiovasc Electrophysiol*. 1993;4:338-55.
2. Schwartz PJ, La Rovere MT and Vanoli E. Autonomic nervous system and sudden cardiac death. Experimental basis and clinical observations for post-myocardial infarction risk stratification. *Circulation*. 1992;85:177-91.
3. Ponikowski P, Anker SD, Chua TP, Szelemej R, Piepoli M, Adamopoulos S, Webb-Peploe K, Harrington D, Banasiak W, Wrabec K and Coats AJ. Depressed heart rate variability as an independent predictor of death in chronic congestive heart failure secondary to ischemic or idiopathic dilated cardiomyopathy. *Am J Cardiol* 1997;79:1645-1650.
4. Boveda S, Galinier M, Pathak A, Fourcade J, Dongay B, Benchendikh D, Massabuau P, Fauvel JM, Senard JM and Bounhoure JP. Prognostic value of heart rate variability in time domain analysis in congestive heart failure. *J Interv Card Electrophysiol* 2001;5:181-187.
5. Smilde TD, van Veldhuisen DJ and van den Berg MP. Prognostic value of heart rate variability and ventricular arrhythmias during 13-year follow-up in patients with mild to moderate heart failure. *Clin Res Cardiol*. 2009;98:233-9.
6. MacLennan DH and Kranias EG. Phospholamban: a crucial regulator of cardiac contractility. *Nature reviews Molecular cell biology*. 2003;4:566-77.
7. Posch MG, Perrot A, Geier C, Boldt LH, Schmidt G, Lehmkühl HB, Hetzer R, Dietz R, Gutberlet M, Haverkamp W and Ozcelik C. Genetic deletion of arginine 14 in phospholamban causes dilated cardiomyopathy with attenuated electrocardiographic R amplitudes. *Heart Rhythm*. 2009;6:480-6.
8. van der Zwaag PA, van Rijsingen IA, Asimaki A, Jongbloed JD, van Veldhuisen DJ, Wiesfeld AC, Cox MG, van Lochem LT, de Boer RA, Hofstra RM, Christiaans I, van Spaendonck-Zwarts KY, Lekanne dit Deprez RH, Judge DP, Calkins H, Suurmeijer AJ, Hauer RN, Saffitz JE, Wilde AA, van den Berg MP and van Tintelen JP. Phospholamban R14del mutation in patients diagnosed with dilated cardiomyopathy or arrhythmogenic right ventricular cardiomyopathy: evidence supporting the concept of arrhythmogenic cardiomyopathy. *European journal of heart failure*. 2012;14:1199-207.
9. Postema PG, Christiaans I, Hofman N, Alders M, Koopmann TT, Bezzina CR, Loh P, Zeppenfeld K, Volders PG and Wilde AA. Founder mutations in the Netherlands: familial idiopathic ventricular fibrillation and DPP6. *Neth Heart J* 2011;19:290-296.
10. Alders M, Koopmann TT, Christiaans I, Postema PG, Beekman L, Tanck MW, Zeppenfeld K, Loh P, Koch KT, Demolombe S, Mannens MM, Bezzina CR and Wilde AA. Haplotype-sharing analysis implicates chromosome 7q36 harboring DPP6 in familial idiopathic ventricular fibrillation. *Am J Hum Genet* 2009;84:468-476.
11. Xiao L, Koopmann TT, Ordog B, Postema PG, Verkerk AO, Iyer V, Sampson KJ, Boink GJ, Mamarbachi MA, Varro A, Jordaens L, Res J, Kass RS, Wilde AA, Bezzina CR and Nattel S. Unique Cardiac Purkinje Fiber Transient Outward Current beta-Subunit Composition: A Potential Molecular Link to Idiopathic Ventricular Fibrillation. *Circ Res* 2013;112:1310-1322.
12. Valdivia CR, Chu WW, Pu J, Foell JD, Haworth RA, Wolff MR, Kamp TJ and Makielski JC. Increased late sodium current in myocytes from a canine heart failure model and from failing human heart. *J Mol Cell Cardiol* 2005;38:475-483.
13. Nattel S, Maguy A, Le Bouter S and Yeh YH. Arrhythmogenic ion-channel remodeling in the heart: heart failure, myocardial infarction, and atrial fibrillation. *Physiol Rev*. 2007;87:425-56.



14. Brugada P and Brugada J. Right bundle branch block, persistent ST segment elevation and sudden cardiac death: a distinct clinical and electrocardiographic syndrome. A multicenter report. *J Am Coll Cardiol* 1992;20:1391-1396.
15. Priori SG, Wilde AA, Horie M, Cho Y, Behr ER, Berul C, Blom N, Brugada J, Chiang CE, Huikuri H, Kannankeril P, Krahn A, Leenhardt A, Moss A, Schwartz PJ, Shimizu W, Tomaselli G and Tracy C. Executive Summary: HRS/EHRA/APHS Expert Consensus Statement on the Diagnosis and Management of Patients with Inherited Primary Arrhythmia Syndromes. *Heart Rhythm* 2013.
16. Matsuo K, Shimizu W, Kurita T, Inagaki M, Aihara N and Kamakura S. Dynamic changes of 12-lead electrocardiograms in a patient with Brugada syndrome. *J Cardiovasc Electrophysiol*. 1998;9:508-12.
17. Priori SG, Napolitano C, Gasparini M, Pappone C, Della BP, Brignole M, Giordano U, Giovannini T, Menozzi C, Bloise R, Crotti L, Terreni L and Schwartz PJ. Clinical and genetic heterogeneity of right bundle branch block and ST-segment elevation syndrome: A prospective evaluation of 52 families. *Circulation*. 2000;102:2509-2515.
18. Antzelevitch C, Brugada P, Borggrefe M, Brugada J, Brugada R, Corrado D, Gussak I, LeMarec H, Nademanee K, Perez Riera AR, Shimizu W, Schulze-Bahr E, Tan H and Wilde A. Brugada syndrome: report of the second consensus conference: endorsed by the Heart Rhythm Society and the European Heart Rhythm Association. *Circulation*. 2005;111:659-670.
19. Priori SG, Napolitano C, Gasparini M, Pappone C, Della Bella P, Giordano U, Bloise R, Giustetto C, De Nardis R, Grillo M, Ronchetti E, Faggiano G and Nastoli J. Natural history of Brugada syndrome: insights for risk stratification and management. *Circulation*. 2002;105:1342-7.
20. Yan GX and Antzelevitch C. Cellular basis for the Brugada syndrome and other mechanisms of arrhythmogenesis associated with ST-segment elevation. *Circulation*. 1999;100:1660-1666.
21. Tukkie R, Sogaard P, Vleugels J, de Groot IK, Wilde AA and Tan HL. Delay in right ventricular activation contributes to Brugada syndrome. *Circulation*. 2004;109:1272-1277.
22. Hoogendijk MG, Potse M, Vinet A, de Bakker JM and Coronel R. ST segment elevation by current-to-load mismatch: an experimental and computational study. *Heart Rhythm* 2011;8: 111-118.
23. Wollert KC, Meyer GP, Lotz J, Ringes-Lichtenberg S, Lippolt P, Breidenbach C, Fichtner S, Korte T, Hornig B, Messinger D, Arseniev L, Hertenstein B, Ganser A and Drexler H. Intracoronary autologous bone-marrow cell transfer after myocardial infarction: the BOOST randomised controlled clinical trial. *Lancet*. 2004;364:141-8.
24. Bolli R, Chugh AR, D'Amario D, Loughran JH, Stoddard MF, Ikram S, Beache GM, Wagner SG, Leri A, Hosoda T, Sanada F, Elmore JB, Goichberg P, Cappetta D, Solankhi NK, Fahsah I, Rokosh DG, Slaughter MS, Kajstura J and Anversa P. Cardiac stem cells in patients with ischaemic cardiomyopathy (SCIPIO): initial results of a randomised phase 1 trial. *Lancet*. 2011;378:1847-1857.
25. Makkar RR, Smith RR, Cheng K, Malliaras K, Thomson LE, Berman D, Czer LS, Marban L, Mendizabal A, Johnston PV, Russell SD, Schuleri KH, Lardo AC, Gerstenblith G and Marban E. Intracoronary cardiosphere-derived cells for heart regeneration after myocardial infarction (CADUCEUS): a prospective, randomised phase 1 trial. *Lancet*. 2012;379:895-904.
26. Askar SF, Ramkisoensing AA, Atsma DE, Schalij MJ, de Vries AA and Pijnappels DA. Engraftment patterns of human adult mesenchymal stem cells expose electrotonic and paracrine proarrhythmic mechanisms in myocardial cell cultures. *Circ Arrhythm Electrophysiol* 2013;6: 380-391.

27. Madonna R, Geng YJ and De Caterina R. Adipose tissue-derived stem cells: characterization and potential for cardiovascular repair. *Arterioscler Thromb Vasc Biol.* 2009;29:1723-9.
28. Nakagami H, Morishita R, Maeda K, Kikuchi Y, Ogihara T and Kaneda Y. Adipose tissue-derived stromal cells as a novel option for regenerative cell therapy. *J Atheroscler Thromb.* 2006;13: 77-81.
29. Rehman J, Traktuev D, Li J, Merfeld-Clauss S, Temm-Grove CJ, Bovenkerk JE, Pell CL, Johnstone BH, Conside RV and March KL. Secretion of angiogenic and antiapoptotic factors by human adipose stromal cells. *Circulation.* 2004;109:1292-8.
30. Miranville A, Heeschen C, Sengenès C, Curat CA, Busse R and Bouloumie A. Improvement of postnatal neovascularization by human adipose tissue-derived stem cells. *Circulation.* 2004; 110:349-55.

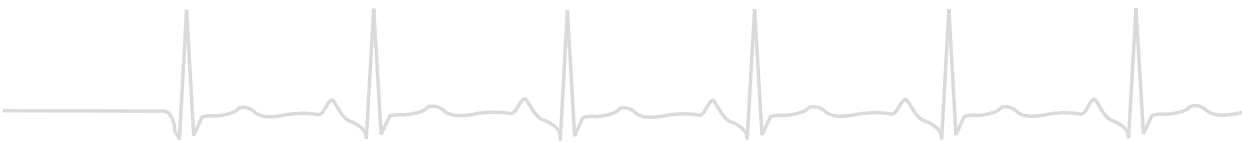


# CHAPTER 9

## Modulatoren van ventriculaire aritmieën in structureel normale en abnormale harten

### Samenvatting en toekomstperspectieven

Judith N. ten Sande



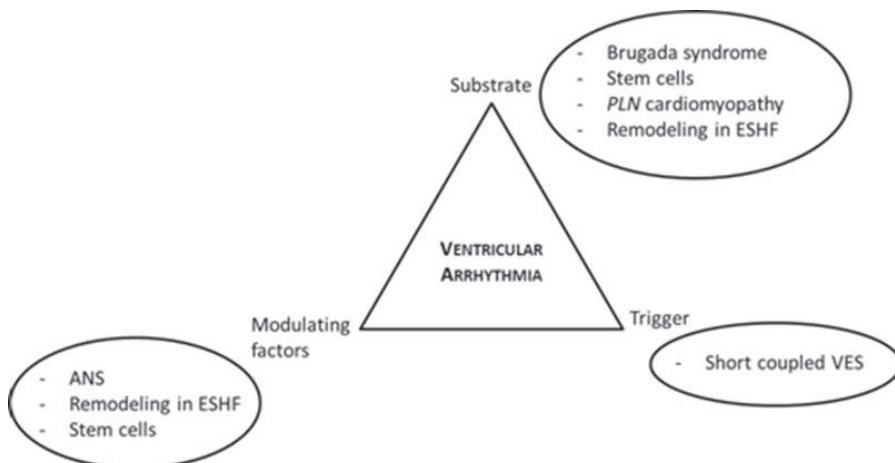


## SAMENVATTING EN TOEKOMSTPERSPECTIEVEN

Dit proefschrift is opgezet om het mechanisme van ventriculaire aritmieën (VA) te onderzoeken en risicofactoren voor VA te bepalen in structureel normale en abnormale harten. Op basis van Coumel's drie componenten van het mechanisme voor aritmieën<sup>1</sup> belichten we de verschillende mechanismen van VA en de variaties in klinisch beeld. Tot nu toe is er zeer veel onderzoek gedaan naar het substraat, de triggers en modulerende factoren die verantwoordelijk zijn voor het optreden van (ventriculaire) aritmieën. Voordat VA optreden moeten de verschillende elementen van de driehoek gelijktijdig aanwezig zijn. Het is dus een kwestie van "de juiste situatie op het juiste moment".

Van patiënten met dezelfde ziekte hebben sommigen een groter risico op het ontwikkelen van VA dan anderen. We hebben aangetoond dat het onderliggende substraat, al dan niet als gevolg van erfelijke aanleg, van groot belang is om VA ontwikkelen. Echter, triggers en modulerende factoren spelen ook een belangrijke rol bij het ontstaan van VA.

Wereldwijd is de incidentie van SCD gedaald als gevolg van betere inzichten in de pathofysiologische mechanismen en de daarbij passende therapie. Toch ontwikkelt nog een groot aantal patiënten dodelijke hartritimestoornissen. Een beter begrip van de verschillende onderdelen die zorgen voor VA kan resulteren in een nauwkeurigere risicostratificatie en uiteindelijk in een betere behandeling van patiënten die risico lopen op VA. De verschillende onderwerpen in dit proefschrift zijn opgenomen in onderstaande figuur met hun relatie tot de driehoek van Coumel.



**Figuur.** De verschillende onderwerpen van het proefschrift opgenomen in de driehoek. ANS: autonome zenuwstelsel, ESHF: eind stadium hartfalen, PLN: phospholamban, VES: ventriculaire extrasystole.

## DEEL I MARKERS VAN VERHOOGDE GEVOELIGHEID VOOR HET OPTREDEN VAN VENTRICULAIRE RITMESTOORNISSEN

In het eerste deel van dit proefschrift werden verschillende klinische parameters onderzocht die invloed hebben op verschillende componenten van de driehoek (figuur) bij patiënten met risico op het optreden van VA.

Eerdere studies hebben aangetoond dat het autonome zenuwstelsel een rol speelt bij de ontwikkeling van VA<sup>2</sup>. Dit is een van de modulerende factoren in de driehoek. Bij patiënten met hartfalen (HF) is er een onbalans tussen het parasympatische en sympathische zenuwstelsel. Hartslagvariabiliteit (HRV) is een maat voor deze onbalans en de HRV is vaak verlaagd bij patiënten met HF<sup>3-5</sup>. In hoofdstuk 2 tonen we aan dat bij patiënten met een implanteerbare cardioverter defibrillator (ICD) als primaire of secundaire preventie, HRV nuttig kan zijn om het optreden van terechte ICD schokken en derhalve VA te voorspellen. We hebben aangetoond dat wanneer de HRV verlaagd is, een verhoogd risico op een terechte ICD schok bestaat. HRV kan dus een hulpmiddel zijn om te bepalen of de patiënt risico loopt op een terechte ICD schok, aangezien de HRV parameters gemakkelijk en direct beschikbaar zijn op verscheidene ICD-apparaten. Steeds meer patiënten nemen deel aan home-monitoringprogramma's. Deze parameters kunnen routinematig geïmplementeerd worden om eventuele aanpassing in de behandeling van hartfalen te bewerkstelligen. Ons onderzoek was een retrospectief onderzoek met verschillende intervallen tussen de metingen en een beperkt aantal patiënten. Ik stel voor om deze parameters prospectief te analyseren in een grotere groep patiënten op vooraf bepaalde tijdstippen.

In hoofdstuk 3 onderzochten we patiënten met een cardiomyopathie met of zonder hartfalen (HF), en met een genetische achtergrond om niet-invasieve parameters te bepalen voor de ernst van de ziekte en mogelijke VA. Deze patiënten hebben een mutatie p.ARG14del in het phospholamban (*PLN*) gen. Het *PLN*-gen is betrokken bij de cellulaire calcium huishouding<sup>6</sup>. Patiënten met deze mutatie krijgen vaak VA, hebben lage QRS voltages op het oppervlakte ECG en ontwikkelen HF<sup>7, 8</sup>. Een laag QRS voltage op het oppervlakte ECG kan de eerste manifestatie zijn van deze ziekte en we onderzochten of de aanwezigheid van laag gevoltageerde QRS-complexen de aanwezigheid van fibrose kan aantonen gebruikmakend van cardiale MRI met late gadolinium enhancement. Dit hoofdstuk past bij het substraat component in de driehoek. We analyseerden verschillende niet-invasieve klinische parameters verkregen uit het oppervlakte ECG (geleiding parameters, lage R-top amplitude en negatieve T-golven). We hebben aangetoond dat bij patiënten met *PLN* cardiomyopathie lage QRS voltages geassocieerd zijn met fibrose op de cardiale MRI. Echter, na correctie voor leeftijd en de aanwezigheid van negatieve T-golven, is deze parameter niet meer voorspellend. Opmerkelijk was dat negatieve T-golven geassocieerd zijn met fibrose op MRI, ook na correctie voor andere voorspellers. Aangezien negatieve T-golven gemakkelijk herkenbaar zijn het ECG, kan de aanwezigheid hiervan

een geschikte risicofactor voor fibrose en eventuele latere VA zijn. Om te bepalen of deze negatieve T-golven en/of lage R-top amplitude daadwerkelijk risicofactoren kunnen zijn voor toekomstige VA zijn wij bezig met een longitudinaal onderzoek bij patiënten met *PLN* cardiomyopathie en het optreden van VA tijdens follow-up.

Een mogelijke verklaring voor de associatie tussen negatieve T-golven en de aanwezigheid van fibrose blijft ook een interessant gegeven voor verder onderzoek. Het kan zijn dat een verminderde compliantie van de ventrikelwand door fibrose resulteert in veranderingen in mechano-electrische feedback.

Dit proefschrift richt zich ook op het familiair voorkomen van idiopathisch kamerebrillen (IVF). Anders dan in het Brugada syndroom (BrS) of het lange QT syndroom zijn er bij deze aandoening geen klinische parameters beschikbaar om het risico op een hartstilstand in te schatten waardoor het moeilijk is om patiënten die risico op VA lopen aan te wijzen. In eerder onderzoek is beschreven dat in onze specifieke familiere subgroep alleen de aanwezigheid van de *DPP6* risico haplotype duidt op een verhoogd risico op een cardiac event<sup>9</sup>. In hoofdstuk 4 hebben we aangetoond dat, ondanks uitgebreide analyse, risicostratificatie moeilijk blijft, omdat er geen klinische parameters konden worden geïdentificeerd anders dan het hebben van een genetische aanleg en een leeftijd tussen de 20 en 50 jaar. Hierdoor blijft het advies tot het implanteren van een profylactische cardioverter defibrillator bij jonge patiënten bestaan met alle bijbehorende complicaties van dien (onterechte schokken, draadbreek, infecties). Daarom is het belangrijk om meer inzicht te krijgen in het mechanisme achter deze dodelijke ziekte. Op dit moment kunnen we alleen speculeren hoe overexpressie van *DPP6* resulteert in het krijgen van IVF. Het is nog steeds niet duidelijk waarom patiënten met IVF kort gekoppelde monomorfe extrasystolen hebben die vaak direct resulteren in VF. In weefselmonsters van 5 risico haplotype-positieve patiënten was er een 22-voudige toename van mRNA expressie van *DPP6*<sup>10</sup>. *DPP6* is betrokken bij de 'transient outward' kaliumstroom (*I<sub>to</sub>*) in het hart. Er worden echter geen ECG afwijkingen waargenomen bij deze patiënten. Een mogelijk mechanisme zou kunnen zijn dat er alleen verkorting van de actiepotentiaal plaats vindt in het Purkinje systeem (door de verhoogd *I<sub>to</sub>*), resulterend in lokale micro-reentry in het specifieke geleidingsstelsel<sup>11</sup>. De kort gekoppelde ventriculaire extrasystolen passen bij de triggers in de driehoek van Coumel. Om te begrijpen hoe overexpressie van *DPP6* resulteert in IVF, zal verder onderzoek zich moeten richten op elektrofysiologisch onderzoek, in het bijzonder op het Purkinje systeem.

Gedetailleerde histologische onderzoek kan meer inzicht geven in veranderingen in hartweefsel. Omdat er slechts een beperkt aantal MRIs beschikbaar was, kan het zijn dat gedurende een langere follow-up met meerdere MRIs er toch met structurele afwijkingen gevonden worden ondanks dat de meeste cardiale events optraden bij jonge patiënten. Tenslotte, misschien zullen meer patiënten die een ICD kregen ter primaire preventie na langere follow-up een terechte schok ervaren wat het mogelijk maakt om andere klinische parameters te vinden.



## DEEL II KENMERKEN VAN HET ARITMOGENE SUBSTRAAT

In het tweede deel van dit proefschrift hebben we ons gericht op de kenmerken van het aritmogene substraat bij patiënten met eindstadium van hartfalen of met het Brugada syndroom (BrS). Daarnaast wordt in het laatste hoofdstuk het effect van het toedienen van stamcellen in een 2D model onderzocht, omdat stamceltherapie een veelbelovende therapeutische optie kan zijn voor de behandeling van HF, maar er ook mogelijk pro-aritmische effecten zijn.

In hoofdstuk 5 onderzochten we de verschillen in substraat op cellulair en moleculair niveau bij patiënten eindstadium HF, die een steunhart kregen. Tijdens de implantatie van het steunhart komt er weefsel vrij van de linker ventrikel en waarbij vervolgens de electrofysiologische remodelering (veroorzaakt door hartfalen) onderzocht kon worden. Het weefsel was afkomstig van patiënten met verschillende etiologie van hartfalen en daarom onderzochten we ook de verschillen in substraat tussen patiënten met ischemische cardiomyopathie (ICM) en dilaterende cardiomyopathie (DCM). In HF is er een toename van fibrose en een afname van connexin43 expressie.<sup>12-14</sup> Ook zijn er veranderingen beschreven in expressie van ionkanalen en microRNAs in patiënten met hartfalen<sup>15, 16</sup>. Daarom hebben we ons gericht op deze specifieke veranderingen.

Onze gegevens tonen aan dat fibrose een andere architectuur heeft bij patiënten met DCM in vergelijking met ICM. Weefsel van patiënten met ICM wordt gekarakteriseerd door 'patchy' fibrose. De fibrose was in grotere hoeveelheid aanwezig in vergelijking tot het weefsel van patiënten met DCM. De expressie van Cx43 vertoonde meer macro-heterogeniteit bij patiënten met DCM. Deze resultaten suggereren dat er verschillen zijn in de pathofysiologie van remodelering afhankelijk van de verschillende etiologieën bij patiënten met eindstadium HF. Er was geen verband tussen de verschillen in deze parameters en het optreden van VA. Hierdoor kunnen we niet bepalen welke parameters richtinggevend zijn voor het optreden van VA. Om daadwerkelijk onderscheid te maken tussen het exacte mechanisme van de VA in relatie tot de etiologie zal men uitgebreid elektrofysiologisch onderzoek moeten uitvoeren wat een uitdaging is. Steeds meer patiënten krijgen een steunhart als definitieve therapie in plaats van een harttransplantatie. Dat maakt dat het aantal te onderzoeken geëxplanteerde harten minder wordt. Door de toegenomen aantallen implantaties van de steunharten, komt er echter wel weer weefsel beschikbaar dat onderzocht kan worden op verschillen in remodelering.

Patiënten met BrS hebben een typisch ECG patroon; coved ST-segment elevatie gevolgd door een negatieve T-golf<sup>17</sup> (type 1 BrS-ECG) in tenminste één van de rechts-precordiale afleidingen in de 2<sup>e</sup>, 3<sup>e</sup> of 4<sup>e</sup> intercostale ruimte. Dit patroon kan spontaan optreden of na provocatie door intraveneuze toediening van klasse I anti-aritmica<sup>18</sup>. De typische ST-segment elevatie gaat vaak vooraf aan het ontstaan van VA<sup>19, 20</sup>, die VA kunnen leiden tot een hartstilstand of syncope<sup>21</sup>. Hierdoor is het type 1 BrS-ECG samen met syncope

een teken van verhoogd risico op VA<sup>22</sup>. Verscheidene hypothesen zijn gevormd om de ST-segment elevatie in BrS te verklaren. De repolarisatie hypothese is gebaseerd op dispersie in repolarisatie als gevolg van transmurale spanningsgradiënten veroorzaakt door heterogeniteit in actiepotentiaal duur tussen het epicard en het endocard van de rechter ventrikel (RV)<sup>23</sup>. De depolarisatie hypothese is gebaseerd op late activering van de rechter ventrikel uitstroombaan (RVOT)<sup>24</sup> en/of 'current-to-load mismatch' met 'excitation failure' in een structureel abnormale subepicardium van de RV/RVOT<sup>25</sup>. Het exacte mechanisme is nog niet volledig duidelijk. Daarom onderzochten we in hoofdstuk 6 het mogelijke pathofysiologische mechanisme van de karakteristieke ST-segment elevatie in BrS patiënten. Door verschillende epicardiale en endocardiale rechter ventrikel mapping procedures waren we in staat om aan te tonen dat de ST-segment elevatie, epicardiale fractionatie en geleidingsvertraging bij BrS patiënten waarschijnlijk veroorzaakt wordt door dezelfde structurele subepicardiale afwijkingen, maar dat het mechanisme verschillend is. Uit de verschillende mapping- en stimulatieprotocollen is gebleken dat BrS patiënten een langere activatieduur hebben met meer gefractioneerde epicardiale elektrogrammen en late potentialen in de RV / RVOT vergeleken met de controlegroep. Bovendien bleek dat alleen lokale fractionatie niet verantwoordelijk is voor de ST-segment elevatie op het oppervlak ECG. De ST-segment elevatie wordt waarschijnlijk veroorzaakt door de current-to-load mismatch. De gefractioneerde elektrogrammen worden veroorzaakt door geleidingsvertraging in hetzelfde gebied met abnormaal myocard. Verder onderzoek zal zich moeten richten op epicardiale mapping met stimulatie van het laatste gedeelte van de RVOT ten tijde van het QRS complex met een stimulussterkte net boven de stimulatierempel om te zien of de typische ST-segment elevatie verdwijnt wanneer het gedeelte wat niet gedepolariseerd is dan wel depolariseert.

In hoofdstuk 7 onderzochten we het effect van toediening van stamcellen op elektrofysiologische parameters aangezien stamceltherapie als een veelbelovende therapeutische optie wordt beschouwd bij patiënten met een verminderde linker ventrikel ejectionfracie door een doorgemaakt myocard infarct en/of HF<sup>26-28</sup>. Door stamcellen verandert de architectuur van het myocard waardoor verschillen in geleiding ontstaan zoals geleidingsvertraging, heterogeniteit van geleiding en geleidingsblokkade. Eerdere studies suggereren dat dit een gevolg kan zijn van elektrotone of paracrine effecten<sup>29</sup>. In dit hoofdstuk analyseerden we verschillende soorten stromale stamcellen verkregen uit vetweefsel (ADSC) van verschillende species (rat, varken en mens) en het effect op voortgeleiding in een monolaag van neonatale rat cardiomyocyten (NRVM). ADSCs werden gekozen omdat ze gemakkelijk te verkrijgen zijn, ze veelvuldig aanwezig zijn (uit vetweefsel), en ook omdat ze een geschikte bron zijn van multipotente cellen die kunnen differentiëren tot verscheidene cellijnen met weinig immunologische effecten<sup>30,31</sup>. Bovendien scheiden ADSCs een groot aantal factoren uit die de angiogenese<sup>32</sup> en neovascularisatie<sup>33</sup> stimuleren.

We hebben aangetoond dat ondanks de veelbelovende resultaten in eerdere studies, men terughoudend moet zijn met het gebruik van stamcellen aangezien er negatieve paracriene en elektrotone effecten zijn op elektrofysiologische parameters. Dit kan resulteren in een hogere gevoeligheid voor VA. Uit dit 2D model blijkt dat ADSCs zorgen voor geleidingsvertraging door paracriene effecten en intercellulaire koppeling met een potentieel aritmogeen substraat als gevolg. Waaruit de paracriene factoren exact bestaan is moeilijk om te bepalen omdat alle cellen factoren uitscheiden die ook met elkaar interfereren. Wij zijn bezig met het onderzoeken van de effecten op de electrofysiologie na van toediening van stamcellen in een 3D varkensmodel. Dit geeft ons de gelegenheid om de effecten te onderzoeken in vivo en in vitro.

Door eerder gepubliceerd onderzoek is er steeds meer duidelijk geworden over VA en het optreden daarvan. Echter, er valt nog steeds veel te leren over deze levensbedreigende VA en de verschillende factoren die hierop van invloed zijn. Dit proefschrift bevat een breed scala van onderwerpen met betrekking tot VA in structureel normale en abnormale harten. Tijdens het onderzoek dat ten grondslag ligt aan dit werk werd het duidelijk dat verder onderzoek nodig is waarbij een nauwe samenwerking bestaat tussen fundamenteel en klinisch onderzoek. Deze samenwerking leidt zo tot een toegenomen inzicht in de modulators van ventriculaire aritmieën, net zoals de nauwe relatie tussen de trigger en het substraat leidt tot het ontstaan van ventriculaire aritmieën.

## REFERENTIES

1. Coumel P. Cardiac arrhythmias and the autonomic nervous system. *J Cardiovasc Electrophysiol*. 1993;4:338-55.
2. Schwartz PJ, La Rovere MT and Vanoli E. Autonomic nervous system and sudden cardiac death. Experimental basis and clinical observations for post-myocardial infarction risk stratification. *Circulation*. 1992;85:177-91.
3. Ponikowski P, Anker SD, Chua TP, Szelemej R, Piepoli M, Adamopoulos S, Webb-Peploe K, Harrington D, Banasiak W, Wrabec K and Coats AJ. Depressed heart rate variability as an independent predictor of death in chronic congestive heart failure secondary to ischemic or idiopathic dilated cardiomyopathy. *Am J Cardiol* 1997;79:1645-1650.
4. Boveda S, Galinier M, Pathak A, Fourcade J, Dongay B, Benchendikh D, Massabuau P, Fauvel JM, Senard JM and Bounhoure JP. Prognostic value of heart rate variability in time domain analysis in congestive heart failure. *J Interv Card Electrophysiol* 2001;5:181-187.
5. Smilde TD, van Veldhuisen DJ and van den Berg MP. Prognostic value of heart rate variability and ventricular arrhythmias during 13-year follow-up in patients with mild to moderate heart failure. *Clin Res Cardiol*. 2009;98:233-9.
6. MacLennan DH and Kranias EG. Phospholamban: a crucial regulator of cardiac contractility. *Nature reviews Molecular cell biology*. 2003;4:566-77.
7. Posch MG, Perrot A, Geier C, Boldt LH, Schmidt G, Lehmkühl HB, Hetzer R, Dietz R, Gutberlet M, Haverkamp W and Ozcelik C. Genetic deletion of arginine 14 in phospholamban causes dilated cardiomyopathy with attenuated electrocardiographic R amplitudes. *Heart Rhythm*. 2009;6:480-6.
8. van der Zwaag PA, van Rijsingen IA, Asimaki A, Jongbloed JD, van Veldhuisen DJ, Wiesfeld AC, Cox MG, van Lochem LT, de Boer RA, Hofstra RM, Christiaans I, van Spaendonck-Zwarts KY, Lekanne dit Deprez RH, Judge DP, Calkins H, Suurmeijer AJ, Hauer RN, Saffitz JE, Wilde AA, van den Berg MP and van Tintelen JP. Phospholamban R14del mutation in patients diagnosed with dilated cardiomyopathy or arrhythmogenic right ventricular cardiomyopathy: evidence supporting the concept of arrhythmogenic cardiomyopathy. *European journal of heart failure*. 2012;14:1199-207.
9. Postema PG, Christiaans I, Hofman N, Alders M, Koopmann TT, Bezzina CR, Loh P, Zeppenfeld K, Volders PG and Wilde AA. Founder mutations in the Netherlands: familial idiopathic ventricular fibrillation and DPP6. *Neth Heart J* 2011;19:290-296.
10. Alders M, Koopmann TT, Christiaans I, Postema PG, Beekman L, Tanck MW, Zeppenfeld K, Loh P, Koch KT, Demolombe S, Mannens MM, Bezzina CR and Wilde AA. Haplotype-sharing analysis implicates chromosome 7q36 harboring DPP6 in familial idiopathic ventricular fibrillation. *Am J Hum Genet* 2009;84:468-476.
11. Xiao L, Koopmann TT, Ordog B, Postema PG, Verkerk AO, Iyer V, Sampson KJ, Boink GJ, Mamarbachi MA, Varro A, Jordaens L, Res J, Kass RS, Wilde AA, Bezzina CR and Nattel S. Unique Cardiac Purkinje Fiber Transient Outward Current beta-Subunit Composition: A Potential Molecular Link to Idiopathic Ventricular Fibrillation. *Circ Res* 2013;112:1310-1322.
12. Kawara T, Derksen R, de Groot JR, Coronel R, Tasseront S, Linnenbank AC, Hauer RN, Kirkels H, Janse MJ and de Bakker JM. Activation delay after premature stimulation in chronically diseased human myocardium relates to the architecture of interstitial fibrosis. *Circulation*. 2001;104:3069-3075.

13. Kitamura H, Ohnishi Y, Yoshida A, Okajima K, Azumi H, Ishida A, Galeano EJ, Kubo S, Hayashi Y, Itoh H and Yokoyama M. Heterogeneous loss of connexin43 protein in nonischemic dilated cardiomyopathy with ventricular tachycardia. *J Cardiovasc Electrophysiol*. 2002;13:865-70.
14. Boulaksil M, Winckels SK, Engelen MA, Stein M, van Veen TA, Jansen JA, Linnenbank AC, Bierhuizen MF, Groenewegen WA, van Oosterhout MF, Kirkels JH, de Jonge N, Varro A, Vos MA, de Bakker JM and van Rijen HV. Heterogeneous Connexin43 distribution in heart failure is associated with dispersed conduction and enhanced susceptibility to ventricular arrhythmias. *European journal of heart failure*. 2010;12:913-21.
15. Valdivia CR, Chu WW, Pu J, Foell JD, Haworth RA, Wolff MR, Kamp TJ and Makielski JC. Increased late sodium current in myocytes from a canine heart failure model and from failing human heart. *J Mol Cell Cardiol* 2005;38:475-483.
16. Nattel S, Maguy A, Le Bouter S and Yeh YH. Arrhythmogenic ion-channel remodeling in the heart: heart failure, myocardial infarction, and atrial fibrillation. *Physiol Rev*. 2007;87:425-56.
17. Brugada P and Brugada J. Right bundle branch block, persistent ST segment elevation and sudden cardiac death: a distinct clinical and electrocardiographic syndrome. A multicenter report. *J Am Coll Cardiol* 1992;20:1391-1396.
18. Priori SG, Wilde AA, Horie M, Cho Y, Behr ER, Berul C, Blom N, Brugada J, Chiang CE, Huikuri H, Kannankeril P, Krahn A, Leenhardt A, Moss A, Schwartz PJ, Shimizu W, Tomaselli G and Tracy C. Executive Summary: HRS/EHRA/APHS Expert Consensus Statement on the Diagnosis and Management of Patients with Inherited Primary Arrhythmia Syndromes. *Heart Rhythm* 2013.
19. Matsuo K, Shimizu W, Kurita T, Inagaki M, Aihara N and Kamakura S. Dynamic changes of 12-lead electrocardiograms in a patient with Brugada syndrome. *J Cardiovasc Electrophysiol*. 1998;9:508-12.
20. Priori SG, Napolitano C, Gasparini M, Pappone C, Della BP, Brignole M, Giordano U, Giovannini T, Menozzi C, Bloise R, Crotti L, Terreni L and Schwartz PJ. Clinical and genetic heterogeneity of right bundle branch block and ST-segment elevation syndrome: A prospective evaluation of 52 families. *Circulation*. 2000;102:2509-2515.
21. Antzelevitch C, Brugada P, Borggrefe M, Brugada J, Brugada R, Corrado D, Gussak I, LeMarec H, Nademanee K, Perez Riera AR, Shimizu W, Schulze-Bahr E, Tan H and Wilde A. Brugada syndrome: report of the second consensus conference: endorsed by the Heart Rhythm Society and the European Heart Rhythm Association. *Circulation*. 2005;111:659-670.
22. Priori SG, Napolitano C, Gasparini M, Pappone C, Della Bella P, Giordano U, Bloise R, Giustetto C, De Nardis R, Grillo M, Ronchetti E, Faggiano G and Nastoli J. Natural history of Brugada syndrome: insights for risk stratification and management. *Circulation*. 2002;105:1342-7.
23. Yan GX and Antzelevitch C. Cellular basis for the Brugada syndrome and other mechanisms of arrhythmogenesis associated with ST-segment elevation. *Circulation*. 1999;100:1660-1666.
24. Tukkie R, Sogaard P, Vleugels J, de Groot IK, Wilde AA and Tan HL. Delay in right ventricular activation contributes to Brugada syndrome. *Circulation*. 2004;109:1272-1277.
25. Hoogendijk MG, Potse M, Vinet A, de Bakker JM and Coronel R. ST segment elevation by current-to-load mismatch: an experimental and computational study. *Heart Rhythm* 2011;8: 111-118.
26. Wollert KC, Meyer GP, Lotz J, Ringes-Lichtenberg S, Lippolt P, Breidenbach C, Fichtner S, Korte T, Hornig B, Messinger D, Arseniev L, Hertenstein B, Ganser A and Drexler H. Intracoronary autologous bone-marrow cell transfer after myocardial infarction: the BOOST randomised controlled clinical trial. *Lancet*. 2004;364:141-8.

27. Bolli R, Chugh AR, D'Amario D, Loughran JH, Stoddard MF, Ikram S, Beache GM, Wagner SG, Leri A, Hosoda T, Sanada F, Elmore JB, Goichberg P, Cappetta D, Solankhi NK, Fahsah I, Rokosh DG, Slaughter MS, Kajstura J and Anversa P. Cardiac stem cells in patients with ischaemic cardiomyopathy (SCIPIO): initial results of a randomised phase 1 trial. *Lancet*. 2011;378:1847-1857.
28. Makkar RR, Smith RR, Cheng K, Malliaras K, Thomson LE, Berman D, Czer LS, Marban L, Mendizabal A, Johnston PV, Russell SD, Schuleri KH, Lardo AC, Gerstenblith G and Marban E. Intracoronary cardiosphere-derived cells for heart regeneration after myocardial infarction (CADUCEUS): a prospective, randomised phase 1 trial. *Lancet*. 2012;379:895-904.
29. Askar SF, Ramkisoensing AA, Atsma DE, Schaliij MJ, de Vries AA and Pijnappels DA. Engraftment patterns of human adult mesenchymal stem cells expose electrotonic and paracrine proarrhythmic mechanisms in myocardial cell cultures. *Circ Arrhythm Electrophysiol* 2013;6: 380-391.
30. Nakagami H, Morishita R, Maeda K, Kikuchi Y, Ogihara T and Kaneda Y. Adipose tissue-derived stromal cells as a novel option for regenerative cell therapy. *J Atheroscler Thromb*. 2006;13: 77-81.
31. Madonna R, Geng YJ and De Caterina R. Adipose tissue-derived stem cells: characterization and potential for cardiovascular repair. *Arterioscler Thromb Vasc Biol*. 2009;29:1723-9.
32. Rehman J, Traktuev D, Li J, Merfeld-Clauss S, Temm-Grove CJ, Bovenkerk JE, Pell CL, Johnstone BH, Considine RV and March KL. Secretion of angiogenic and antiapoptotic factors by human adipose stromal cells. *Circulation*. 2004;109:1292-8.
33. Miranville A, Heeschen C, Sengenès C, Curat CA, Busse R and Bouloumie A. Improvement of postnatal neovascularization by human adipose tissue-derived stem cells. *Circulation*. 2004; 110:349-55.



## PORTFOLIO

PhD student: J.N. ten Sande

PhD period: 2010-2017

Supervisor: Prof. dr. ir. J.M.T. de Bakker and prof. dr. A.A.M. Wilde

Co-supervisor: Dr. P.F.H.M. van Dessel and dr. R. Coronel

PhD training		
Year	Courses	ECTS
2010	AMC world of Science (introduction course)	0.7
2010	Laboratory Animals; Article 9 certified	3.9
2010	Practical biostatistics	1.5
2011	ICH-Good clinical practice certified (BROK course)	0.9
2011	Clinical data management	0.5
	<b>Specific courses and master classes</b>	
2010	CVOI Electrophysiology course	0.3
	CVOI Electrocardiography course	0.3
2012	ICD essentials course	1.0
	ERC ALS course: certified ALS provider	1.0
2013	Masterclass ECG interpretation	0.3
	Masterclass Stem Cells	0.3
2014	Young Cardiologists Electrophysiology course	0.5
	Presentations and conferences	
2010	European Society of Cardiology Congress, Stockholm, Sweden	1.5
2012	European Society of Cardiology Congress, Munich, Germany	1.5
	Netherlands Heart Rhythm Association, Ermelo (oral presentation)	0.7
2013	American Heart Association Congress, Los Angeles, USA (poster presentation)	1.5
	BioMedical Material congress, Ermelo (oral presentation)	0.7
	Utrecht Stem Cell Conference, Utrecht	0.5
	Denis-Escande Symposium, Amsterdam	0.5
	European Society of Cardiology Congress, Amsterdam, The Netherlands (oral presentation)	1.5
	Netherlands Heart Rhythm Association, Ermelo (oral presentation)	0.7
2014	Heart Rhythm Society Congress, San Francisco, USA (poster presentation)	1.5
	European Society of Cardiology Congress, Barcelona, Spain	1.5
	Netherlands Heart Rhythm Association, Ermelo (oral presentation)	0.7
2015	Heart Rhythm Society Congress, Boston, USA (poster presentation)	1.5
	European Society of Cardiology Congress, London, UK (poster presentation)	1.5
	<b>Teaching</b>	
2011 - 2014	Lecturer electrocardiography for advanced nursing courses	3.0
2010 - 2014	Lecturer electrocardiography for medical students	2.5





## CONTRIBUTING AUTHORS

### **Boekholdt SM**

Heart Center, Department of Clinical and Experimental Cardiology, Academic Medical Center, University of Amsterdam, Amsterdam, The Netherlands

### **Boersma LVA**

Department of Cardiology, St. Antonius Hospital, Nieuwegein, The Netherlands

### **Christiaans I**

Department of Clinical Genetics, Academic Medical Center, University of Amsterdam, Amsterdam, The Netherlands

### **Conrath CE**

Heart Center, Department of Clinical and Experimental Cardiology, Academic Medical Center, University of Amsterdam, Amsterdam, The Netherlands

### **Coronel R**

Heart Center, Department of Clinical and Experimental Cardiology, Academic Medical Center, University of Amsterdam, Amsterdam, The Netherlands  
L'Institute de RYthmologie et de modélisation Cardiaque (LIRYC), Université Bordeaux Segalen, Bordeaux, France

### **Damman P**

Heart Center, Department of Clinical and Experimental Cardiology, Academic Medical Center, University of Amsterdam, Amsterdam, The Netherlands

### **De Bakker JMT**

Heart Center, Department of Clinical and Experimental Cardiology, Academic Medical Center, University of Amsterdam, Amsterdam, The Netherlands  
Interuniversity Cardiology Institute of the Netherlands, Utrecht, The Netherlands

### **De Boer RA**

Department of Clinical and Experimental Cardiology, University of Groningen, University Medical Center Groningen, Groningen, the Netherlands

### **De Groot JR**

Heart Center, Department of Clinical and Experimental Cardiology, Academic Medical Center, University of Amsterdam, Amsterdam, The Netherlands

**De Groot NMS**

Department of Cardiology, Erasmus Medical Center, Rotterdam, The Netherlands

**Driessen AHG**

Heart Center, Department of Cardiothoracic Surgery, Academic Medical Center, Amsterdam, The Netherlands

**Gorter TM**

Department of Clinical and Experimental Cardiology, University of Groningen, University Medical Center Groningen, Groningen, the Netherlands

**Harmsen MC**

Department of Pathology and Medical Biology, University Medical Center Groningen, University of Groningen, The Netherlands

**Knops RE**

Heart Center, Department of Clinical and Experimental Cardiology, Academic Medical Center, University of Amsterdam, Amsterdam, The Netherlands

**Nademanee K**

Pacific Rim Electrophysiology Research Institute, Los Angeles, CA, USA

**Nannenberg EA**

Department of Clinical Genetics, Academic Medical Center, University of Amsterdam, Amsterdam, The Netherlands

**Parvizi M**

Department of Pathology and Medical Biology, University Medical Center Groningen, University of Groningen, The Netherlands

**Planken RN**

Department of Radiology, University of Amsterdam, Academic Medical Center, Amsterdam

**Plantinga JA**

Department of Pathology and Medical Biology, University Medical Center Groningen, University of Groningen, The Netherlands

**Postema PG**

Heart Center, Department of Clinical and Experimental Cardiology, Academic Medical Center, University of Amsterdam, Amsterdam, The Netherlands

**Smit NW**

Heart Center, Department of Clinical and Experimental Cardiology, Academic Medical Center, University of Amsterdam, Amsterdam, The Netherlands

**Tan HL**

Heart Center, Department of Clinical and Experimental Cardiology, Academic Medical Center, University of Amsterdam, Amsterdam, The Netherlands

**Te Rijdt WP**

Department of Clinical and Experimental Cardiology, University of Groningen, University Medical Center Groningen, Groningen, the Netherlands

**Tijssen JGP**

Heart Center, Department of Clinical and Experimental Cardiology, Academic Medical Center, University of Amsterdam, Amsterdam, The Netherlands

**Van Amersfoort SCM**

Heart Center, Department of Clinical and Experimental Cardiology, Academic Medical Center, University of Amsterdam, Amsterdam, The Netherlands

**Van den Berg MP**

Department of Clinical and Experimental Cardiology, University of Groningen, University Medical Center Groningen, Groningen, the Netherlands

**Van der Zwaag PA**

Department of Clinical and Experimental Cardiology, University of Groningen, University Medical Center Groningen, Groningen, the Netherlands

**Van Dessel PFHM**

Heart Center, Department of Clinical and Experimental Cardiology, Academic Medical Center, University of Amsterdam, Amsterdam, The Netherlands

**Van Haelst PL**

Department of Cardiology, Antonius Hospital, Sneek, the Netherlands and Roche Diagnostics, Basel, Switzerland

**Van der Heijden JF**

Department of Cardiology, University Medical Center Utrecht, Utrecht, The Netherlands

**Van Rijsingen IA**

Heart Center, Department of Clinical and Experimental Cardiology, University of Amsterdam, Academic Medical Center, Amsterdam, The Netherlands

**Van Veldhuisen DJ**

Department of Clinical and Experimental Cardiology, University of Groningen, University Medical Center Groningen, Groningen, the Netherlands

**Van Tintelen JP**

Department of Clinical Genetics, University of Amsterdam, Academic Medical Center, Amsterdam, the Netherlands

**Volders PGA**

Department of Cardiology, Maastricht University Medical Center, The Netherlands

**Wilde AAM**

Heart Center, Department of Clinical and Experimental Cardiology, Academic Medical Center, University of Amsterdam, Amsterdam, The Netherlands

Princess Al-Jawhara Albrahim Center of Excellence in Research of Hereditary Disorders, King Abdulaziz University, Jeddah, Saudi Arabia

**Willems TP**

Department of Radiology, University of Groningen, University Medical Center Groningen, Groningen, the Netherlands

**Zeppenfeld K**

Department of Cardiology, Leiden University Medical Center, The Netherlands

## DANKWOORD

Hier is het “boekje” dan eindelijk!

Tijdens het promotietraject heb ik veel mensen in meer en mindere mate leren kennen en ik wil graag iedereen bedanken die bijgedragen heeft aan de totstandkoming van dit proefschrift. Een aantal personen wil ik graag specifiek bedanken.

Mijn promotores prof. dr. ir. J.M.T de Bakker en prof. dr. A.A.M. Wilde.

Beste Jacques, het was een eer om met u te mogen samenwerken. Of het nu ging om samen experimenten uitvoeren of om uw commentaar op de manuscripten: altijd was het met geduld en precisie, hartelijke bedankt hiervoor.

Beste Arthur, ondanks je drukke schema stond je deur altijd open. Bedankt voor de opbouwende kritiek en de juiste sturing op het juiste moment.

Mijn co-promotores dr. P.F.H.M. van Dessel en dr. R. Coronel.

Beste Pascal, wat hebben wij veel meegemaakt gedurende de afgelopen jaren. Altijd en onvoorwaardelijk ben je achter mij blijven staan. Dit waardeer ik zeer en zal ik niet vergeten. Ik mis de woensdagochtenden waarbij er naast wetenschap ook ruimte was voor jouw visie op meer persoonlijke zaken. Onze samenwerking zal zich vast voortzetten op een of andere manier.

Beste Ruben, wat later raakte jij betrokken bij mijn promotietraject. Dit heeft zeker een toegevoegde waarde gehad. Ik vond het erg ‘leuk’ en boeiend om met jou de basale elektrofysiologie te bespreken. Altijd kritisch en rekening houdend met mijn ongeduld

De leden van de promotiecommissie, bestaande uit prof. dr. R.J.G. Peters, prof. dr. Y.M. Pinto, prof. dr. D.J. van Veldhuisen, prof. dr. M.A. Vos, dr. C.E. Conrath, dr. P.G. Postema en dr. J.P. van Tintelen, ben ik zeer erkentelijk en bedank ik van harte voor het beoordelen van het manuscript en voor hun bereidheid om zitting te nemen in mijn promotiecommissie.

Medeauteurs, bedankt voor alle commentaren en discussie om de manuscripten tot een hoger niveau te brengen.

Afdeling Assist Device van het UMC Utrecht, hartelijk bedankt voor het meedenken en voor het creëren van de mogelijkheid om hartweefsel te verkrijgen. Met name door Nelienke en Anne-Marie konden de patiënten op tijd geïncubeerd worden.

Graag bedank ik de afdeling Cardiologie, de afdeling Electrofysiologie en Pacemaker-ertechniek en de afdeling Experimentele Cardiologie voor al hun hulp en adviezen. In het

bijzonder Rena, Gerrie, Marieke, Tobias, Charly, Carel, André, Carol Ann, Cees, Ton, Jan, Antoni en Shirley.

Regina, Anita, Lieve, Piety en Margreet, bedankt voor alle hulp en ondersteuning de afgelopen jaren!

Collega onderzoekers van de klinische en experimentele cardiologie (wat zijn het er inmiddels veel...excuses als ik iemand vergeet):

Peter, Wichert, Annemarie, Bimmer, Anja, Harald, Marcel, Krischan, Carlijne, Wouter K., Ze-Yie, Loes, Ronak, Kirsten, Tim, Maik, Ralf, Esther, Ling, Mariëlle, Ties, Dagmar, Joëlle, Susan, Debbie, Martijn v L., Ivo, Martijn v M., Juliëtte, Martina, Michiel, Niels, Robin, Sangeeta, Maayke, Michiel, Jeroen, Piet, Paul, Zeliha, Teun, Mark, Romy, Alexander, Jouke, Annelieke, Josephine, Joey, Ilja, Fleur, Lonneke, Jolien, Gilbert, Ruben, Hayang, Yolan, Michiel, Noline S., Christiaan, Maaïke, Dénise, Geert, Bas, Mathilde, Krystien, enorm bedankt voor de super tijd in het AMC, de gezellige borrels en de feestjes.

Mijn kamergenootjes/mede-EP-ers: Christian, Sébastien, Wouter, Madelon, Suzanne, Yuka, Jim, Tom en Noline. Wat een feest om met jullie op de kamer te zitten en te ontspannen na werktijd. Van luchtige gesprekjes tot aan heftige discussies: ik heb van alles genoten. Een mooie tijd hebben we gehad, iets wat ik niet zal vergeten.

Opleidingsgenoten, wat fijn en gezellig om samen dit traject te doorlopen. In het bijzonder noem ik Louise en Pier. Lieve Louise, eerst samen op de kamer en daarna in opleiding. Naast een betrokken collega ben je ook een vriendin geworden en vooral je directheid waardeert ik. Ik kijk uit naar de komende jaren! Lieve Pier, samen zijn we gestart en we hebben het eerste gedeelte erop zitten: wat is er veel gebeurd. Je bent een enthousiaste en fijne collega. Ik hoop dat we nog vele jaren kunnen samenwerken.

Lieve vrienden, dank voor een luisterend oor en voor het relativiseringsvermogen (Hilversum gang: Judith, Mirjam, Cathinca, Lisa en Laura. Gevaarlijke vissen: Albertine, Ilse, Jeldau, Kenza, Lineke, Nicolien en Sanne).

Lieve Nina, bij jou kon ik mijn hart luchten over het wel en wee in het AMC en alles wat daarbij kwam kijken. Het is niet te beschrijven wat dit voor mij betekende en jouw visie heeft er zeker toe geleid dat het makkelijker was.

Mijn paranimfen, Lenneke en Veronique.

Lieve Veronique, kamergenoot vanaf het begin, maar inmiddels ook vriendinnetje. Samen sporten, cellen isoleren, op jacht naar harten en natuurlijk bij de "experimentele" op

bezoek. Wat fijn dat we elkaars paranimf kunnen zijn. Ik hoop dat we in de toekomst onze goede samenwerking kunnen voortzetten.

Lieve Lenneke, wie had vijftien jaar geleden kunnen bedenken dat we hier zo zouden staan. Ik denk met plezier terug aan de momenten dat we op donderdagavond nog tot laat in de MB zaten te studeren op de oogzenuwen, de handbotjes en de inhoud van een cel. Wat bijzonder dat je naast me staat.

Lieve familie en schoonfamilie, niet altijd was het duidelijk waar ik mee bezig was en geregeld kwam de vraag wanneer het eens af was. Moeilijke vragen, maar dit neemt niet weg dat ik de berichtjes en belletjes zeer op prijs heb gesteld.

Lieve pap en mam, door jullie ben ik geworden wie ik ben en sta ik hier. Altijd ben ik vrij gelaten om dingen te ontdekken en heb ik kunnen doen wat ik wilde met hier en daar wat sturing. Het was niet altijd even makkelijk, maar heel erg bedankt voor jullie vertrouwen. Dit boekje is voor jullie.

Lieve Peter, zo lang al zij aan zij en het verveelt nooit. Dank voor je steun, geduld en adviezen. Nu met onze kleine rakker is het leven nog rijker. Ik ben dankbaar voor mijn twee Peters. Ik houd van jullie!





## CURRICULUM VITAE

Judith ten Sande was born in Amersfoort, the Netherlands, on January 4<sup>th</sup> 1983, to Hans Willem and Annelies ten Sande. Together with her older sister Eveline and her younger brother Erwin she grew up in Kortenhoef. In 2001 she graduated from high school at the Comenius College in Hilversum after which she moved to Utrecht to study Biology and subsequently Medicine at the University of Utrecht. In April 2009 she obtained her medical degree and started working at the cardiology department at the Sint Lucas Andreas Hospital (under supervision of dr. W.G. de Voogt). During the last two years of medical school Judith developed an interest in cardiology and this interest progressed while working at the cardiology department. Subsequently in 2010 she started her PhD project at the Department of Cardiology at the AMC under supervision of prof. dr. ir. Jacques de Bakker, prof. dr. Arthur Wilde, dr. Pascal van Dessel and dr. Ruben Coronel.

In April 2015 she started her training in Cardiology at the AMC under supervision of dr. R.B.A. van den Brink and dr. M.M. Vis with a two years residency at the Department of Internal Medicine under supervision of prof. dr. S.E. Geerlings, prof. dr. J.M. Prins and prof. dr. J.A. Romijn.

Judith is married to Peter Bierdrager and together they have one son, Peter.

